Structural Dynamics and Novel Biological Function of Topoisomerase 2

by

Yu-tsung Shane Chen

Department of Biochemistry
Duke University

Date:_____

Approved:

_____
Tao-shih Hsieh, Co-Supervisor

_____
Paul Modrich, Co-Supervisor

_____
Kenneth Kreuzer

_____
Sue Jinks-Robertson

_____
Aziz Sancar

Dissertation submitted in partial fulfillment of
the requirements for the degree of Doctor
of Philosophy in the Department of
Biochemistry in the Graduate School
of Duke University

2015

ABSTRACT

Structural Dynamics and Novel Biological Function of Topoisomerase 2

by

Yu-tsung Shane Chen

Department of Biochemistry
Duke University

Date:_____

Approved:

_____
Tao-shih Hsieh, Co-Supervisor

_____
Paul Modrich, Co-Supervisor

_____
Kenneth Kreuzer

_____
Sue Jinks-Robertson

_____
Aziz Sancar

An abstract of a dissertation submitted in partial
fulfillment of the requirements for the degree
of Doctor of Philosophy in the Department of
Biochemistry in the Graduate School of
Duke University

2015

Abstract

Eukaryotic Topoisomerase 2 is an essential enzyme that solves DNA topological problems such as DNA knotting, catenation, and supercoiling. It alters the DNA topology by introducing a transient double strand break in one DNA duplex as a gate for the passage of another DNA duplex. Two different aspects of studies about eukaryotic Topoisomerase 2 will be covered in this thesis. In the first half of the thesis, we investigated conformational changes of human Topoisomerase 2α (*hs*Top2α) in the presence of cofactors and inhibitors. In the second half, we focused on an unknown regulatory function in the C-terminal domain (CTD) of *Drosophila* Topoisomerase 2 (Top2).

In the project of studying enzyme conformational changes, we adapted a previously developed methodology, Pulse-Alkylation Mass Spectrometry, with monobromobimane to study the protein dynamics of *hs*Top2α. Using this method, we captured the evidence of conformational changes in the presence of ATP and Mg^{2+} or the Top2 inhibitor, ICRF-193 which were not previously observed. Lastly, by using CTD truncated *hs*Top2α, the increasing reactivity of Cys427 suggested the CTD domain might be tethered adjacent to the core enzyme.

Following the study of enzyme conformational changes, we examined an interaction between *Drosophila* Top2 and Mus101, the homolog of human TopBP1. We

first found that Mus101 interacts with the CTD of Top2 in a phosphorylation-dependent manner. Next, in co-immunoprecipitation and pull-down experiments using truncated or mutant Top2 with various Ser to Ala substitutions, we mapped the binding motif to the last amino acids of Top2 and identified that phosphorylation of Ser1428 and Ser1443 is important for Top2 to interact with the N-terminus of Mus101, which contains BRCT1/2 domains (BRCT, BRCA1 C-terminus). The binding affinity of the N-terminal Mus101 with a synthetic phosphorylated peptide covering the last 25 amino acids of Top2 (with pS1428 and pS1443) was determined by surface plasmon resonance with a K_d of 0.57 μM. In an *in vitro* decatenation assay, Mus101 can specifically reduce the decatenation activity of Top2, and dephosphorylation of Top2 attenuates this response to Mus101. Next, we endeavored to establish a cellular system for testing the biological function of Top2-Mus101 interaction. Top2-silenced S2 cells rescued by Top2Δ20, truncation of 20 amino acids from the C-terminus of Top2, developed abnormally high chromosome numbers, which implies an infidelity in chromosome segregation during mitosis. Lastly, Top2-null flies rescued by Top2 with S1428A and S1443A were found to be viable but sterile. After investigating spermatogenesis, telophase of meiosis I was delayed, indicating Top2-Mus101 interaction is also important in segregating DNA in meiosis.

Dedication

This thesis is dedicated to my parents, Yung-Chang Chen and Pi-ju Wu.

Contents

List of Tables

List of Figures

Acknowledgements

I would like to first thank my adviser, Dr. Tao-shih Hsieh, for equipping me with all his firsthand lab experience and skills which have helped me to overcome many obstacles along the entire Ph.D. training. I especially appreciated that he always kept me motivated and told me not to turn away but to learn from every failure for which is the key to any success. Next, my project would not have gone this far without my co-adviser, Dr. Paul Modrich, who took me in after Tao moved back to Taiwan. Although my project was not directly linked to the lab, he considered me as his own student on the first day and gave me guidance no less than any other people in the lab. I would also like to thank my committee members, Dr. Aziz Sancer, Dr. Kenneth Kreuzer, and Dr. Sue Jinks-Robertson for their insightful suggestions in every committee meeting. Furthermore, I am also grateful to have useful advice and encouragement from the lab mates throughout my time in the Hsieh lab and the Modrich lab.

Outside the lab, life at Duke would not be as cheerful if it were not for my classmates and friends, who were always there to share my happy moments or to make my worries vanish. I am also lucky to have strong bonds with friends in Taiwan Student Associations at Duke who helped me to get familiar with the environment and cheer me up with heartwarming Chinese holiday events. Lastly, I would like to thanks my wife, Han-Yu Shih, who has always believed in me and supported me unconditionally.

1. Introduction

1.1 Eukaryotic Topoisomerase 2

DNA topoisomerases are a family of enzymes that solve DNA topological problems. Based on the DNA scission activity, these enzymes can be categorized into two types, I and II. While type I topoisomerases cleave one strand of DNA to relax the DNA tension (Depew et al., 1978; Liu and Wang, 1979), type II topoisomerases change DNA topology by creating a transient DNA double strand breakage which allows a second DNA duplex to pass through (Liu et al., 1983; Morrison and Cozzarelli, 1979; Sander and Hsieh, 1983). Based on the structure and mechanism, there are two subfamilies, IIA and IIB, among type II topoisomerases (Bergerat et al., 1997; Gadelle et al., 2003). Type IIA topoisomerases include bacterial gyrase, TopoIV, and the main focus of this thesis, eukaryotic topoisomerase 2 (Gadelle et al., 2003).

1.1.1 Structure and Mechanism of Eukaryotic Topoisomerase 2

Eukaryotic topoisomerase 2 (Top2) functions as a homodimer, and it is composed of three major domains, an N-terminal ATPase domain, a core cleavage/religation domain and a C-terminal regulatory domain (CTD) (Schoeffler and Berger, 2008). Based on the structure, ATPase and cleavage/religation domains can be divided into several subdomains (**Figure. 1**).

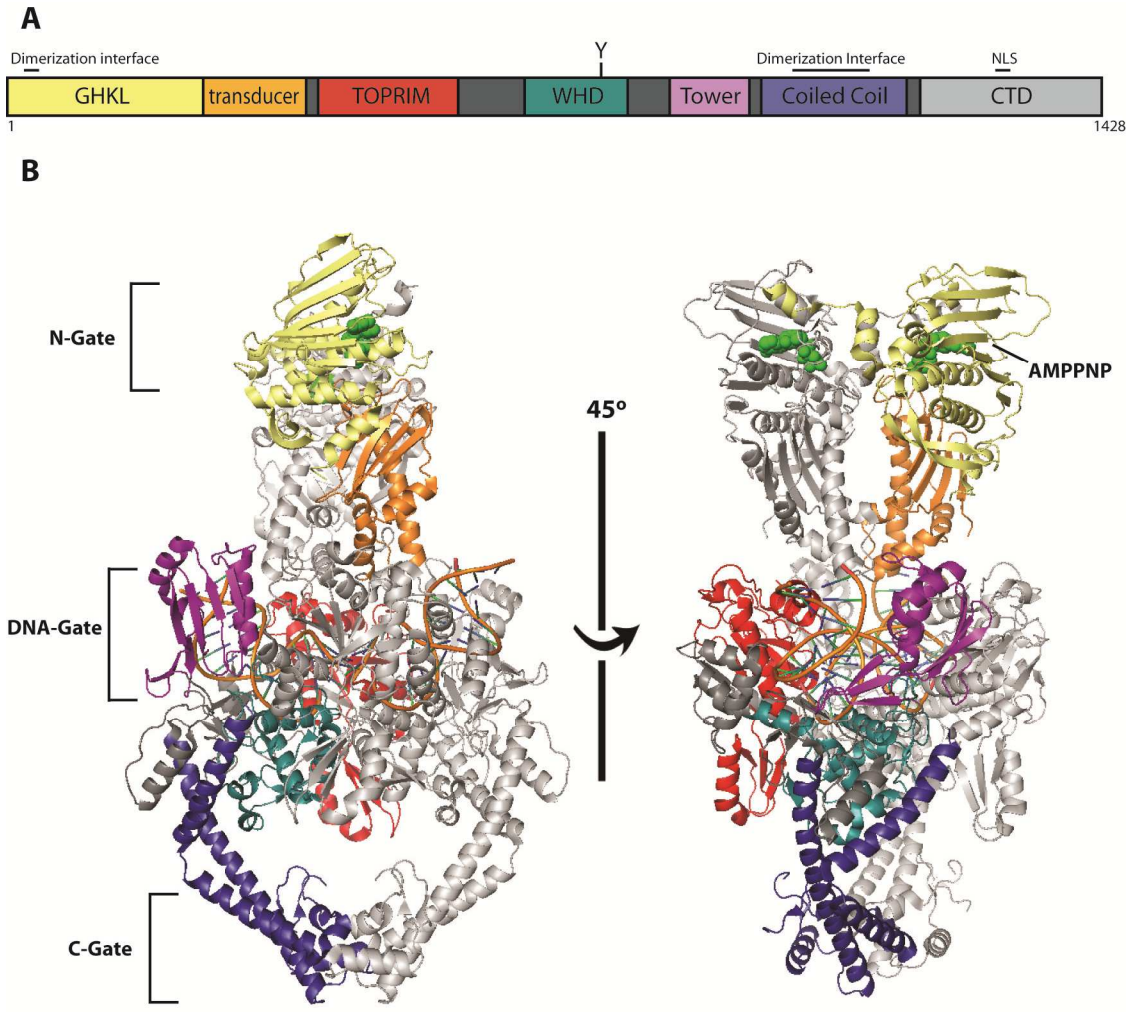

Figure 1: Organization and structure of eukaryotic Topoisomerase 2. A. Primary structure of Topoisomerase 2 from *Saccharomyces cerevisiae*. B. Structure of Topoisomerase 2 holoenzyme (aa 1-1177) from *Saccharomyces cerevisiae* (DPB ID 4GFH) (Schmidt et al., 2012). Domains are color-coded according to A. Closed N-gate is stabilized by the binding of non-hydrolyzable ATP analogs, AMPPNP. A crossover configuration is shown by the ATPase domain of one protomer, containing GHKL and transducer, resides on the top of the other protomer.

The ATPase domain consists of a GHKL fold which forms a major dimerization interface upon the binding of ATP, also termed N-gate, and a transducer domain which is believed to signal the conformational changes between ATPase and cleavage/religation domains (Bellon et al., 2004; Classen et al., 2003). In the cleavage/religation domain, the first two subdomains, TOPRIM and WHD, coordinate DNA cleavage with the assistance of divalent metal(s), resulting in covalently linkage of the 5′ phosphate at the break with the catalytic tyrosine in WHD (Schoeffler and Berger, 2008). Following the WHD is the tower domain and the coiled coil domain. This coiled coil domain at the C-terminus of cleavage/religation domain forms another major dimerization interface, also is commonly referred to as the C-gate (Schoeffler and Berger, 2008).

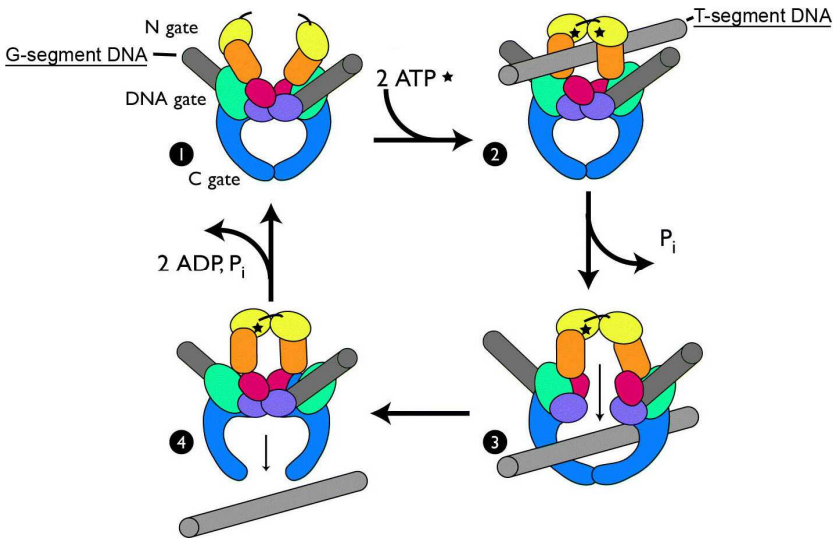

Figure 2: Individual steps in the catalytic cycle of eukaryotic Topoisomerase 2. Adapted from *Quarterly Reviews of Biophysics* (Schoeffler and Berger, 2008).

The catalytic reaction requires the coordination of the ATPase domain and cleavage/religation domains (**Figure 2**). Upon the binding of two ATP molecules, the N-terminal gate in ATPase domain is capable of trapping one DNA duplex (transport or T-segment) (Roca and Wang, 1992; Wigley et al., 1991). The hydrolysis of one ATP facilitates the T-segment to pass through a second segment of DNA (gate or G-segment) which has been cleaved and covalently linked to a catalytic tyrosine in each WHD domain of the dimeric enzyme (Baird et al., 1999; Harkins et al., 1998; Liu et al., 1983; Sander and Hsieh, 1983). The crossover configuration between ATPase domain and cleavage/religation domain prevents the T-segment from moving backward to guarantee a unidirectional movement of the T-segment (Schmidt et al., 2012). The G-segment is then religated and the T-segment can leave via the simultaneously opened C-terminal gate. After the second ATP is hydrolyzed and dissociates from ATPase domain, the enzyme is reset for another round of reaction (Baird et al., 1999; Harkins et al., 1998).

Contrary to the extensively studied structures and functions of conserved ATPase domain and core domain, the conformation of CTD in eukaryotic Top2 has not been determined. Although the CTD is not required for the DNA strand passing activity, it is, however, indispensable for the physiological function *in vivo*.

1.1.2 C-terminal Domain of Eukaryotic Topoisomerase 2

The Top2 CTD shares relatively low similarity between species and there is no well-conserved domain. However, the common features that eukaryotic Top2 CTDs have are nuclear localization signals and patches of positively-charged residues for DNA binding (Crenshaw and Hsieh, 1993; Mirski et al., 1997). A recent study of human Top2α indicated that independent from the DNA binding patches, a chromatin tethering sequence that resides at the C-terminal end of the CTD allows Top2 to form stable anchors to chromatin via interaction with DNA and histone 3 (Lane et al., 2013). In addition to subcellular localization, the CTD mediates a more complex regulation by protein-protein interactions and post-translational modifications, which fine-tunes the activity, half-life, and localization of eukaryotic Top2 for specific cellular events. The CTD also determines the isoform-specific functions (Vos et al., 2011). In vertebrates, there are two Top2 isoforms, Top2α and Top2β, which have distinct CTD sequences for different cellular functions. Top2α is essential for all cells and its function is required during DNA replication and DNA segregation. Top2β is important for transcription and the development of neural cells but is not required for the growth of most of cells (Nitiss, 2009a). Due to the essential role of Top2α in DNA replication, Top2 poisons, i.e. etoposide, doxorubicin, and mitoxantrone, have been clinically useful for cancer treatment. However, some cell types relying on the activity of Top2β would be severely

affected by Top2 poisons as well, for example, cardiotoxicity caused by doxorubicin (Lyu et al., 2007; Nitiss, 2009e). Exploring the structural differences of the two isoforms may help to develop isoform-selective drugs to prevent the unwanted side effects during chemotherapy.

1.1.3 Regulation of Eukaryotic Topoisomerase 2 via Post-translational Modifications and Protein-protein Interactions

To understand the mechanism, Top2 has been mostly examined *in vitro* as a single enzyme catalyzing supercoiled, knotted, or catenated DNA substrates. However, to understand the role of Top2 *in vivo*, the communications between the enzyme and the surrounding environment must be understood. Thus, many studies have addressed protein regulation of eukaryotic Top2, including effects of post-translational modifications and protein-protein interactions.

One post-translational modification, phosphorylation, was first found in the early studies of *Drosophila* Top2. The enzyme was discovered to be effectively phosphorylated by protein kinase C (PKC) *in vitro* and the phosphorylation of Top2 enhances the rate of DNA relaxation (Sander et al., 1984). *Drosophila* Top2 was also found to be phosphorylated at multiple sites by casein kinase II (CK2) *in vitro* (Ackerman et al., 1985). Similar activity stimulation by CK2 was also found in yeast Top2 and human Top2α (Cardenas et al., 1993; Chikamori et al., 2003).

In more recent studies, human Top2α has been found to be phosphorylated by p38γ mitogen-activated protein kinase (p38γ), Aurora B kinase, polo-like kinase 1 (Plk1), and polo-like kinase 3 (Plk3) (Iida et al., 2008; Li et al., 2008; Morrison et al., 2002; Qi et al., 2011). Similar to the effect of phosphorylation by CK2 and PKC, phosphorylation by Plk1 or p38γ enhances catalytic activity of human Top2α. Increasing the phosphorylation level by CK2, p38γ has been shown to sensitize human Top2α to Top2-targeting anticancer drugs, which could indicate a potential mechanism for resistance of cancer cells (Chikamori et al., 2003; DeVore et al., 1992; Qi et al., 2011).

One of the serines located at the very end of human Top2α, serine1524, happened to be a common target for CK2, Plk1, and p38γ (Li et al., 2008; Qi et al., 2011; Wells et al., 1994). Not only does the phosphorylation of serine1524 affect directly the activity and stability of the enzyme, but also plays a role in mediating protein-protein interaction. Phosphorylation of human Top2α Ser1524 is required for the binding of C-terminal BRCT domain of Mdc1 (Mediator of DNA damage checkpoint 1). Using siRNA to knock down endogenous Top2α in HT1080 cells, treatment with the Top2 inhibitor, ICRF-193, causes mitotic arrest in cells ectopically expressing wildtype Top2α but not in cells expressing Top2αS1524A, indicating the Mdc1-Top2α interaction serves an important role in activating the decatenation checkpoint (Luo et al., 2009).

Another important post-translational modification is the conjugation of the small ubiquitin-like modifier, SUMO. In yeast, mutations of lysines for SUMO conjugation and deletion of E3 ligases, SIZ1 and SIZ2, result in loss of Top2 SUMOylation and a chromosome segregation defect (Bachant et al., 2002; Takahashi et al., 2006). Mediated through an E3 ligase, PIASy, SUMOylation of *Xenopus* Top2α has also been found to be critical for proper chromosome segregation (Azuma et al., 2005). Similar conclusions were drawn from Hela cell studies with PIASy knockdown, supporting the idea that SUMOylation on the CTD of eukaryotic Top2 is required for the localization of Top2 and its decatenation function at the centromere (Agostinho et al., 2008). Although most of the studies showed SUMOylation conjugates on conserved ψ-K-X-E/D motifs (ψ :hydrophobic residue) of the CTD of eukaryotic Top2, one recent study showed Lys660 of *Xenopus* Top2α can be SUMOylated as well (Johnson and Blobel, 1999; Ryu et al., 2010; Sampson et al., 2001). The SUMO moiety is not only conjugated on a motif different from any other SUMOylations on CTD, but the function of Lys660 SUMOylation is also surprisingly different. Instead of functioning as a signal for localization at the centromere, SUMOylation on Lys660 inhibits *Xenopus* Top2α decatenation activity. Furthermore, the structurally hidden Lys660 would only become accessible for SUMOylation in the presence of DNA, suggesting the enzyme activity is modified when bound to DNA *in vivo*. It was proposed that this inhibition is temporally

required for preventing overly active *Xenopus* Top2α from recatenating nearby centromere DNA during metaphase, with the enzyme becoming active to finalize the segregation of DNA at anaphase upon the removal of SUMOylation (Ryu et al., 2010).

Some regulation of eukaryotic Top2 is mediated by protein-protein interaction. PCNA and HMGB1 (High-mobility group protein box-1) are two proteins that have been found to bind Top2 directly *in vitro* (Niimi et al., 2001; Stros et al., 2007). Using chicken embryonic fibroblast cells, Top2α, but not Top2β, co-localizes with sites of DNA replication. The minimal requirement of the sequence for co-localization with DNA replication sites was narrowed down to amino acids 1280-1294 of chicken Top2α. Comparing the α and β isoforms, this short chicken Top2α sequence (aa 1280-1294) is conserved only in Top2α between chicken, mouse and human. Moreover, this sequence and other PCNA binding proteins all share a common motif which is a QTxhxF motif (x: any residue; h: hydrophobic residue) immediately followed by a KR-rich sequence (Montecucco et al., 1998; Niimi et al., 2001; Warbrick, 1998). The direct binding between PCNA and a fragment of chicken Top2α (aa 1158-1294) was validated by *in vitro* pull-down assay (Niimi et al., 2001). Although Top2α-PCNA interaction was not further examined *in vivo*, this interaction could explain how Top2 solves DNA topological problems associated with the DNA replication machinery.

HMGB1 was originally found to bind distorted DNA and promote the ligase-mediated intramolecular association of DNA (Sheflin and Spaulding, 1989; Stros et al., 2000; Stros et al., 1994; Thomas and Travers, 2001). After confirming the direct interaction between purified human Top2α and HMGB1 by pull-down experiment, catenation, decatenation, and relaxation activities of human Top2α were all found to be stimulated by HMGB1. In a series of *in vitro* assays, two critical steps in Top2 catalytic cycle, DNA binding and DNA cleavage, were found enhanced by the binding of HMGB1 (Stros et al., 2007).

The interaction between human Top2α and BAF complexes is another example of how Top2α is modulated on segregating replicated sister chromatids (Dykhuizen et al., 2013). BAF (BRG1 associated factors) complexes are ATP-dependent chromatin-remodeling complexes. In addition to its ability to alter the position of nucleosomes along the DNA, the complexes have been shown to be tumor suppressors (Imbalzano et al., 1994). Mutations in BRG1, one subunit of BAF complexes, are responsible for some cases of medulloblastoma and Burkitt's lymphoma (Jones et al., 2012; Love et al., 2012; Parsons et al., 2011; Pugh et al., 2012; Richter et al., 2012; Robinson et al., 2012). Evidence provided by a recent study has shown that BRG1 mutations reduce the chromatin binding of human Top2α over certain regions, resulting in an increase of anaphase bridge formation and decatenation defects. The defect resembles the phenotype of loss

of human Top2α. Human Top2α was later discovered to associate with BAF complexes through the BAF250a subunit. Although the BRG1 subunit is not a direct human Top2α binding partner, it was suggested that human Top2α has a specific role at certain chromatin loci mediated through BAF complexes (Dykhuizen et al., 2013).

1.2 TopBP1 and Homologs

Human TopBP1, topoisomerase IIβ binding protein 1, is a scaffold protein mediating signals for cellular events by recruiting different protein partners through its tandem BRCT domains. It was first discovered in a yeast two-hybrid system using the C-terminus of human Top2β as a bait to screen a HeLa cDNA library (Yamane et al., 1997). However, the interaction between Top2β and TopBP1 was found to be weak *in vitro*, and the biological role of TopBP1 binding to Top2β has never been elucidated. Based on recent studies, TopBP1 has been shown to be an initiating factor in DNA replication and the activator of the ATR kinase in DNA damage signaling (Pospiech et al., 2010; Wardlaw et al., 2014).

The roles of TopBP1 in DNA replication and DNA damage signaling were initially shown by its homologs in other species. Homologs of TopBP1 include Xmus101/Xcut5 in *Xenopus*, Mus101 in *Drosophila*, Mus101/Rad4 in *C. elegans*, Dpb11 in *Saccharomyces cerevisiae*, and Cut5/Rad4 in *Schizosaccharomyces pombe* (Garcia et al., 2005; Makiniemi et al., 2001). Although different in size, these homologs all contain 4 to 9

BRCT domains (4 in yeast Rad4/Cut5 and Dpb11, 6 in *C. elegans* Mus101/Rad4, 7 in *Drosophila* Mus101, 8 in *Xenopus* Xmus101/Xcut5, and 9 in human TopBP1) (Garcia et al., 2005; Rappas et al., 2011). Most of the BRCT domains function in pairs and some BRCT domains have a critical lysine residue in the pocket that binds phosphorylated proteins (Rappas et al., 2011). Based on the sequence homology, BRCT1/2 and BRCT3/4 of Dpb11 are conserved as BRCT1/2 and BRCT4/5 of Mus101/Xmus101/ TopBP1, (Garcia et al., 2005).

1.2.1 TopBP1 in DNA Replication

TopBP1 and its homologs have essential roles in DNA replication. The protein function in DNA replication was first shown in yeast. Dpb11 (Dpb, DNA polymerase ε subunit B) was found to be required for cell viability in yeast genetic studies. Recent studies further confirmed that Dpb11 is the crucial component for assembling the DNA replication pre-initiation complex, pre-IC, by interacting with phosphorylated Sld2 and Sld3 (Araki et al., 1995; Zegerman and Diffley, 2007).

The main goal of assembling pre-IC is to bring DNA polymerase ε to a replication origin that has been loaded with the replicative helicase, MCM, in late M phase. In the early stage of G1 phase, Sld3 and Cdc45 are first recruited to the pre-replication complex (pre-RC), which is composed of the MCM 2-7 complex, Cdc6, and Cdt1 (Labib, 2010; Pospiech et al., 2010). During S phase, Sld2 is phosphorylated by S-

CDK at Thr84 which allows Sld2 to interact with BRCT3/4 of Dpb11 (Masumoto et al., 2002; Tak et al., 2006). With the assistance of the GINS complex, Sld2, Dpb11, and polε are brought together to form the pre-loading complex, pre-LC (Araki, 2011). In S phase, S-CDK also phosphorylates Sld3 at Thr600 and Ser622 for binding to BRCT1/2 of Dpb11 (Tanaka et al., 2007; Zegerman and Diffley, 2007). With the polε-containing pre-LC docking onto MCM-containing pre-RC via Dpb11-Sld2-Sld3 interaction, the pre-IC is completed and ready for DNA replication. After DNA replication begins, Dpb11, Sld2, and Sld3 dissociate from the complex (Bruck and Kaplan, 2011; Masumoto et al., 2002).

The function of Dpb11 in replication is conserved in other eukaryotes. Two *Drosophila* mutations, mus101^{SM}, and mus101^{K451}, show defects related to DNA replication (Yamamoto et al., 2000). mus101^{SM} is a null allele, which has a frameshift mutation in BRCT2 of Mus101 (Kondo and Perrimon, 2011). Homozygous null mus101^{SM} mutants are lethal at the early larval stages due to loss of cell proliferation in imaginal discs (Yamamoto et al., 2000). mus101^{K451} has a missense mutation, leading to a substitution of valine675 with aspartate (Kondo and Perrimon, 2011). Based on sequence alignment and the information from the crystal structure of BRCT4/5 of human TopBP1, Val675 is in the middle of a β-sheet and mutation from valine to aspartate may cause a misfolding in BRCT4 and prevent substrate binding (Leung et al., 2013).

In genetic tests, flies carrying a homozygous mus101^{K451} mutant show impaired eggshell formation due to defective amplification of the chorion gene, which is related to origin dependent and locus specific DNA replication (Yamamoto et al., 2000). The relationship between TopBP1 and replication was further elucidated in experiments with Mus101-depleted *Xenopus* egg extracts which showed Mus101 is required for the loading of Cdc45 for the initiation of replication (Hashimoto and Takisawa, 2003; Van Hatten et al., 2002). Coincidently, upon siRNA knockdown of human TopBP1, U2OS cells were observed to arrest at G1/S transition implying a defect in assembling pre-replication complexes (Jeon et al., 2007).

The discovery of the functional homolog of Sld3 in human and *Xenopus*, Treslin/Ticcr, also helps to confirm the conservation of Dpb11/Mus101/TopBP1 function in DNA replication (Boos et al., 2011; Kumagai et al., 2010). The rate of the chromosomal DNA replication from Treslin-depleted *Xenopus* egg extracts is greatly reduced, and in the human system, an S-phase arrest was also observed in Treslin-silenced U2OS cells, suggesting Treslin is required for replication (Kumagai et al., 2010). Like Sld3, Treslin was found to bind BRCT1/2 of TopBP1 in a doubly phosphorylation dependent manner. The CDK-2/cyclin E phosphorylation sites on human Treslin were identified to be Thr969 and Ser1001, and substitutions of alanine for these two residues were unable to rescue the S-phase arrest in Treslin-depleted HeLa-Kyoto cells (Boos et al., 2011).

Demonstrated by studies of Dpb11/Mus101/TopBP1 mutants and their binding partners, TopBP1 and its homologs have a conserved, critical function in DNA replication.

1.2.2 TopBP1 in DNA Damage Signaling

The relevance of TopBP1 in DNA damage signaling was revealed in genetic studies by its homologs, *Drosophila* Mus101 and *C. elegans* Rad4. In 1976, a series of mutants were isolated in *Drosophila* that are sensitive to methyl methanesulfonate (MMS). Six genes on the X-chromosome characterized in this study were designated MUS101 to MUS106 (MUS, mutagen sensitive). In addition to MMS, a $mus101^{D1}$ mutant is also hypersensitive to nitrogen mustard and γ-radiation (Boyd et al., 1976). Similarly, in 1982, mutation in rad4 of *C. elegans* was found to confer hypersensitivity to γ-radiation and MMS (Hartman and Herman, 1982). Due to the sensitivity to multiple DNA damaging agents in these mutants, *Drosophila* Mus101 and *C. elegans* Rad4 were individually considered to be involved in DNA repair. The role of TopBP1 in DNA damage signaling was not understood until recent studies.

The co-localization of TopBP1 and BRCA1 in response to DNA damage first suggested a role of TopBP1 in DNA damage signaling (Makiniemi et al., 2001). This signaling was subsequently found to be mediated through interaction with Rad9 and ATR kinase (Choi et al., 2007; Delacroix et al., 2007; Kumagai et al., 2006). Rad9 is a component of a 9-1-1 complex (Rad9, Rad1, and Hus1) which forms PCNA-like ring

structure and functions as a DNA clamp during DNA damage signaling (Sohn and Cho, 2009). When DNA damage occurs, the single strand DNA binding protein, RPA, first protects the single strand region formed after DNA damage. The ATR-ATRIP complex and 9-1-1 complex are then recruited to the vicinity of the DNA damage labeled by RPA (Sokka et al., 2010). Through the interaction between BRCT1/2 of TopBP1 and phosphorylated Rad9 (by casein kinase 2 at S341 and S387), TopBP1 is recruited to the site of DNA damage (Rappas et al., 2011; Takeishi et al., 2010). Recruitment of ATR-ATRIP by RPA promotes the autophosphorylation of ATR kinase in *trans* at T1989 which then interacts with BRCT7/8 of TopBP1 (Liu et al., 2011). Following the binding to TopBP1, the activity of ATR kinase is greatly enhanced by a region between BRCT6 and BRCT7 of TopBP1 called the ATR-activation domain (AAD). ATR kinase phosphorylates Chk1, which in turn activates downstream responses (e.g., prevention of origin firing and stabilization of stalled replication folks) (Choi et al., 2007; Choi et al., 2009; Kumagai et al., 2006).

TopBP1 can also be recruited to the DNA damage site in a Rad9-independent manner. Demonstrated in *Xenopus* egg extracts, the Mre11-Rad50-Nbs1 (MRN) complex interacts with BRCT3/4/5 and recruits Xmus101 to single-stranded/double-stranded DNA junctions (Duursma et al., 2013). Besides the MRN complex, in human U2OS cells,

phosphorylated Mdc1 also helps TopBP1 localize at stalled DNA replication forks via the binding of BRCT-5 of TopBP1 (Leung et al., 2013; Wang et al., 2011).

1.2.3 Other Functions of TopBP1

Recent studies also showed TopBP1 is involved in regulation of transcription. TopBP1 binds directly to transcription factors and co-regulators, including E2F-1, Miz1, and SPBP, to enhance or repress their transcriptional activities. The binding of TopBP1 to these transcription factors requires Akt-mediated TopBP1 oligomerization. TopBP1 is first phosphorylated by Akt at S1159, and then oligomerized through BRCT7/8. TopBP1 binding to these proteins has similar outcomes, which are repression of apoptosis and promotion of proliferation, suggesting that TopBP1 may serve as a general modulator to balance cellular stress responses (Herold et al., 2008; Liu et al., 2013; Liu et al., 2006; Sjottem et al., 2007).

There is evidence showing TopBP1 participates in mitosis as well. Flies carrying mus101^{lcd} allele die at the late third instar larval stage. The metaphase chromosomes in neuroblasts of these larva appear to be undercondensed or broken (Yamamoto et al., 2000). The authors suggested that *Drosophila* Top2, which is required for DNA compaction, may be recruited by Mus101 to promote chromatin condensation (Yamamoto et al., 2000). On the other hand, in later stages of the mitosis, chicken TopBP1 and yeast Dpb11 were found localized to anaphase bridges, including both

ultrafine DNA bridges and chromatin bridges. The depletion of TopBP1 causes accumulation of the chromatin bridges in chicken DT40 cells. Because chromatin bridges represents sites of topological problems, TopBP1 was assumed to collaborate with Top2 or the BLM-Top3 complex to resolve topological problems and ensure DNA segregation (Germann et al., 2014).

1.3 Chapter Preface

Many X-ray crystal structures have been solved to study eukaryotic Top2. However, the static conformations may not provide sufficient mechanistic information due to complex dynamics involved in changing states. In the first part of our work in chapter 2, we developed a new probing method involving pulse-alkylation mass spectrometry with monobromobimane (mBrB) to study the protein dynamics of human Top2α. We also used this method to successfully locate the position of the CTD of human Top2α.

Chapter 3 describes regulatory interactions of the CTD of eukaryotic Top2. Using the *Drosophila* system, we have addressed the significance of the Top2β-TopBP1 interaction, including the binding mechanism and the biological functions. Using co-immunoprecipitation and pull-down assays, we mapped the binding interfaces of Top2 and Mus101. After identifying the key Top2 residues for the interaction, mutant Top2 was generated to abolish the binding of Mus101. Using the mutant Top2, we were able

to determine the function of the Top2-Mus101 interaction by 1) *in vitro* functional assay; 2) cellular assays; 3) fly genetics.

2. Probing Topoisomerase II Conformational Changes and Position of Dynamic C-terminal Domain by Pulse-Alkylation Mass Spectrometry

The research presented in this chapter was originally published in the Journal of Biological Chemistry. Chen, Y.-t., Collins, T.R., Guan Z., Chen V. B., Hsieh T.-s. "Probing Conformational Changes in Human DNA Topoisomerase IIα by Pulsed Alkylation Mass Spectrometry" *J Biol Chem*. 2012, 287, 25660–25668.

2.1 Introduction

Eukaryotic Top2 proteins have a two-fold symmetrical architecture. A key step in the catalytic cycle of the enzyme reaction is to pass a DNA segment through a transient double strand break. In such a strand passage step, a segment of DNA is cleaved to create a staggered double strand break with 4-nucleotide protrusion at 5′ ends. Each 5′ end of the DNA break is covalently linked to a catalytic tyrosine to form a transient DNA gate which will be religated after the passage of the transit DNA segment (Liu et al., 1983; Morrison and Cozzarelli, 1979; Sander and Hsieh, 1983). By repeating the cycle of this reaction, Eukaryotic Top2 is capable of reducing/introducing supercoils, decatenating/catenating DNA or knotting/unknotting DNA.

Due to the sophisticated coordination between individual subdomains in eukaryotic Top2, we are interested in developing methods to monitor the dynamic nature of the enzyme during the catalytic cycles. Chemical protein footprinting

methodologies have been previously used to detect protein conformational changes. Some studies utilized chemical reagents to selectively label the ε-amine group of lysine (Hanai and Wang, 1994; Li and Wang, 1997), the guanidino group of the arginine (Atassi et al., 1972; Wood et al., 1998) or the thiol group of cysteine (Apuy et al., 2001; Habeeb et al., 1972; Kim et al., 2004; Tu and Wang, 1999). Labeled proteins were then cleaved and separated by gel electrophoresis, followed by the examination of pattern changes between different conformations (Atassi et al., 1972; Habeeb et al., 1972; Hanai and Wang, 1994; Li and Wang, 1997; Tu and Wang, 1999). More recent works combined protein modification with mass spectrometry to study protein dynamics and conformational change at a higher resolution (Apuy et al., 2001; Carven and Stern, 2005; Kim et al., 2004; Wood et al., 1998). For instance, Apuy *et al.* used pulse-alkylation of cysteines followed by mass spectrometry to study the folding/unfolding of luciferase (Apuy et al., 2001). Kim *et al.* also developed mass spectrometric measurement of differential cysteine modification to probe conformational changes of tubulin (Kim et al., 2004). In this study, we used pulse-alkylation of cysteines followed by analysis with mass spectrometry to examine the protein dynamics of human Top2α (*hs*Top2α). We first determined that the reactivities of all 13 cysteines in *hs*Top2α are highly correlated with the accessibilities predicted from a structural model of *hs*Top2α. Based on such information, we detected conformational changes in the presence of cofactors and the

Top2 inhibitor, ICRF-193, and a possible positioning of the CTD domain with respect to the linker region between ATPase and cleavage/religation domains.

2.2 Results

The study of the dynamics of high molecular weight proteins with flexible regions such as *hs*Top2α is challenging. In an effort to monitor the conformational changes of *hs*Top2α, specific labeling of side chains of amino acids offers an opportunity to capture the movement of the protein. This approach depends on labeling amino acids that have reactive side chains, such as the nucleophilic thiol of cysteine. Because *hs*Top2α has 13 cysteines in each monomer of the homodimer evenly distributed throughout different domains, we applied pulse-alkylation combined with mass spectrometric analysis on *hs*Top2α to study the dynamics of *hs*Top2α in response to cofactors and inhibitors. In the schematic shown in **Figure 3**, cysteine-specific labeling reagents combined with LC-ESI-MS were utilized in this study.

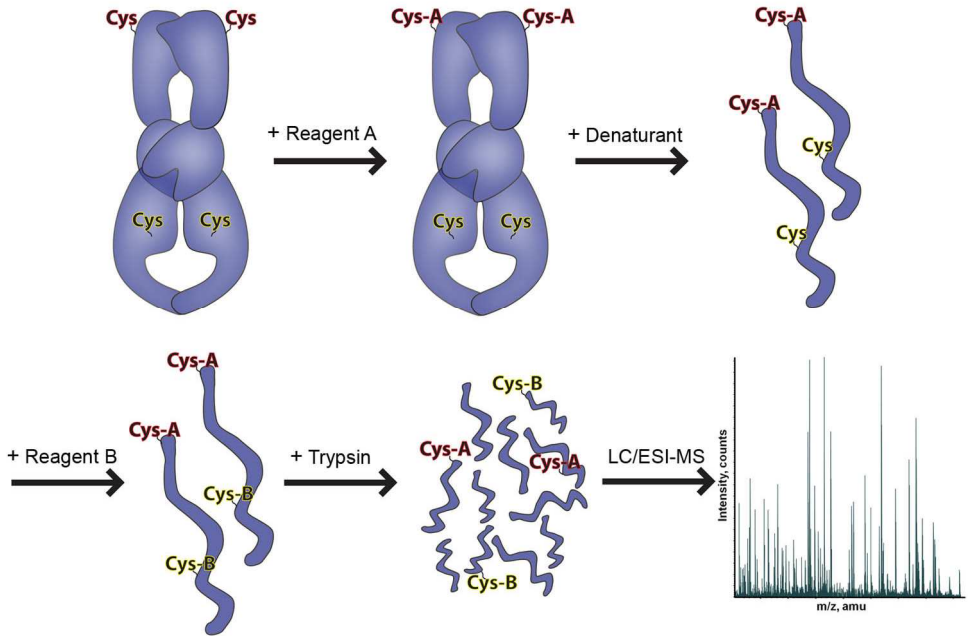

Figure 3: Schematic of cysteine footprinting using LC/ESI-MS. *hs*Top2α was first treated with a thiol alkylator (reagent A, D6-mBrB), which reacts with solvent-accessible cysteines. Upon denaturation, less solvent-accessible cysteines reacted with excess amount of a second thiol alkylator (reagent B, H6-mBrB). The protein was next digested with trypsin, and peptide fragments were analyzed with liquid chromatography/electrospray ionization-mass spectrometry (LC/ESI-MS).

2.2.1 Labeling Reagents and Calibration Curve

Two alkylation reagents, iodoacetamide (IAM) and monobromobimane (mBrB), were tested in our experiments to label cysteines. While they both gave qualitatively similar results, we found mBrB is a better reagent to distinguish between buried and exposed cysteines because it is sufficiently bulky to selectively label only surface cysteines within a given time. We also took advantage of its six non-exchangeable hydrogens to synthesize a deuterated derivative (D_6-mBrB). This pair of labeling

reagents should have similar chemical properties, equal labeling efficiency, but distinguishable m/z signals, allowing us to perform a quantitative measurement by LC-MS. Thus, the results in this study are mainly shown with mBrB.

We first examined whether cysteine-containing peptides modified with either mBrB or D_6-mBrB could be detected by the LC-MS and whether the intensities of the peptide signals were linearly proportional to their concentrations. After trypsin digestion, we were able to detect all cysteine-containing peptides by LC-MS (**Table 1**). Eleven of the thirteen cysteines are located in different peptides, and only a pair of cysteines (Cys997, 1008) is in the same peptide. As cysteines are completely labeled with either mBrB or D_6-mBrB and mixed in various ratios, the signals of the cysteine-modified peptides can be easily tracked and quantified by the integrated area of the mono-isotopic peaks (Cys170 is shown as an example in **Figure 4A**). The percentage of a fragment modified by D_6-mBrB or the reactivity of a cysteine obtained from pulse-alkylation experiments is determined by dividing the signal from the D_6-mBrB labeled peptides by the total signal from the peptides labeled by both reagents.

Reactivity = D_6-mBrB / (D_6-mBrB + H_6-mBrB)

When the experimental ratios are plotted against the theoretical ratios (pre-determined mixing ratios), calibration curves can be obtained (**Figure 4B**). The linearity of the calibration curves reveals that the ratios of the intensities closely reflect their

relative concentrations. Because the ion abundance of peptides labeled with either light or heavy mBrB was nearly equivalent, we can use these reagents to quantitatively measure the degree of reactivity of cysteines in *hs*Top2α in response to ligand binding.

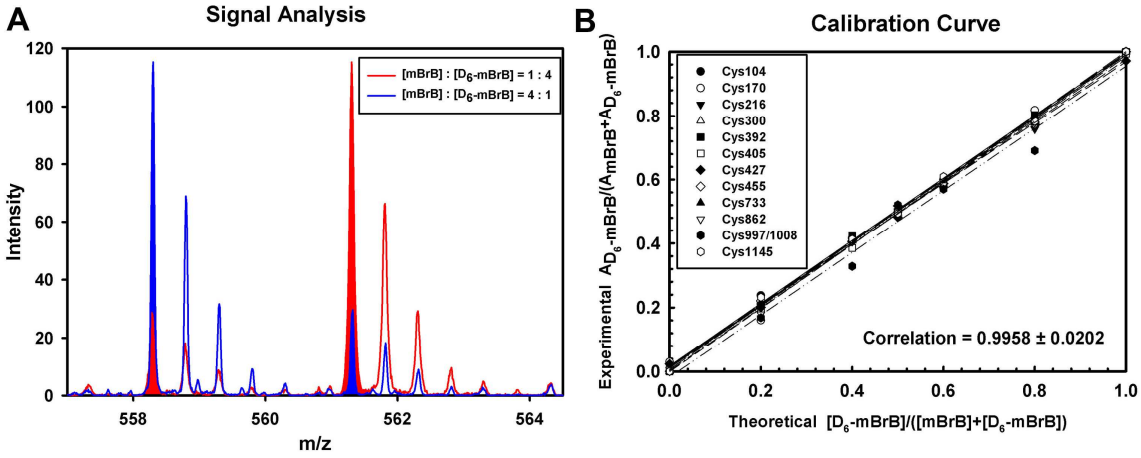

Figure 4: Correlation between the ratio of the calculated peak area and the pre-determined concentration ratio of the mixtures of D_6- and H_6-mBrB modified tryptic peptides. A. The signals of the Cys170 containing peptide are quantified by measuring the integrated area of the highest m/z peaks (symbolized by filling with red or blue color). The ratios of the peak area integration, 3.7:1(in blue) and 1:3.8 (in red), agree with the ratios of the pre-determined concentration, 4:1 and 1:4 respectively. B. The overall correlation of all cysteines between concentration ratio and the peak area integration ratio.

Table 1: Amino Acid Sequences and Masses of H_6-mBrB or D_6mBrB-Labeled Tryptic Peptides of *hs*Top2α

Cysteinyl Residue	Amino Acid Sequence of Human Topoisomerase IIα	Obs. Mass for H_6-mBrB Adduction (m/z)	Calc. Mass for H_6-mBrB Adduction (m/z)	Obs. Mass for D_6-mBrB Adduction (m/z)	Calc. Mass for D_6-mBrB Adduction (m/z)
Cys104	MSCIR (102-106) $[M+2H]^{2+}$	400.183	400.179	403.203	403.198
Cys170	LCNIFSTK (169-176) $[M+2H]^{2+}$	558.276	558.278	561.299	561.297
Cys216	AGEMELKPFNGEDYTCITFQPDLSK (201-225) $[M+3H]^{3+}$	1008.451	1008.460	1010.458	1010.473
Cys300	WEVCLTMSEK (297-306) $[M+2H]^{2+}$	708.314	708.317	711.333	711.336
Cys392	SFGSTCQLSEK (387-397) $[M+2H]^{2+}$	688.805	688.808	691.825	691.826
Cys405	AAIGCGIVESILNWVK (401-416) $[M+2H]^{2+}$	931.983	931.992	935.003	935.010
Cys427	CSAVK (427-431) $[M+H]^{+}$	697.321	697.334	703.364	703.371
Cys455	NSTECTLILTEGDSAK (451-466) $[M+2H]^{2+}$	936.426	936.435	939.437	939.453
Cys733	VLFTCFK (729-735) $[M+2H]^{2+}$	524.269	524.267	526.272	527.285
Cys862	VEPEWYIPIIPMVLINGAEGIGTGWSCK (836-863) $[M+3H]^{3+}$	1088.197	1088.210	1090.204	1090.223
Cys997/1008	LQTSLTCNSMVLFDHVGCLK (991-1010) $[M+3H]^{3+}$	863.739	863.743	867.723	867.768
Cys1145	DELCR (1142-1146) $[M+H]^{+}$	825.345	825.356	831.375	831.394

2.2.2 Reactivities of Cysteines in human Top2α

In order to correctly evaluate the correlation between cysteine labeling reactivity and the solvent accessibility, DNA unknotting activity of the pulse-labeled protein was measured to confirm the enzyme was not over-labeled and denatured. Compared with the unlabeled *hs*Top2α, labeled proteins retained 30% of the unknotting activity indicating the condition we used should be valid for evaluating solvent accessibility (**Figure 5**).

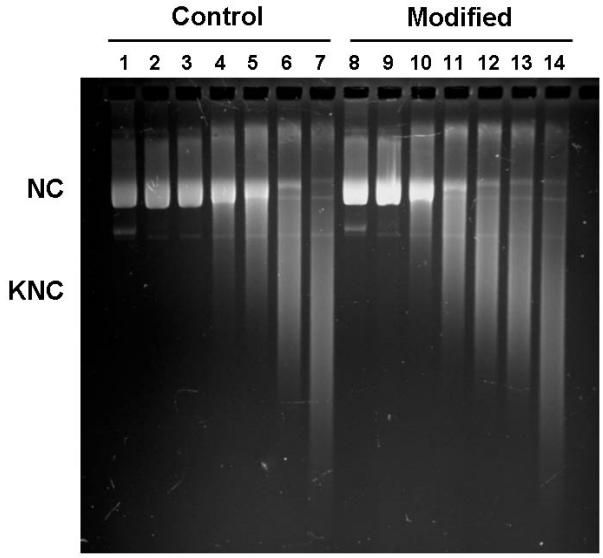

Figure 5: The unknotting activity of *hs*Top2α with or without labeling. *hs*Top2α was treated with either 0.5 mM D6-mBrB or DMSO for 1 min before the unknotting reaction. The unknotting activity of the labeled *hs*Top2α was not completely abolished upon cysteine-labeling but reduced to 30% of the activity in mock-unlabeled proteins (NC: nicked circle; KNC: knotted nicked circle).

After pulse-alkylation mass spectrometric analysis of *hs*Top2α in the absence of Mg^{2+} and ATP, the 13 cysteines can be separated into three categories based on reactivity

with D_6-mBrB (**Figure 6A**). (1) High reactivity (> 10%): Cys104, Cys216, Cys427, and Cys1145; (2) Medium reactivity (2% ~ 10%): Cys170, Cys300, Cys392, and Cys405; (3) Low reactivity (< 2%): Cys455, Cys733, Cys862, and Cys997-1008. The reactivity experiment was also conducted with IAM and its deuterated derivative (D_2-IAM) and both results distinguish these cysteines in similar manner (**Figure 7**).

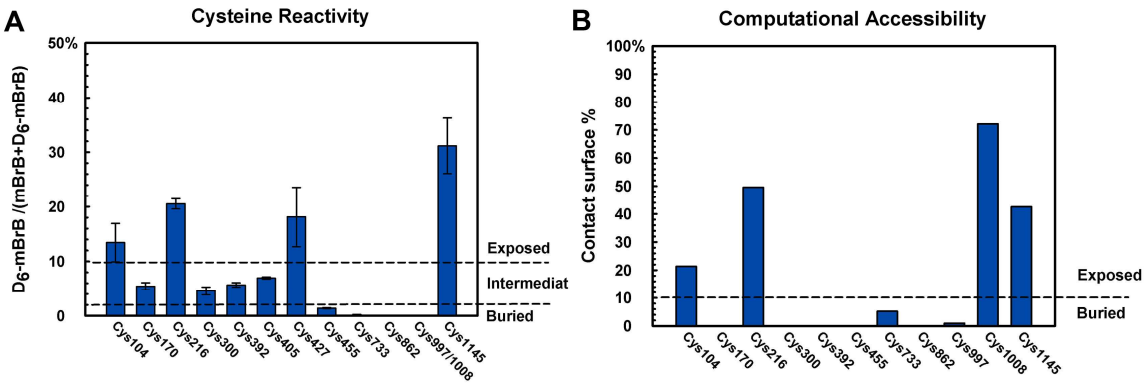

Figure 6: The result of the reactivities of cysteines in *hs*Top2α. A. Using pulse-alkylation with MS analysis, 13 cysteines can be separated into three categories based on reactivity with D6-mBrB. 1) High reactivity (> 10%); 2) Medium reactivity (2% ~ 10%); 3) Low reactivity (< 2%). B. Based on the information from the homology model, the accessibilities of all cysteines are predicted by Probe software. The cysteines can be categorized as exposed (> 10%) or buried (< 10%).

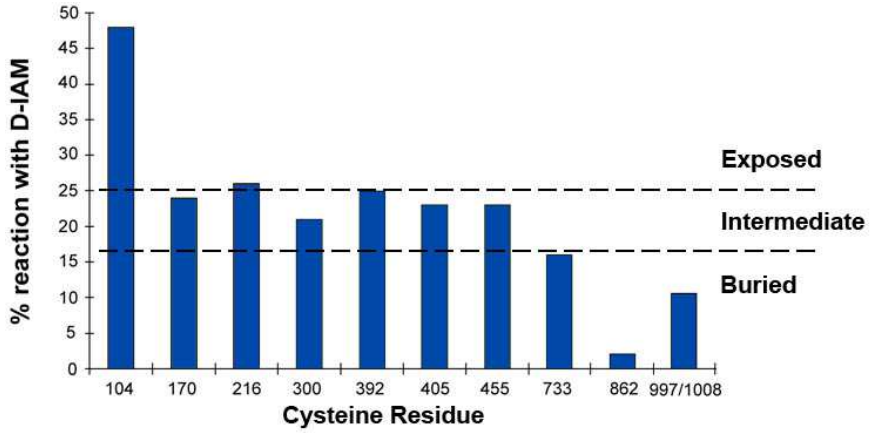

Figure 7: The reactivities of cysteines in *hs*Top2α probed by D_2-IAM/IAM pair. *hs*Top2α was first pulsed with D2-IAM before being denatured and treated with excess amount of IAM. Three classes of thiols result were determined, exposed (> 25%), intermediate (16~25%), and buried (< 16%)

To investigate if the reactivity of each cysteine is related to its solvent accessibility, we constructed a human Top2*α* homology model from the partial structures of yeast Top2 and human Top2*α*, and compared our experimental result with the predicted cysteine accessibilities analyzed by Probe software (Word et al., 1999). By using a water molecule as a probe to scan around the thiol groups of cysteines in *hs*Top2α homology model, contact dots representing the level of solvent accessibility can be generated. Counting the contact dots of each cysteine allows us to differentiate two groups of cysteines, exposed and buried (**Figure 8B, C**). The cysteines that are detected with intermediate reactivity might be caused by the "breathing" of the enzyme and thus cannot be distinguished from static structures. The comparison showed that the reactivity of each cysteine approximately agrees with the solvent accessibility predicted

from the homology model with the exception of Cys997-1008 (**Figure 6B**). The accessibility of Cys405 and Cys427 are excluded in our results because Cys427 is absent in *hs*Top2α crystal structures and Cys405, which is located at the interface of two docked structures (see materials and methods), may not accurately reflect its accessibility in the holoenzyme (**Figure 8A**).

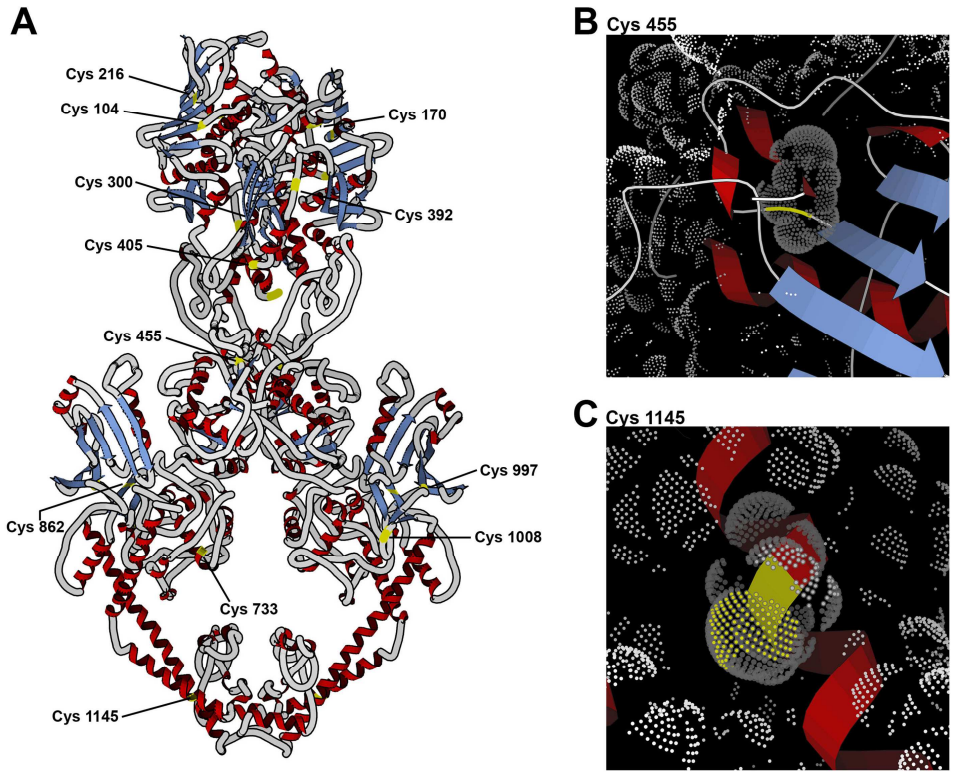

Figure 8: Surface of cysteines and homology model of *hs*Top2α. A. Ribbon diagram of our combined model of *hs*Top2α. The location of each cysteine is highlighted in yellow color. B, C. Dot surface of cysteines were calculated by Probe all-atom contact analysis software. The number of yellow dots represents the exposed area of a sulfhydryl group. While buried cysteines have few or no yellow dots (for example, Cys455, B), solvent-exposed cysteines show a cluster of yellow dots (for example, Cys1145, C).

It is notable that Cys427 is highly reactive suggesting that the linker region between the transducer and TOPRIM subdomains is very much exposed to solvent. The other three highly reactive cysteines, Cys1145, Cys104, and Cys216, are predicted as exposed cysteines and can be easily found to have a massive patch of surface contacts in the homology model (**Figure 8C**). Compared to Cys104 and Cys216 in the same GHKL subdomain, Cys170 has moderate reactivity with D_6-mBrB because it is partially shielded from the solvent by a β-sheet near the ATP binding site. A second part of the ATP gate, the transducer subdomain, contains three cysteines (Cys300, Cys392, and Cys405) with intermediate reactivities. The thiol groups of these three cysteines are also partially shielded by different parts of secondary structures. These cysteines in the GHKL and transducer subdomains are in a prime location to exhibit reactivity changes upon cofactor-induced conformational changes in *hs*Top2α, while five of the least reactive cysteines (Cys455, Cys733, Cys862, and Cys997-1008) are potential candidates to monitor larger conformational dynamics in TOPRIM, WHD, and Tower subdomains. Based on the homology model, the positions of Cys455, Cys733, and Cys862 in *hs*Top2α are predicted to be covered inside rigid secondary structures preventing the labeling by D_6-mBrB. Nevertheless, the reactivity of Cys997-1008 is the only result that is not consistent with the predicted accessibility in the structure, which shows the side chains of Cys997 and 1008 pointing outward and appearing to be exposed to the solution. One interesting possibility is that the low reactivity of Cys997-1008 could result from the

presence of the regulatory CTD not included in the crystal structure. Taken together, this approach allows us to easily detect the accessibilities of cysteines in the entire protein, including the flexible regions. Furthermore, it also provides a possibility to explore the local environment around these cysteines.

2.2.3 *hs*Top2α ATP gate conformational change in the presence of Mg^{2+} and AMPPNP

In order to examine the ATP gate movement, the reactivities of cysteines in *hs*Top2α were measured in the presence of 10 mM Mg^{2+} only, 1 mM AMPPNP only, or both 10 mM Mg^{2+} and 1 mM AMPPNP. Compared with the control (absence of Mg or AMPPNP), no obvious conformational changes were detected in the presence of Mg^{2+} only or AMPPNP only (**Figure 9**).

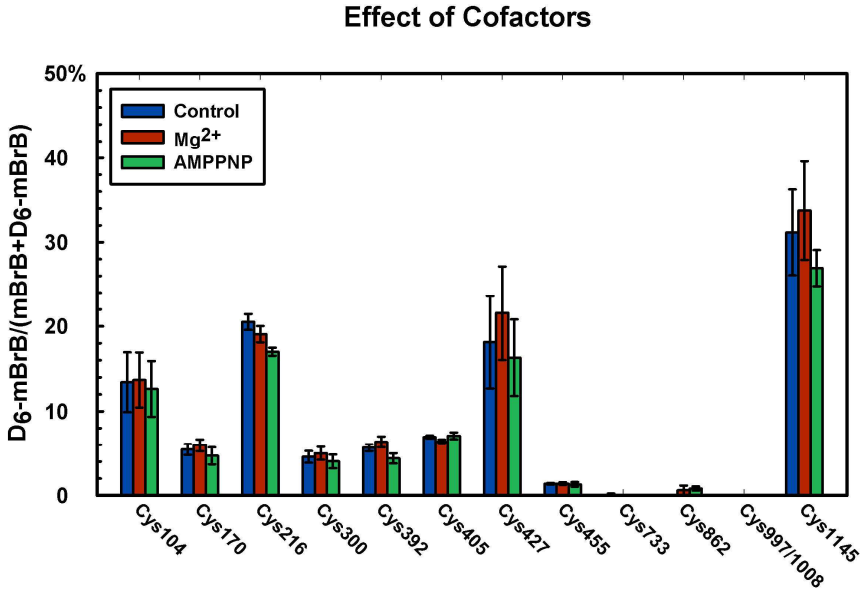

Figure 9: Investigation of the reactivity changes in the presence of Mg^{2+} or AMPPNP. The reactivities of all cysteines in *hs*Top2α do not change significantly in response to Mg^{2+} or AMPPNP.

However, with 10 mM Mg^{2+} present, AMPPNP triggers a significant conformational change in the ATP gate region (**Figure 10A**), and a similar result was also obtained with a different pair of labeling reagents, mBrB and IAM (**Figure 11**). This change noticeably alters the reactivities of two groups of cysteines (**Figure 10A**): (1) Cys170, Cys216, Cys300, and Cys392; (2) Cys405 and Cys455. The reactivities of the cysteines in the first group decrease while those in the second group increase. The reactivities of Cys170, Cys216, Cys300, and Cys392 decrease by 3-fold, 2-fold, 2-fold, and 2.5-fold, respectively. A possible explanation is that GHKL and transducer subdomains on individual units move toward each other upon AMPPNP binding in the presence of Mg^{2+}, decreasing the accessibility of the cysteines on these two subdomains (**Figure 10B**). This conformational change is consistent with a previous study which showed the ATP gate closes in the presence of ATP and Mg^{2+} (Hu et al., 2002; Roca and Wang, 1992). Cys405, located at the bottom of the transducer subdomain, increases 1.5-fold in reactivity. This location might be the hinge region of the movement, so instead of pulling the individual units together, this region may bend and become more accessible to solvent (**Figure 10B**). Cys455 is located near the DNA gate (TOPRIM subdomain) and has a 2-fold increase in reactivity upon Mg^{2+} and AMPPNP binding, suggesting that AMPPNP-induced ATP gate closure causes a conformational change in the DNA gate that renders Cys455 more solvent-accessible. As an interesting control, Cys427 does not

change in reactivity to D_6-mBrB upon Mg^{2+} and AMPPNP binding. Last, the reactivities of cysteines beyond the DNA gate remain unchanged, for example, Cys1145 in the C-terminal coiled-coil subdomain. After adding Mg^{2+} and AMPPNP, no conformational change can be probed in C-terminal gate region. However, we cannot rule out the possibility that the change is beyond detection limit with our method.

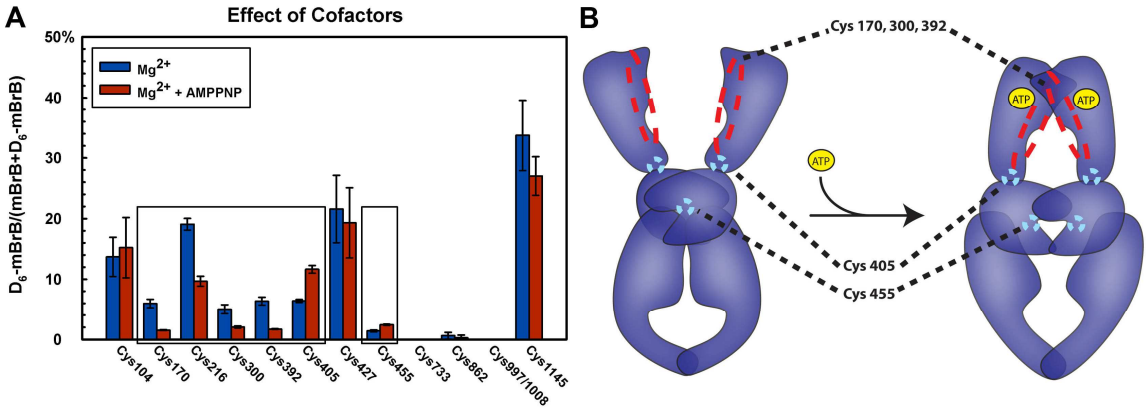

Figure 10: Conformational changes of *hs*Top2α in the presence of AMPPNP. A. In the presence of AMPPNP, the reactivities of Cys170, Cys300, and Cys392 decrease while the reactivities of Cys405 and Cys455 increase. B. The deduced movement of Top2 is shown in the model. The decreasing reactivities of Cys170, Cys300, and Cys392 might result from the N-gate closing and the increasing reactivities of Cys405 and Cys455 might be due to the DNA-gate opening.

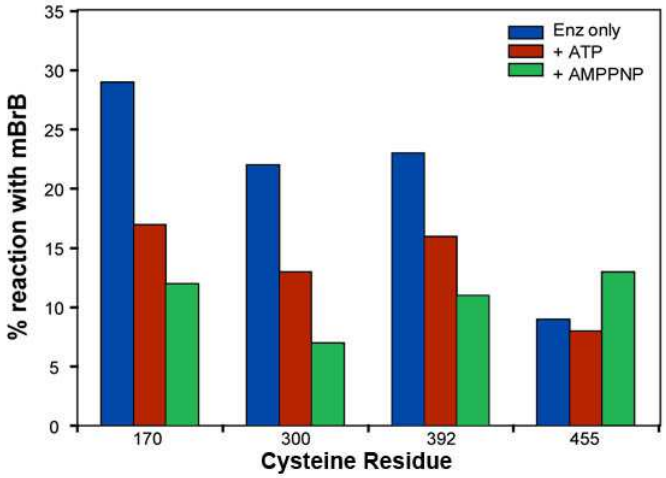

Figure 11: Probing reactivity changes upon adding ATP or AMPPNP by mBrB and IAM. Cysteine residues in the GHKL domain and upper transducer domain (Cys170, Cys300, and Cys392) decrease in reactivity upon AMPPNP binding while Cys455 located in the lower transducer domain increases in reactivity, suggesting coordinated opposing movements between the two domains. (This experiment was performed by Dr. Tammy L. Collins)

2.2.4 Capturing the ICRF-193 Linked ATP gate conformation

ICRF-193, also known as bisdioxopiperazine, is an antitumor agent that targets Top2 and forms a closed clamp protein complex by locking the ATP gate. In this study, we measured the reactivities of cysteines in the closed clamp structure triggered by ICRF-193 binding. Comparing this result to that of AMPPNP and Mg^{2+}, we were interested in knowing whether pulse-alkylation could distinguish differences between the closed ATP gate conformation formed by AMPPNP versus ICRF-193 (Roca et al., 1994). With 150 μM ICRF-193, the reactivities of Cys170, Cys216, Cys300, and Cys392 have a similar decrease compared to AMPPNP-induced changes (**Figure 12**).

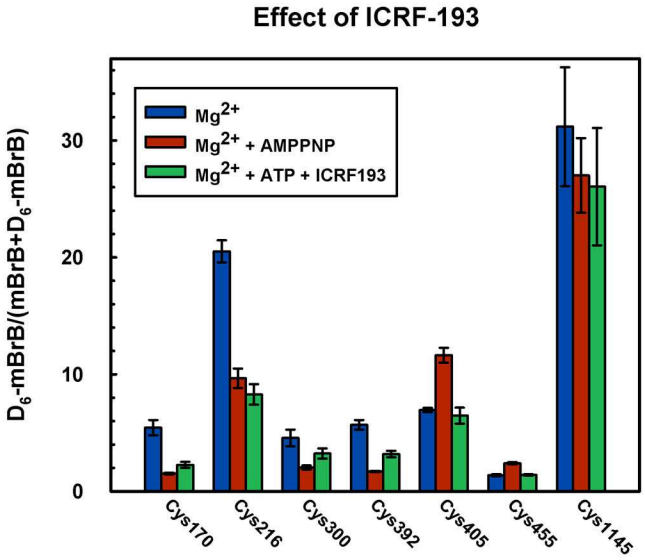

Figure 12: Differences between two close-clamp complexes triggered by AMPPNP and ICRF-193. In the presence of ICRF-193, while the reactivities of Cys170, Cys300, and Cys392 decrease to the similar level as the enzyme with AMPPNP, Cys405 and Cys455 remain at the same level as the condition with Mg^{2+} only.

This similarity implies that the GHKL subdomain and part of the transducer domain are both required to move toward each other to close the ATP gate no matter by which mechanisms. In contrast with the effect of AMPPNP, Cys405 and Cys455 near or at the DNA gate do not significantly change in reactivity with ICRF-193. Therefore, the closed-clamp complexes induced by AMPPNP and ICRF-193 could have different overall conformations. While AMPPNP/Mg^{2+} triggers the closure of ATP gate, the DNA gate opens along with the conformational change at N-terminal domain. The simultaneous downstream movement in the DNA gate, however, is not triggered by

ICRF-193. Cys1145 at the C-terminal coiled-coil domain again serves as a control which is not affected by ICRF-193.

2.2.5 Relationship between CTD and DNA gate

When probing the reactivitities of cysteines, Cys997 and Cys1008 were found to be two of the least reactive cysteines, which is not consistent with the predicted analysis from *hs*Top2α homology model. To rule out the possible coverage by flexible CTD which was not shown in the structure, *hs*Top2α with a C-terminal 310 amino acids truncation (*hs*Top2α-CΔ310t) was tested. The CTDs of eukaryotic Top2 proteins have been previously found to be dispensable for catalytic activity (Caron et al., 1994; Crenshaw and Hsieh, 1993; Meczes et al., 2008). We tested *in vitro* DNA unknotting activity of *hs*Top2α-CΔ310t and it retains robust activity, implying the protein maintains intact enzyme structure with limited coverage of CTD (data not shown). However, as shown in **Figure. 13**, the Cys997-1008 reactivity remains at the low level. It is possible that we did not truncate the CTD to the same extent as the yeast Top2 that was previously used for crystal structure (22 amino acids shorter than *hs*Top2α-CΔ310t), or there might be a difference between the crystal structure of yeast Top2 vs. the solution structure of humanTop2α around Cys997 and Cys1008. Unexpectedly, in *hs*Top2α-CΔ310t, the reactivity Cys427 near DNA-gate increases about 10% (**Figure 13**).

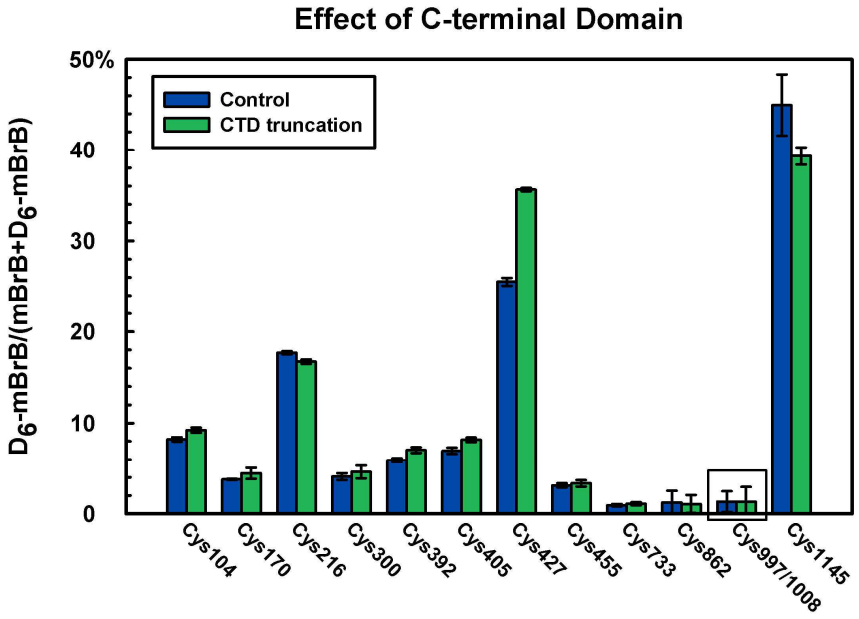

Figure 13: CTD truncated *hs*Top2α has higher reactivity in Cys427. Comparing among all the cysteines of *hs*Top2α with or without CTD, the reactivity of Cys427 is the only one that showed a significant difference while others remain at similar level.

We speculated that the CTD might be anchored near the DNA gate region in an arrangement similar to bacterial Topo IV (CTD of ParC (Corbett et al., 2005)), even though the sequence homology between these two CTDs are very low. We attempted to see if there is a direct interaction between the CTD and holoenzyme using pull-down assay and pulse-alkylation experiment with purified GST-tagged CTD and *hs*Top2α-CΔ310t (**Figure 14**). However, no strong interaction between CTD and holoenzyme can be detected. Given the fact that CTD affects the labeling efficiency of Cys427 without a strong interaction, our result suggests the CTD might tether around DNA-gate for its potential regulatory functions.

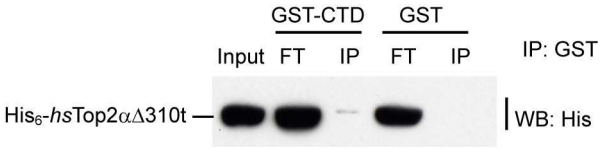

Figure 14: *hs*Top2α CTD does not directly interact with *hs*Top2α-CΔ310t. Purified *hs*Top2α-CΔ310t was incubated with immobilized *hs*Top2α CTD with N-terminal GST fusion protein (GST-CTD) or GST protein only. His-tagged *hs*Top2α-CΔ310t was detected by anti-His antibodies. No significant amount of *hs*Top2α-CΔ310t was pulled down by GST-CTD or GST only.

2.3 Discussion

In this study, we have demonstrated that by using pulse-alkylation with mass spectrometric analysis, we were able to differentiate the levels of alkylating reactivities of cysteines in *hs*Top2α and probe the protein dynamics. There are two main determinants for the alkylation reactivity. One is chemical, with thiol nucleophilicity being influenced by its environment, and one is physical, with the reactivity being determined by the accessibility of a thiol group to solvent. Because there is a close correlation between the solvent accessibility calculated from a structural model and the measured reactivity, the accessibility factor is likely a critical one. However, the most useful information will be what can be extracted from the difference in reactivities under different reaction conditions, which can pinpoint the conformational changes occurring near a particular cysteine residue. We have shown here that we could detect the conformational changes in N-gate closure induced by AMPPNP and Top2 inhibitor, ICRF-193. Furthermore, we also detected distinct conformational differences in closed clamp complexes resulting from the addition of either AMPPNP or ICRF-193, which

were not observed previously upon comparing the crystal structures of the yeast ATPase domain bound to AMPPNP with or without ICRF-187 (Classen et al., 2003). In our experiments, both AMPPNP and ICRF-193 lead to N-gate closure as indicated by the decreased reactivities of cysteines in both the GHKL domain (Cys170 and Cys216) and the upper transducer domain (Cys300 and Cys392) (**Figure. 12**). Besides N-gate closure, AMPPNP simultaneously enhanced accessibility at the DNA gate as well. In an interesting contrast, ICRF-193 limited solvent accessibility of the DNA gate in *hs*Top2α.

The flexible linker region between ATPase and cleavage/religation domains, disordered in crystal structures, was found to be highly accessible to solvent in our previous work with limited trypsin digestion (Lee and Hsieh, 1994). In this study, Cys427 at linker region was used to monitor the possible motion around this local environment, and this cysteine unsurprisingly remains solvent exposed in all conditions. However, we noticed a significant increase in the reactivity of Cys427 when the CTD of *hs*Top2α was completely truncated. The GST pull-down assay suggested the CTD does not strongly interact with the core enzyme but merely affects the solvent accessibility of Cys427 by anchoring around this region. Although we cannot rule out the possibility that the GST-tagged CTD purified from *E.coli* might not fold correctly or the interaction requires post-translational-modifications, evidence suggests this similar positioning of the CTD is common for bacterial type II topoisomerases. For example, *E. coli*

topoisomerase IV (Topo IV) has a globular CTD next to the tower domain with a consensus short peptide sequence (Corbett et al., 2005).

Others have also shown that the CTD of Topo IV helps the core enzyme preferentially recognize the positive-supercoiled DNA due to its higher affinity for the local left-handed crossover DNA (Corbett et al., 2005). The position of the CTD of bacterial gyrase is not as certain as Topo IV, but the CTD of bacterial gyrase is required to stay near the DNA-gate to stabilize the T-segment DNA to introduce negative supercoils into the DNA (Costenaro et al., 2005). Although the sequence homology of CTDs between prokaryotic and eukaryotic type II topoisomerase is low, the preference of recognizing positive supercoiled DNA in *hs*Top2α is CTD dependent (McClendon et al., 2008). Thus, we suspect *hs*Top2α has a similar arrangement of the CTD to the core enzyme.

Protein side chain modification in combination with mass spectrometric analysis can be clearly applied to amino acids other than cysteine. However, previous studies demonstrated that *hs*Top2α is sensitive to thiol-reacting reagents and that cysteine modifications participate in a number of unique reactions (Bender et al., 2007; Bender et al., 2006; Jensen et al., 2005; Wu et al., 2008). For instance, thimerosal, a mercury-containing compound that rapidly reacts with thiol group, inhibited the Top2 decatenation activity (Wu et al., 2008). Thiopurines also inhibited Top2 ATPase activity by alkylating thiol groups of cysteines (Jensen et al., 2005). Both inhibitory effects can be

abolished by adding reducing reagents, implicating cysteine modification in such reactions. However, it remains to be determined which cysteines are responsible for the inhibition. The mechanism of *hs*Top2α inhibition by quinone drugs is better characterized. Modification of Cys392 and Cys405 by benzoquinone prevents the DNA religation step in the *hs*Top2α catalytic cycle, resulting in the accumulation of DNA breakage (Bender et al., 2007). In a recent study, the chemopreventive effect of dietary isothiocyanates was also shown to be related to cysteine modification of *hs*Top2α. In an *in vitro* assay, cysteines in the ATPase domain were found to be modified by benzyl isothiocyanate (Lin et al., 2011). The studies of cysteine modification of *hs*Top2α shed light not only on Top2 conformational dynamics and catalytic mechanism but also on the action of novel inhibitors that have potential application as antineoplastic agents.

2.4 Experimental Procedures

2.4.1 Enzyme Preparation

Recombinant *hs*Top2α was created by replacing the first 28 amino acids of *hs*Top2α with the first 5 amino acids of yeast Top2 (Wasserman et al., 1993), and the N-terminus was tagged with a heart muscle kinase (HMK) phosphorylation site and hexahistidine (H_6) tag. The HMK motif was added to potentially allow for end-labeling of the protein for detection in an alternate gel-based cysteine footprinting method. The HMK site contains the Protein Kinase A (PKA) consensus sequence, RRASV (Kennelly

and Krebs, 1991). The C-terminus was truncated (amino acids 1405 to 1530) to remove an intrinsic PKA consensus sequence (RKPST).

Recombinant *hs*Top2α-CΔ310t was generated by truncating *hs*Top2α 310 amino acids at C-terminus (amino acids 1221 to 1530). Both *hs*Top2α and *hs*Top2α-CΔ310t were overexpressed in the yeast strain BCY123, and purified by Ni^{2+}-affinity (Ni-NTA resin, Qiagen) and ion exchange chromatography (POROS® HS column, Applied Biosystems). The tagged and truncated enzymes displayed activity comparable to that of the wild type protein.

2.4.2 Liquid Chromatography Electrospray Ionization Mass Spectrometry (LC/ESI-MS)

Tryptic peptides were analyzed by reverse phase liquid chromatography (RP-LC) coupled with electrospray ionization mass spectrometry. A Shimadzu Scientific Instruments (Columbia, MD) LC system (comprising a solvent degasser, two LC-10A pumps, and a SCL-10A system controller) was coupled to a QSTAR XL quadrupole time-of-flight tandem mass spectrometer (ABI/MDS-Sciex, Foster City, CA) equipped with an electrospray source. LC was operated at a flow rate of 200 μL/min with a linear gradient as follows: 100% A was held isocratically for 2 min and then linearly increased to 60% B over 18 min and then increased to 100% B over 5 min. Mobile phase A consists of water:acetonitrile (98:2 v/v) with 0.1% acetic acid. Mobile phase B consists of acetonitrile:water (90:10 v/v) with 0.1% acetic acid. A Zorbax C8 column (SB-C8, 2.1mm

ID × 50 mm (5μm), Agilent Technology) was used for LC/MS analysis with injection volume of 10 μL.

The mass spectra were acquired in the positive mode in the range of 200 to 2000 m/z (a.m.u). The acquired spectra were then reprocessed using LCMS reconstruct software (Analyst QS software with the BioAnalyst extension) to obtain the integrated peak area.

2.4.3 Sample preparation for evaluating the quantitative ability of monobromobimane (mBrB)

Two batches of 210 μg of *hs*Top2α were individually prepared in 700 μL of TNE buffer (10 mM Tris·HCl, pH 7.9/ 50 mM NaCl/ 0.1 mM EDTA). One was incubated with 50mM mBrB while the other was labeled with 50 mM D_6-mBrB. After 10 min incubation at 37°C, the samples were further labeled in a denaturing condition with 6M guanidinium hydrochloride for 2 h at 37°C. After the completion of the labeling, the mBrB- and D_6-mBrB-treated samples were then mixed in seven different ratios (5:0, 4:1, 3:2, 1:1, 2:3, 1:4, 0:5). To remove the excess labeling reagents (mBrB or D_6-mBrB), the samples were dialyzed 4 times against 1 L of 100 mM NH_4HCO_3 solution with 5mM 2-mercaptoethanol for 2 h each time at 4°C. Dialysis was followed by trypsin digestion (overnight, 37°C), lyophilization, and resuspension with 50 μl of dH_2O before LC/ESI-MS analysis.

2.4.4 Procedure of Pulse-alkylation Mass Spectrometry

100 µl samples of 30 µg *hs*Top2α in TNE buffer (10 mM Tris·HCl, pH 7.9/ 50 mM NaCl/ 0.1 mM EDTA) was preincubated at 37°C for 5 minutes. Samples were then pulsed with 0.5 mM D_6-mBrB for 1 min and immediately quenched with 5 mM 2-mercaptoethanol for 1 min at 37°C. After the first labeling, the samples were incubated with second reagent mBrB (50 mM) for 10 min at 37°C. The second labeling process was completed by denaturing the samples with 6M guanidinium hydrochloride for 2 h at 37°C. The samples were then dialyzed 4 times against 1 L of 100 mM NH_4HCO_3 solution with 5mM 2-mercaptoethanol for 2 h each time at 4°C. Dialysis was followed by trypsin digestion (overnight, 37°C), lyophilization, and resuspension with 50 µl of dH_2O before LC/ESI-MS analysis. In experiment with cofactors, Mg^{2+} or/and AMPPNP were added during the preincubation step, while ICFR-193, Mg^{2+}, and ATP were preincubated in the experiment with the Top2 inhibitor.

2.4.5 Homology Model and Accessibility Analysis

A homology model of the cleavage/religation and CTDs of *hs*Top2α was constructed using the I-TASSER protein structure prediction server (Roy et al., 2010; Zhang, 2007). The sequence of *hs*Top2α, starting from residue 400, was submitted to the I-TASSER server. The crystal structure of yeast Top2 DNA-binding and cleavage domains (PDB: 1bjt (Fass et al., 1999)) was specified as a template in order to produce a homology model which could be dimerized more easily. The crystal structure of the

ATPase domain of *hs*Top2α (PDB: 1zxm (Wei et al., 2005)) was manually docked into its approximate location on the I-TASSER homology model using the KiNG visualization software program (Chen et al., 2009).

The solvent accessibility of the cysteines in our constructed model of *hs*Top2α was calculated using the Probe all-atom contact analysis software (Word et al., 1999). This software allowed us to roll a 1.4 Å radius ball around the model in order to calculate a visual dot representation of the solvent-accessible surface for the whole model. Then, for each cysteine in the model, similar dot representations were calculated, excluding all other residues. The overlap between the surface for the whole model and the surfaces for each cysteine's sulfhydryl group gives an approximation of the solvent-accessibility of each cysteine. This solvent-accessibility was calculated by dividing the number of dots for a particular cysteine's sulfhydryl in the whole model surface by the number of dots for that sulfhydryl if that cysteine was alone.

3. Unveiling the Interaction between *Drosophila* Top2 and Mus101, Homolog of Human TopBP1

3.1 introduction

Eukaryotic topoisomerase 2 (Top2) is an essential enzyme that solves DNA topological problems in DNA replication, transcription, and DNA segregation. During the catalytic cycle, Top2 introduces a transient double strand break in one DNA segment for the passage of a second DNA segment, which results in altered DNA topology (Liu et al., 1983; Morrison and Cozzarelli, 1979; Sander and Hsieh, 1983). The general mechanism of eukaryotic Top2 has been established using *in vitro* kinetic and structural analysis (Baird et al., 1999; Harkins et al., 1998; Schmidt et al., 2012). The current emerging question is how eukaryotic Top2 is regulated *in vivo*, which is hypothesized to be mediated by post-translational modifications and protein-protein interactions involving the C-terminal domain (CTD) of eukaryotic Top2 (Chen et al., 2013; Nitiss, 2009a).

TopBP1 (Top2β binding protein 1) was found to interact with the CTD of human Top2β via a yeast two-hybrid (Yamane et al., 1997). Perhaps due to the lack of phosphorylation, fragments of Top2 and TopBP1 expressed in *E. coli* interacted only weakly. Thus, the biological function of Top2-TopBP1 remains obscure. As discussed in chapter 1, TopBP1 has been shown to play important roles in the initiation of DNA replication and as an activator of ATR kinase in the DNA damage response (Pospiech et al., 2010; Wardlaw et al., 2014).

However, some functions of TopBP1 in mitosis seems closely linked with Top2 functions. Cut5 (Cut, cell untimely torn) is a TopBP1 homolog in fission yeast that has been shown to be essential for the DNA replication. In a genetic analysis screening mutants showing abnormal nuclear division, cut5 was identified along with top2, suggesting Cut5 and Top2 may coordinate closely in the same cellular event (Hirano et al., 1986). In a recent study of yeast Dpb11 and chicken TopBP1, Dpb11 and TopBP1 were found enriched on the anaphase bridges (Germann et al., 2014). The depletion of chicken TopBP1 causes accumulation of anaphase bridges in chicken DT40 cells. Because anaphase bridges can be sites of topological problems, TopBP1 was assumed to collaborate with Top2 or the BLM-Top3 complex to solve topological problems and to ensure faithful DNA segregation (Germann et al., 2014). Mus101, the *Drosophila* TopBP1 homolog, has also been shown to be functionally linked to Top2. Flies carrying the $mus101^{lcd}$ lethal allele die at the late third instar larval stage, and metaphase chromosomes appear to be undercondensed or broken in neuroblasts of these larva. It is postulated *Drosophila* Top2, which is required for DNA compaction, may be recruited by Mus101 to promote chromatin condensation (Yamamoto et al., 2000).

Using the *Drosophila* system, we have examined the interaction between Top2 and Mus101 in the hope of obtaining more insights of the regulation of eukaryotic Top2. We generated various truncated Top2 and Mus101 constructs to map the binding interface of these two proteins. The CTD of *Drosophila* Top2 interacts with the BRCT1/2

containing N-terminus of Mus101. Resembling Sld3-Dpb11, Tresline-TopBP1, and Rad9-TopBP1 interactions (Boos et al., 2011; Moyer et al., 2006; Takeishi et al., 2010), doubly phosphorylated Top2 CTD at Ser1428 and Ser1443 is required for the interaction. In an *in vitro* assay, we found binding of Mus101 significantly inhibits Top2 decatenation activity.

We further used a plasmid-based shRNA system and fly genetics to address the biological functions of the Top2-Mus101 interaction. Endogenous Top2 in *Drosophila* Schneider 2 (S2) cells can be nearly depleted by two sets of shRNA and these cells conferred a G2/M arrest phenotype. Both Top2(S1428A, S1443A) and Top2Δ20 can rescue the G2/M arrest in Top2-depleted S2 cells. However, in an experiment with long-term induction, Top2-depleted S2 cells rescued by Top2Δ20 show an abnormally high number of chromosomes, indicating the role of Top2-Mus101 interaction in maintaining the fidelity of chromosome segregation. The result of our genetic analysis shows the viability of the flies carrying *top2* null mutation can be rescued by Top2(S1428A, S1443A). However, both male and female flies have severe defects in fertility. By examining spermatogenesis, primary spermatocytes from flies rescued by Top2(S1428A, S1443A) exhibited a delay in DNA segregation during meiosis I, suggesting the Top2-Mus101 interaction also participates in chromosome segregation during meiosis.

3.2 Results

3.2.1 Confirming the interaction between *Drosophila* Top2 and Mus101

Prior to investigating the role of the interaction, we first verified the interaction between Top2 and Mus101, the *Drosophila* TopBP1 homolog. Incubating anti-Flag agarose resin with nuclear extracts from *Drosophila* S2 cells overexpressing Flag-tagged Mus101 demonstrated Top2 complexes with Mus101 (**Figure 15A**). To further confirm the direct contact between these two proteins, we purified both proteins for a pull-down experiment. HA-tagged Top2 was overexpressed and purified from S2 cells in the presence of phosphatase inhibitors to preserve the post-translational modification of Top2, and 6×His-tagged Mus101 was purified from *E. coli*. Mus101 and Top2 can pull down each other in the pull-down assays, using anti-HA agarose resin or Ni-NTA resin, which show the interaction does not require any other mediators (**Figure 15B and C**).

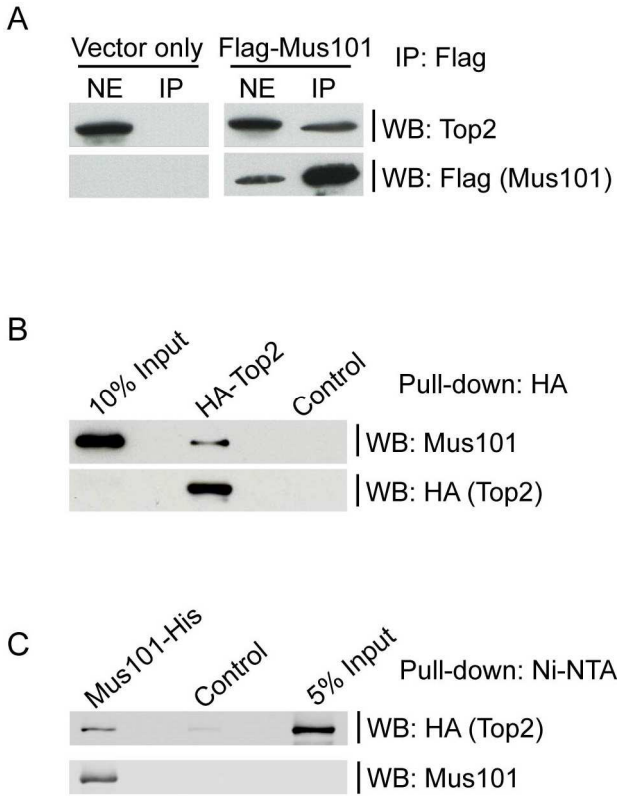

Figure 15: Interaction between Top2 and Mus101. A. Anti-Flag agarose beads were incubated with nuclear extract from Drosophila S2 cells overexpressing Flag- Mus101. Endogenous Top2 and Flag-Mus101 were immunoblotted with rabbit anti-Top2 antibodies and rabbit anti-Flag antibodies, respectively. Top2 was co-immunoprecipitated with Flag-Mus101. B. and C. Direct binding between Top2 and Mus101 were examined with purified proteins by pull-down assays. His-Mus101 was pulled down by HA-Top2 immobilized on anti-HA agarose beads. In a reciprocal experiment using Ni-NTA resin, HA-Top2 was pulled down by anchored His-Mus101. Empty anti-HA agarose beads and Ni-NTA resin are used as controls. HA-Top2 and His-Mus101 were immunoblotted with mouse anti-HA antibodies and rabbit anti-Mus101 antibodies, respectively (The immunoprecipitation assay in A was performed by Dr. Jianhong Wu).

3.2.2 BRCT1/2 containing N-terminal domain of Mus101 is required for Top2 binding

In previous studies, it was shown that the C-terminal human TopBP1 domain, containing BRCT6/7/8, is involved in the binding of human Top2β (Yamane et al., 1997).

To confirm that *Drosophila* proteins behave similarly, we used S2 cells expressing Flag-tagged fragments of Mus101, residues 1-350, residues 351-800, residues 801-1150, and residues 1151-1425 (**Figure 16A**), in the background of HA-tagged full-length Top2 to map the binding domain of Mus101. Nuclear extracts prepared from these cells were subjected to a co-immunoprecipitation (co-IP) assay. Only residue 1-350, Mus101[1-350], which contains the first two BRCT domains (BRCT1/2), co-immunoprecipitated with Top2 (**Figure 16B**). The reciprocal co-IP experiment also yielded consistent results (**Figure 16C**). Unlike human the Top2β-TopBP1 interaction, the first 350 amino acids of Mus101 that contain BRCT1/2 are responsible for the binding of Top2 in the *Drosophila* system.

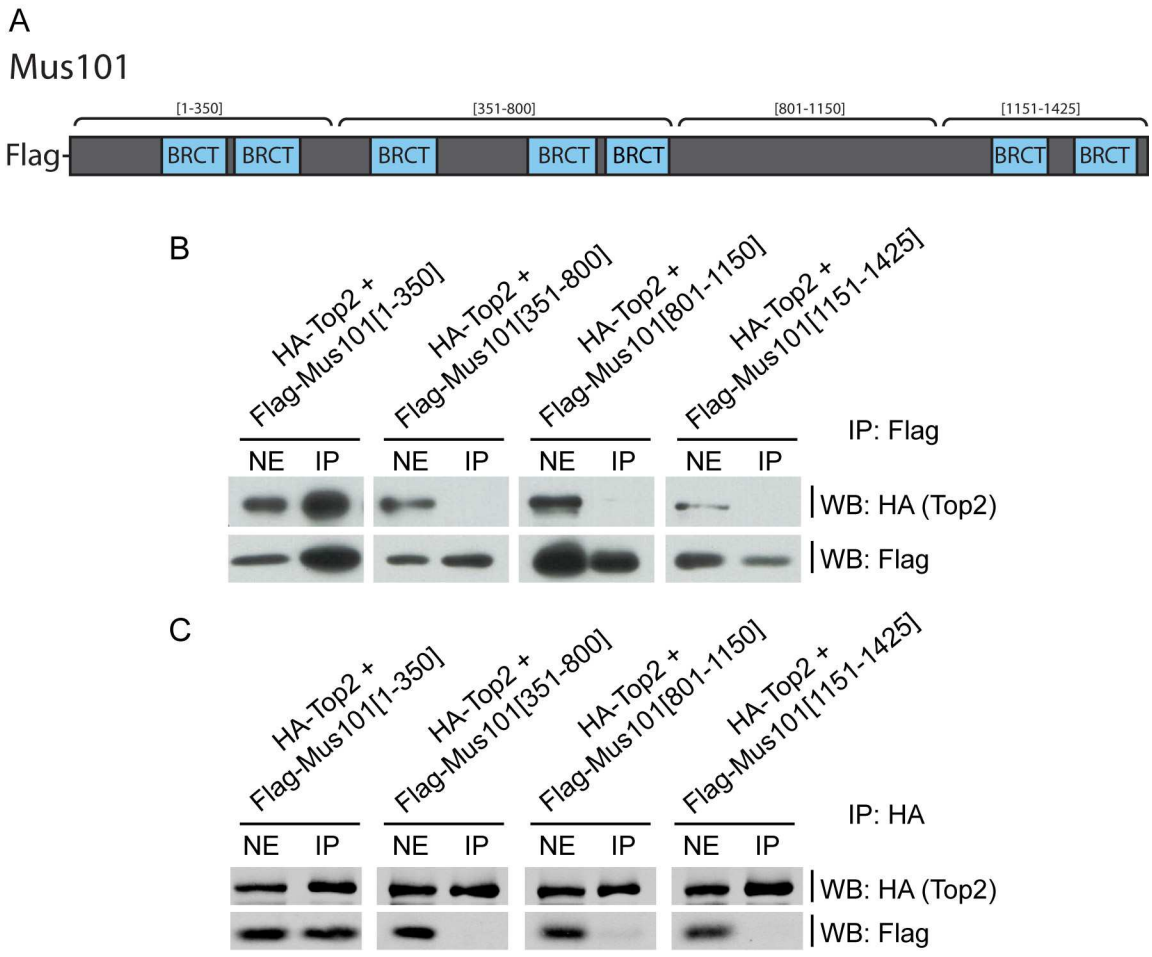

Figure 16: N-terminal Mus101 containing BRCT1/2 interacts with Top2. A. Domains of Mus101. The position and length of each Mus101 fragment is indicated above the diagram. B. and C. Each strain of S2 cells was transfected with one of the four Flag-tagged fragments of Mus101, aa 1-350, aa 351-800, aa 801-1150, and aa 1151-1425, along with HA-Top2. The nuclear extracts were harvested from lysed cells and then subjected to immunoprecipitation using anti-Flag or anti-HA agarose beads. Products of immunoprecipitation were then immunoblotted by rabbit anti-Flag antibodies for Mus101 fragments and mouse anti-HA antibodies for Top2. Flag-Mus101[1-350] was co-immunoprecipitated with HA-Top2 and vice versa. (The constructs of Mus101 fragments were generated by I-Jay Chen at Academia Sinica)

3.2.3 Top2 C-terminal regulatory domain is required for the binding of Mus101

To examine if Top2 binds Mus101 via its C-terminal regulatory domain as has been reported for the human Top2β-TopBP1 interaction (Yamane et al., 1997), we conducted the co-IP experiments using S2 cells overexpressing Flag-tagged full-length Mus101 and HA-tagged Top2 with a truncation of N-terminus (ATPase domain), C-terminus (regulatory domain), or both termini (**Figure 17A**). The result shows that the interaction is completely abolished with the removal of the CTD (Top2Δ240 and -core in **Figure 17B**). Although the sequences of CTDs of eukaryotic Top2 proteins are not conserved between different species and isoforms, based on our result, the C-terminus of *Drosophila* Top2 has the conserved function for the binding to Mus101.

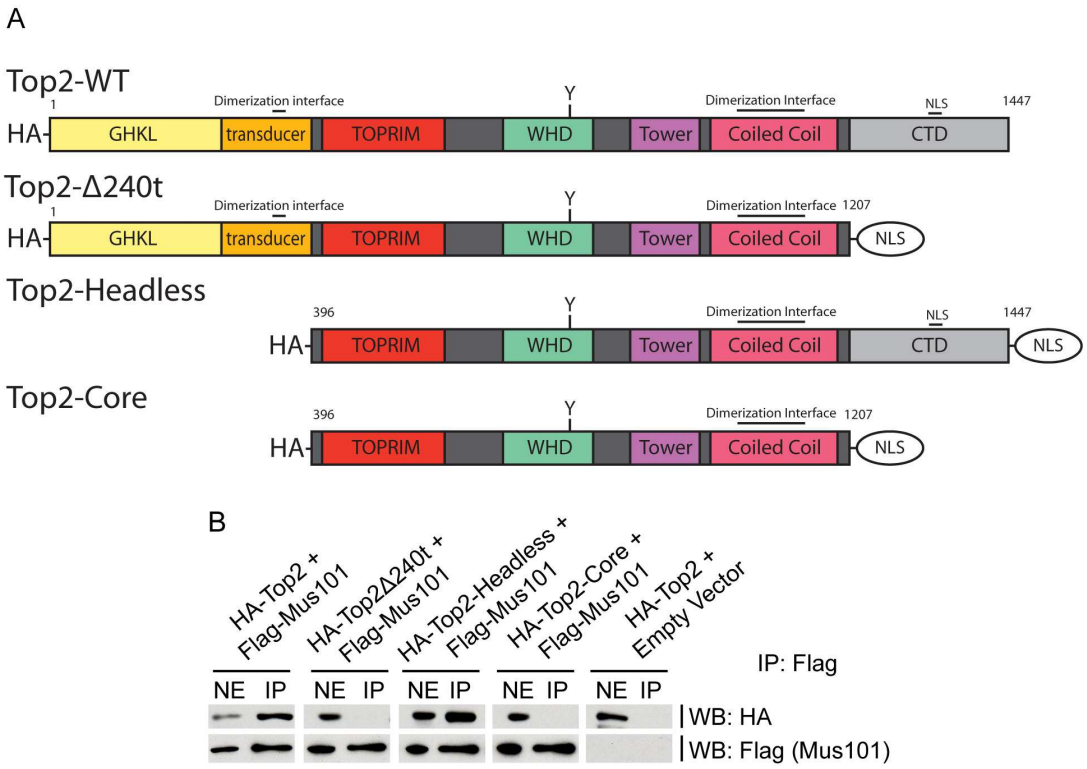

Figure 17: C-terminal regulatory domain of Top2 is required for the binding of Mus101. A. Schematic representation of the HA-tagged Top2 truncation constructs. B. Nuclear extracts harvested from S2 cells overexpressing full-length Top2 (HA-Top2), C-terminus truncated Top2 (HA-Top2Δ240t), N-terminus truncated Top2 (HA-Top2-Headless), or Top2 with truncation at both termini (HA-Top2-Core) along with Flag-Mus101 were incubated with anti-Flag agarose beads. The products of immunoprecipitation were then immunoblotted with rabbit anti-Flag antibodies for Mus101 fragments and mouse anti-HA antibodies for Top2. HA-Top2 and HA-Top2-Headless were co-immunoprecipitated with Flag-Mus101.

3.2.4 The requirement for Mus101 binding resides at the last 20 amino acids of Top2

To dissect Mus101-binding related function from the essential catalytic part of Top2, we sought to build a Top2 construct with altered sequence that abolishes the binding of Mus101 without affecting Top2 DNA strand passage activity. To this end, we aimed to find the minimal C-terminal elements of Top2 required for the binding of

Mus101. In a pull-down experiment using purified Top2 proteins with 59 residues, 125 residues, or 240 residues truncated from C-terminus (Top2Δ59t, Top2Δ125t, and Top2Δ240t, respectively), we found Mus101 fails to bind any of these truncated Top2 proteins **(Figure 18)**.

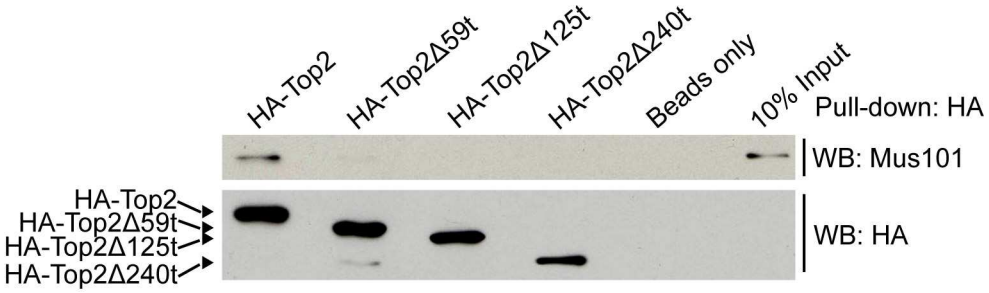

Figure 18: Truncation of 59 amino acids from the C-terminus of Top2 abolishes the binding of Mus101. Purified full-length Mus101 was incubated with immobilized full-length Top2 (HA-Top2), truncated Top2 lacking C-terminal 59, 125, or 240 amino acid residues (HA-Top2Δ59t, HA-Top2Δ125t, and HA-Top2Δ240t) on anti-HA agarose beads. The pull-down products were then detected by anti-Mus101 antibodies for Mus101 and anti-HA antibodies for Top2. Mus101 was only pulled down by HA-Top2.

Due to the low abundance and instability of full-length Mus101 protein, we continued the mapping of Top2 interacting motif with the N-terminal 350 aa of Mus101, Mus101[1-350]. Comparing purified Top2 proteins truncated at the last 5 residues, and 20 residues (Top2Δ5t, and Top2Δ20t, respectively), Mus101[1-350] does not bind to Top2Δ20t while it binds Top2Δ5t at a reduced level, which suggests that the last 20 amino acids are required for interacting with Mus101 **(Figure 19)**.

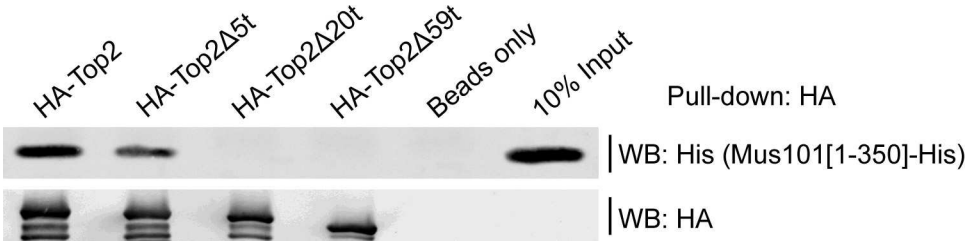

Figure 19: The last 20 amino acids are the minimal requirement for the binding of Mus101. Purified N-terminal Mus101, Mus101[1-350]-His, was incubated with immobilized full-length Top2 (HA-Top2), truncated Top2 lacking C-terminal 5, 20, or 59 amino acid residues (HA-Top2Δ5t, HA-Top2Δ20t, and HA-Top2Δ59t) on anti-HA agarose beads. The pull-down products were then detected by anti-His antibodies for Mus101[1-350]-His and anti-HA antibodies for Top2. Mus101[1-350]-His was pulled down by HA-Top2 and HA-Top2Δ5t, but not HA-Top2Δ20t.

3.2.5 Phosphorylation of both Ser1428 and Ser1443 is required to bind Mus101

The conserved BRCT1/2 domains of TopBP1 and its homologs have been found to interact with several binding partners in their doubly phosphorylated forms (Boos et al., 2011; Moyer et al., 2006; Takeishi et al., 2010). After the N-terminal 350 aa of Mus101, which contains BRCT1/2 domains, were found to be required for Top2 binding, we were curious if Top2 also interacts with Mus101 in a phosphorylation dependent manner, and furthermore, if a doubly phosphorylated form is required. In a pull-down experiment with Top2 dephosphorylated by λ-phosphatase, we found that phosphorylation indeed is required for Mus101 binding **(Figure 20)**.

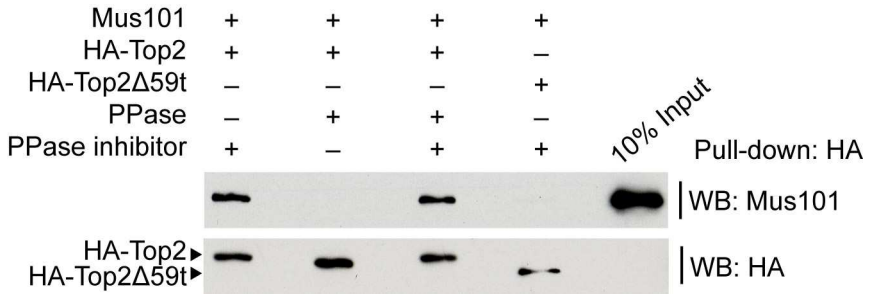

Figure 20: Top2 interacts with Mus101 in a phosphorylation-dependent manner. Binding of Mus101-His to HA-Top2 without any treatment, treatment with λ-phosphatase, and treatment with inhibited λ-phosphatase was compared by a pull-down assay. λ-phosphatase treated HA-Top2 (without inhibitors) failed to pull down Mus101-His. HA-Top2Δ59t, Top2 with partial CTD truncation, serves as a negative control. The protein level of HA-Top2 remains the same after λ-phosphatase treatment.

Taken together with our mapping results, two serine residues, Ser1428 and Ser1443, among the last 20 amino acids could be phosphorylated for the binding of Mus101 (**Figure 21A**). In a pull-down experiment with purified Top2(S1428A), Top2(S1443A), and Top2(S1428A, S1443A), the interaction can only be abolished completely by substituting both Ser1428 and Ser1443 with alanines (**Figure 21B**). We have also examined Top2 with 4 serines upstream of Ser1428 and Ser1443 substituted with alanines, Top2(S1392A, S1396A, S1409A, S1410A), and found none of the serine to alanine substitutions affected the binding of Mus101[1-350]. Thus, among the last 59 amino acids, Ser1428 and Ser1443 are apparently the only two phosphorylated sites required for the interaction (**Figure 21C**).

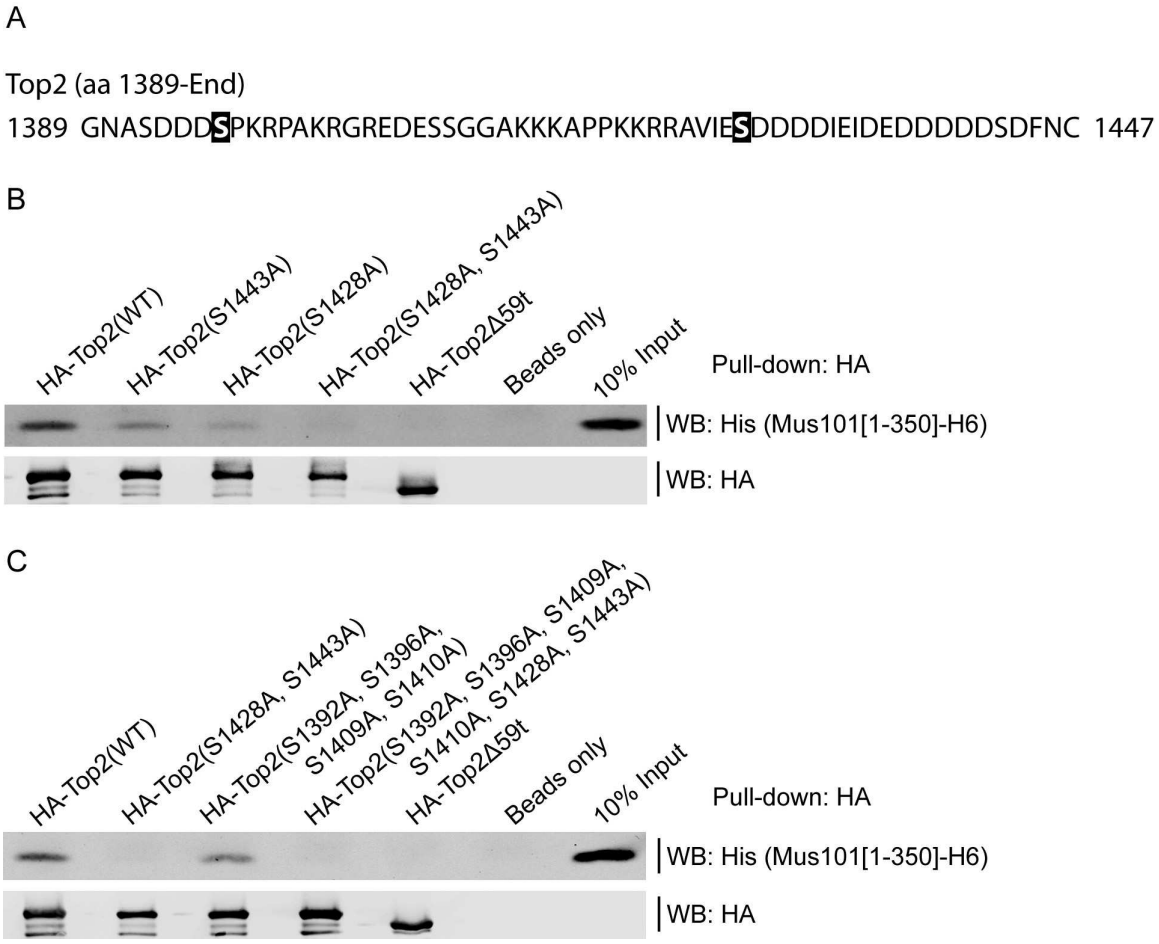

Figure 21: pS1428 and pS1443 of Top2 are required for the binding of Mus101. A. Sequence of the last 59 amino acids of Top2. B. Top2 with alanine substituted for serine at residue 1428, residue 1443, or both (HA-Top2(S1428A), HA-Top2(S1443A), and HA-Top2(S1428A, S1443A)), were tested in the pull-down experiment. After incubating Mus101[1-350]His with immobilized wild type or mutant Top2 proteins, Mus101[1-350]His was barely pulled down by HA-Top2(S1428A, S1443A) and was pulled down at a significant reduced level by HA-Top2(S1428A), HA-Top2(S1443A) comparing to wild type Top2. C. Substitutions of serine 1392, 1396, 1410, and 1409 for alanines do not abrogate the binding of Mus101. HA-Top2(S1392A, S1396A, S1409A, S1410A, S1428A, S1443A), HA-Top2(S1392A, S1396A, S1409A, S1410A), and HA-Top2(S1428A, S1443A) were tested in the pull-down experiment. Mus101[1-350]His was pulled down only by both HA-Top2(S1392A, S1396A, S1409A, S1410A) and wild type Top2.

3.2.6 The binding of Mus101 to Top2 CTD is not affected by the C-terminal GFP fusion protein

For studying the biological function of the Top2-Mus101 interaction, we generated C-terminal GFP tagged wild type or mutant Top2 for fluorescence-based cellular assay and fly tissue analysis. To confirm that the Top2-Mus101 interaction remain unaffected with the GFP fusion protein, we tested the binding of Mus101[1-350] to the C-terminal GFP-tagged Top2 by pull-down assay, and the interaction was not affected by the fusion of GFP protein (**Figure 22**).

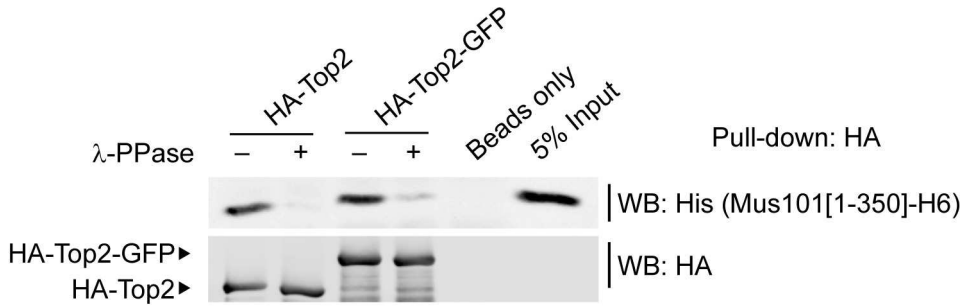

Figure 22: The binding of Mus101[1-350] to Top2 is not hindered by the C-terminal GFP fusion protein. HA-tagged Top2 with or without C-terminal GFP fusion protein was immobilized on anti-HA agarose beads for the pull-down experiment. Mus101[1-350] can be pulled down by both HA-Top2 and HA-Top2-GFP at the similar level. Mus101[1-350] does not bind HA-Top2 nor HA-Top2-GFP after the treatment with λ-phosphatase (λ-PPase).

3.2.7 Phosphorylated Top2 peptide interacts with Mus101[1-350]

We then confirmed the Mus101 binding motif at the C-terminus of Top2 by synthesizing phosphorylated and unphosphorylated peptides spanning the last 25 amino acids of Top2 with a C-terminal biotinylation. After peptide immobilization on

streptavidin agarose beads, Mus101[1-350] was pulled down by phosphorylated peptide but not unphosphorylated peptide **(Figure 23A)**. The binding affinity between the phosphorylated Top2 peptide and Mus101[1-350] was determined by a surface plasmon resonance with a K_d of 0.57 ± 0.04 μM, while the binding affinity between unphosphorylated Top2 peptide and Mus101[1-350] was too weak to be measured **(Figure 23B)**. Our pull-down and surface plasmon resonance experiments strongly support the requirement of phosphorylation in Top2-Mus101 binding, and demonstrate that the last 25 amino acids of Top2 itself are sufficient for high-affinity Mus101 binding.

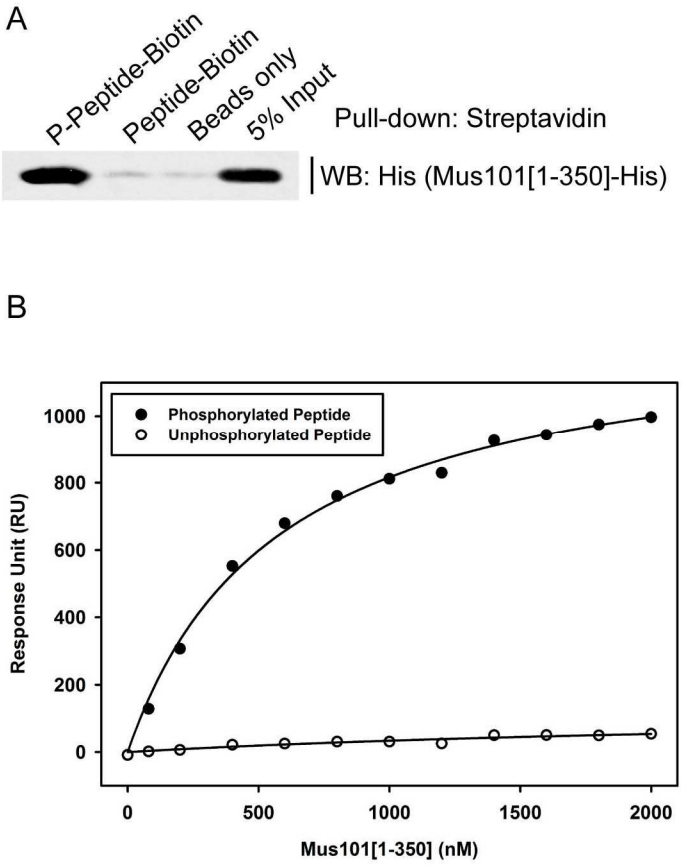

Figure 23: Phosphorylated Top2 peptide interacts with Mus101[1-350]. C-terminal biotinylated synthetic peptides, phosphorylated (pS1428 and pS1443) or unphosphorylated, containing the last 25 amino acids of Top2 were generated for pull-down assay and surface plasmon resonance experiment. A. Mus101[1-350]His was incubated with immobilized peptides on streptavidin agarose beads in the pulldown experiment, and Mus101[1-350]His was only pulled down by phosphorylated peptide. B. 145 response unit (RU) of phosphorylated or unphosphorylated peptides were immobilized on separate channels of a streptavidin chip for SPR experiment. Different concentrations of Mus101[1-350]His (from 0 to 2 μM) were tested and sensorgrams were recorded. Saturated RU of each condition was plotted against the concentration of Mus101[1-350]His. Dissociation constant (K_d) of Mus101[1-350]His to phosphorylated Top2 peptide was determined to be 0.57 ± 0.04 μM.

3.2.8 The binding of Mus101 inhibits Top2 decatenation activity

Phosphorylation and protein binding (HMBG1 and 14-3-3ε) at the C-terminus of Top2 have both been shown to modulate Top2 activity (Ackerman et al., 1985; Chikamori et al., 2003; DeVore et al., 1992; Kurz et al., 2000; Qi et al., 2011; Sander et al., 1984; Stros et al., 2007). Therefore, it was of our interest to see how Top2 function was affected by the binding of Mus101. Before testing Top2 decatenation activity in the presence of Mus101, a set of Top2 samples was purified after λ-phosphatase treatment to abolish the interaction with Mus101. In the presence of Mus101, we noticed the activity of phosphorylated Top2 decreased with the increasing amount of Mus101, while the activity of dephosphorylated Top2 was unaffected until the Mus101 concentration exceeded 1.5 μM, suggesting that binding of Mus101 inhibits Top2 decatenation activity **(Figure 24A and B)**.

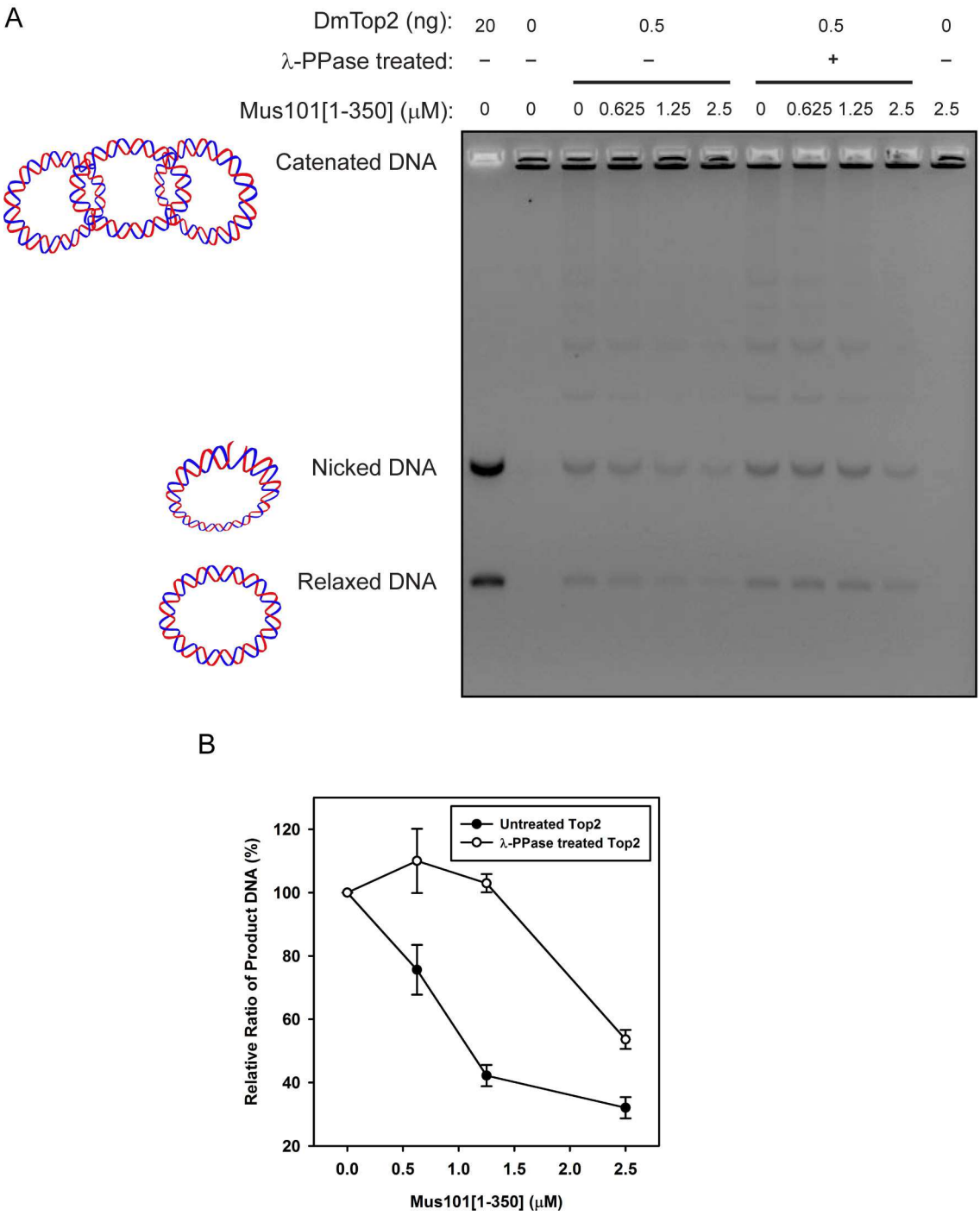

Figure 24: Mus101 inhibits Top2-mediate kinetoplast DNA decatenation. A. 0.5 μg of untreated or λ-phosphatase (λ-PPase) treated Top2 was incubated with 0.1 μg kinetoplast DNA in the present of Mus101[1-350]His (0, 0625, 1.25, or 2.5 μM) at 30 °C for 15 min. The samples were analyzed by electrophoresis in 1% agarose gel with

EtBr. B. Triplicate results were quantified and relative ratios of DNA product were plotted against Mus101[1-350]His concentrations. Top2 (untreated) decatenation activity reduces significantly with the increasing amount of Mus101, while λ-PPase treated Top2 remains unaffected until the presence of 2.5 μM of Mus101[1-350]His.

3.2.9 Top2-silenced S2 cells accumulate products of incomplete DNA segregation.

Due to the essential functions of *Drosophila* Top2 and Mus101, it is difficult to decipher the biological function of Top2-Mus101 interaction by using loss-of-function genetic analysis. In order to study the function at cellular level, we adapted an intron-mediated shmiR expression design from Haley *et al*. to build an inducible plasmid-based shRNA system to simultaneously silence endogenous Top2 and express the wild-type or mutant Top2 (Haley et al., 2010). Using the DSIR, Designer of Small Interfering RNA, algorithm, we chose two sets of shRNA sequences for the TOP2 gene with one targeting the protein coding region and the other targeting the 3'UTR (Vert et al., 2006). In case of insufficient knock-down efficiency by one shRNA, we considered two ways to combine the effect of two shRNAs. One was to co-transfect two shRNAs on separate plasmids, and the other was to tandem-link shRNAs on a single plasmid following the design of Haley *et al.* (Haley et al., 2010). As described in the previous design, the shRNA sequence is embedded in an *ftz* intron in upstream of GFP reporter gene which allows us to track the induction of the shRNA at the single cell level by fluorescence-activated cell sorting (Haley et al., 2010). By examining the protein level of endogenous Top2, all four of our constructs of shRNA expression system successfully knocked down the endogenous Top2 (**Figure 25**).

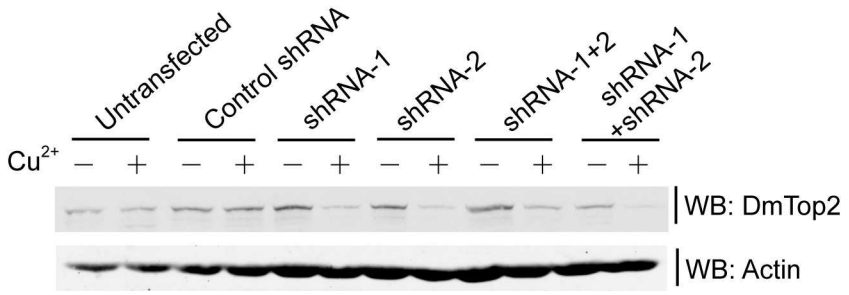

Figure 25: Efficiency of inducible plasmid-based shRNA system on silencing endogenous Top2. Drosophila S2 cells transfected with indicated shRNA constructs were incubated with or without 500 μM $CuSO_4$ for 4 days. Endogenous Drosophila Top2, DmTop2 was detected by anti-DmTop2 antibodies. "shRNA-1+2" represents a single construct carrying a tandem-linked shRNA-1 and shRNA-2 cassette, and "shRNA-1 + shRNA-2" represents a co-transfection of shRNA-1 and shRNA-1 constructs. Top2 in S2 cells co-transfected with shRNA-1, shRNA-2 or both constructs is nearly depleted.

Since Top2 is essential for cell growth, depleting Top2 using shRNA should show defects in cell cycle. We used flow cytometry to monitor the cell cycle profile in S2 cells transfected with shRNAs. S2 cells transfected with shRNA-1 or shRNA-2 accumulated at S and G2/M phases (**Figure 26**). However, the severe cell cycle arrest and cell death only happened to the cells transfected with both shRNA-1 and shRNA-2, which indicates the combination of two sets of shRNAs achieved a near-complete depletion of Top2 (**Figure 26 and 27**).

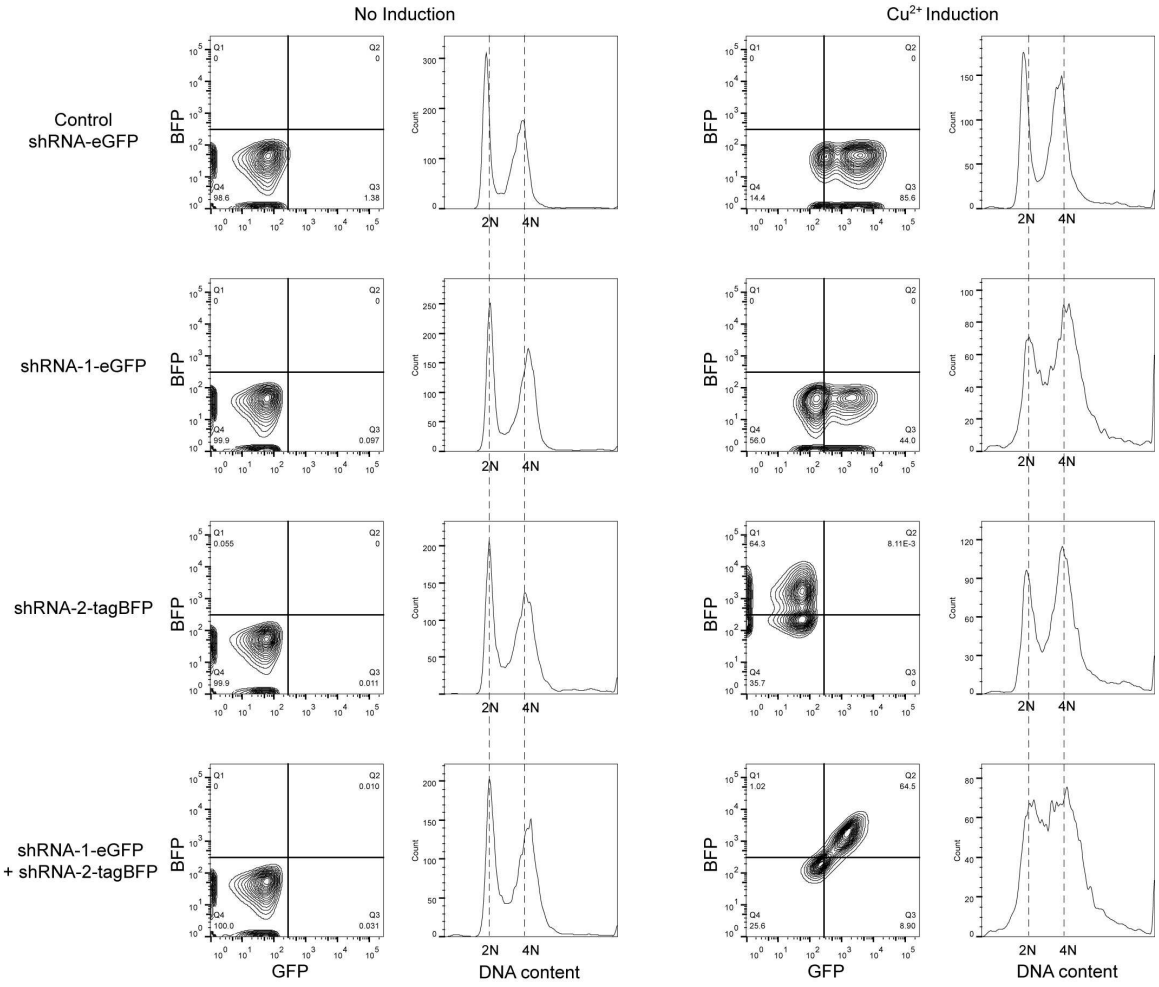

Figure 26: Cell cycle profiles of cells transfected with inducible shRNA constrcuts silencing Top2. Four groups of cells were individually transfected with 1) control shRNA-eGFP; 2) shRNA-1-eGFP; 3) shRNA-2-tagBFP; 4) shRNA-1-eGFP + shRNA-2-tagBFP. The cells without $CuSO_4$ were shown as un-induced control, and they expressed undetectable level of fluorescent reporter gene (eGFP or tagBFP). Thus, the histograms of GFP and BFP negative cells were plotted to represent the normal cell cycle profiles. Induced by 500μM $CuSO_4$, cells with the fluorescent signal of the corresponding reporter genes were gated, and the histograms show the cell cycle profiles of GFP positive, BFP positive or both positive cell. Cells transfected with shRNA-1-eGFP or shRNA-2-tagBFP show mild S-phase and G2/M accumulation. With the transfection of both shRNA-1-eGFP and shRNA-2-tagBFP, severe accumulation of cells at S-phase and G2/M were observed.

For simultaneous expression of shRNA and Top2 rescuing gene, we replaced one of the GFP reporter genes by an RNAi resistant wild-type Top2, Top2(S1428A,S1443A) (hereafter Top2-2SA), or Top2Δ20 with GFP fused at the C-terminus. As mentioned previously, fusion of GFP does not affect the binding of Mus101.

In addition to S and G2/M accumulation, the viability of Top2-silenced S2 cells was severely affected after 14-day copper induction (**Figure 27**). More than 50% of Top2-silenced cells were at sub-G1 population, which represents cells with DNA fragmentation, likely caused by cell apoptosis. Probed by permeability of propidium iodide, Top2-silenced cells were found to be less than 25% viable (**Figure 27**). The cell cycle defect and inviability caused by depletion of endogenous Top2 was rescued by expression of wild-type Top2, Top2-2SA, or Top2Δ20 (**Figure 27**).

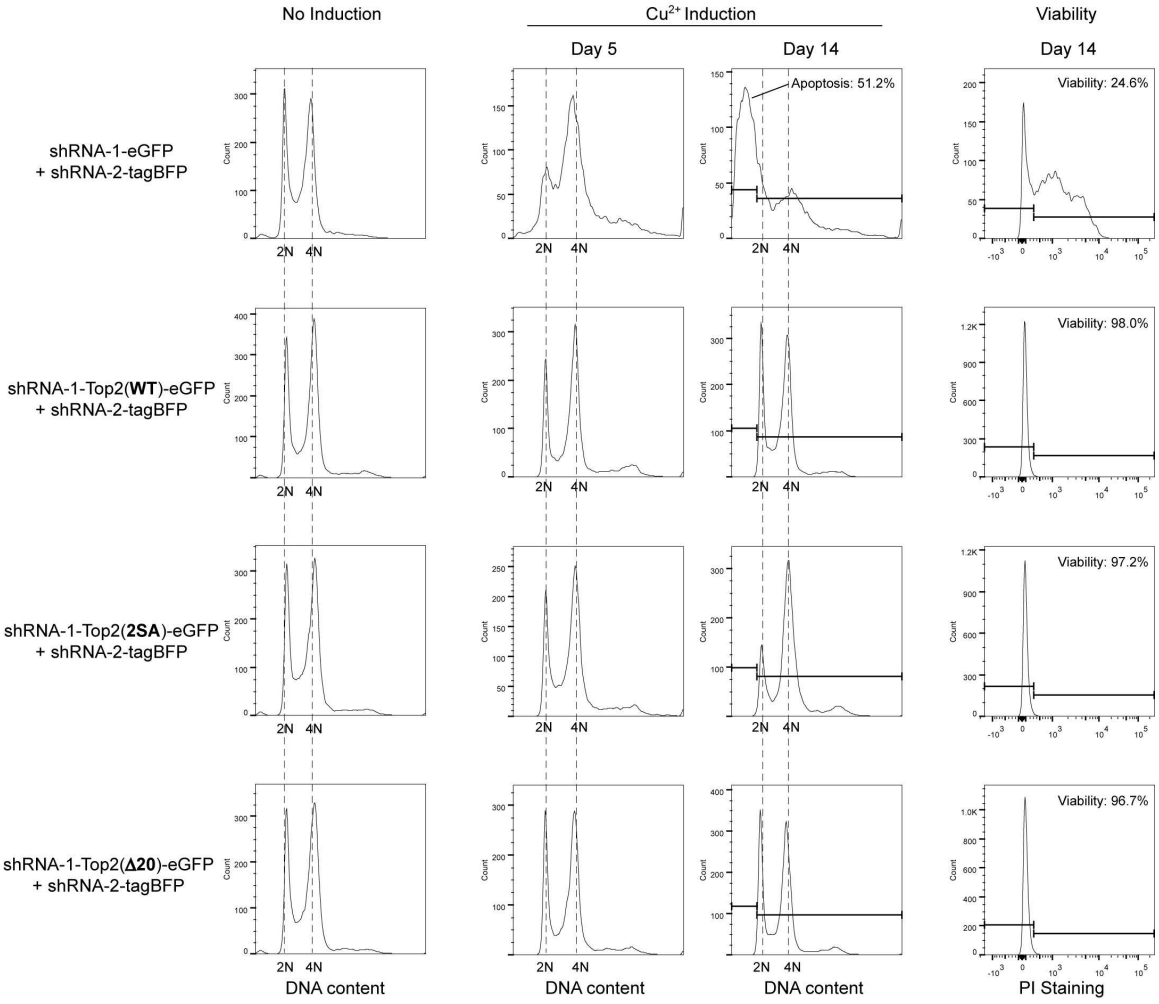

Figure 27: Cell cycle defect and cell inviability caused by Top2 depletion was rescued by Top2(WT), Top2(2SA), or Top2(Δ20). Four groups of cells were transfected with constructs indicated on the left. After 100 μM $CuSO_4$ induction, the cell cycle profiles were recorded on Day 5 and Day 14. The cells without $CuSO_4$ induction were shown as controls for normal cell cycle distribution. After 14 days of induction, cells expressing shRNA-1-eGFP and shRNA-2-tagBFP accumulated at sub-G1 on day 14, and only 24.6% of cells remained viable. Top2-depleted cells rescued by Top2(WT), Top2(2SA), and Top2(Δ20) appeared to be viable and normal in cell cycle distribution on Day 14.

No apparent cell cycle defects were observed after replacing endogenous Top2 with Top2-2SA, and Top2Δ20 for 14 days. However, after 29 days of copper induction,

Top2-silenced cells rescued by Top2Δ20 showed an increasing population at high DNA content (**Figure 28**). We were curious if the additional DNA content was from the increasing the copy number of chromosomes or the alteration in genome size through fusion or insertion. Thus, we compared the karyotype of these cells with untransfected S2 cells and Top2-silenced S2 cells rescued by wildtype-Top2. Higher copy numbers of chromosomes were observed in the Top2-silenced S2 cells rescued by Top2Δ20, indicating the incomplete segregation during mitosis (**Figure 28**).

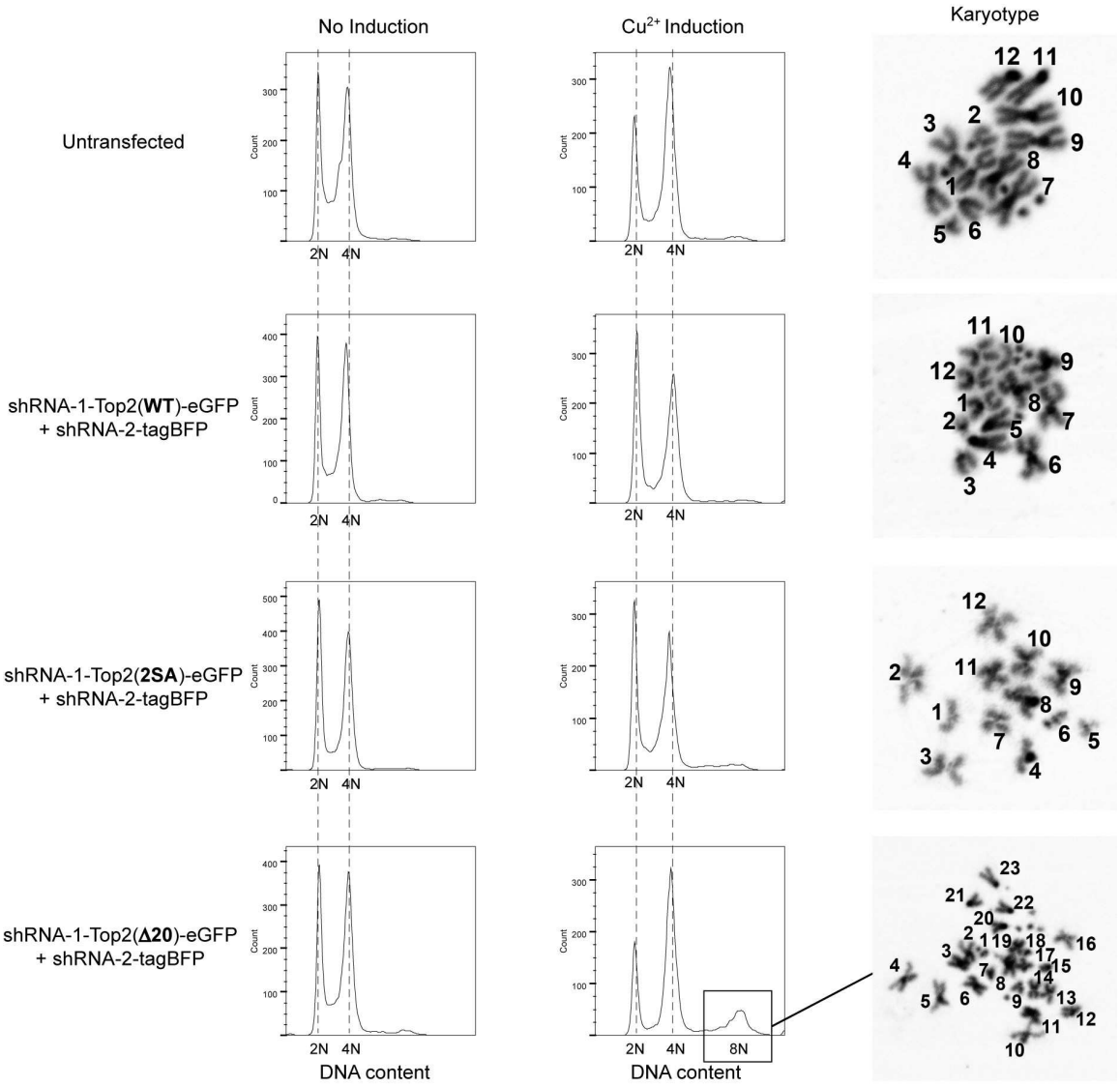

Figure 28: Long-term expression of Top2(Δ20) in Top2-depleted cells triggers the accumulation of a population with high DNA content. On Day 29 of CuSO4 induction, cell cycle profiles of S2 cells transfected with indicated constructs were recorded. Top2-depleted cells rescued by Top2(Δ20) showed a peak representing high DNA content, while cells rescued by Top2(WT) or Top2(2SA) showed no significant difference from untransfected cells. More than 20 chromosomes (compared to 12 long chromosomes in normal cells) were observed in the karyotype analysis of Top2-depleted cells rescued by Top2(Δ20).

3.2.10 Flies with Top2 null mutation complemented with Top2(S1428A, S1443A) and Top2Δ20 are viable but severely defective in fertility.

To test the biological consequences of abolishing Top2-Mus101 interaction in *Drosophila*, we generated transgenic flies carrying Top2-GFP (wild-type), or Top2-2SA-GFP by P-element transposition. We found Top2-2SA-GFP rescued the viability of Top2 null mutants (Data not shown). However, Top2 null mutant flies complemented by Top2-2SA-GFP had a severe fertility defect in both males and females (**Table 2**).

Table 2: Top2-2SA mutant cannot rescue fertility of top2 null flies. (Experiment was performed by Chia-hsiang Wu).

Female × Male	Number of female offspring	Number of male offspring
P2 × P2	174±19	172±27
P2 × $Top2^{17}/Top2^{35}$; P*{Top2-GFP}f*	143±38	142±31
P2 × P*{Top2-2SA-GFP}*/Y; $Top2^{17}/Top2^{35}$	0	0
$Top2^{17}/Top2^{35}$; P*{Top2-GFP}* × P2	166±30	186±27
P*{Top2-2SA-GFP}*; $Top2^{17}/Top2^{35}$ × P2	7±6	10±7

We further examined the spermatocytogenesis and found a delay in telophase of meiosis I in primary spermatocytes from Top2-null flies rescued by Top2-2SA-GFP, indicating that the Top2-Mus101 interaction is likely involved in DNA segregation during meiosis (**Figure 29**).

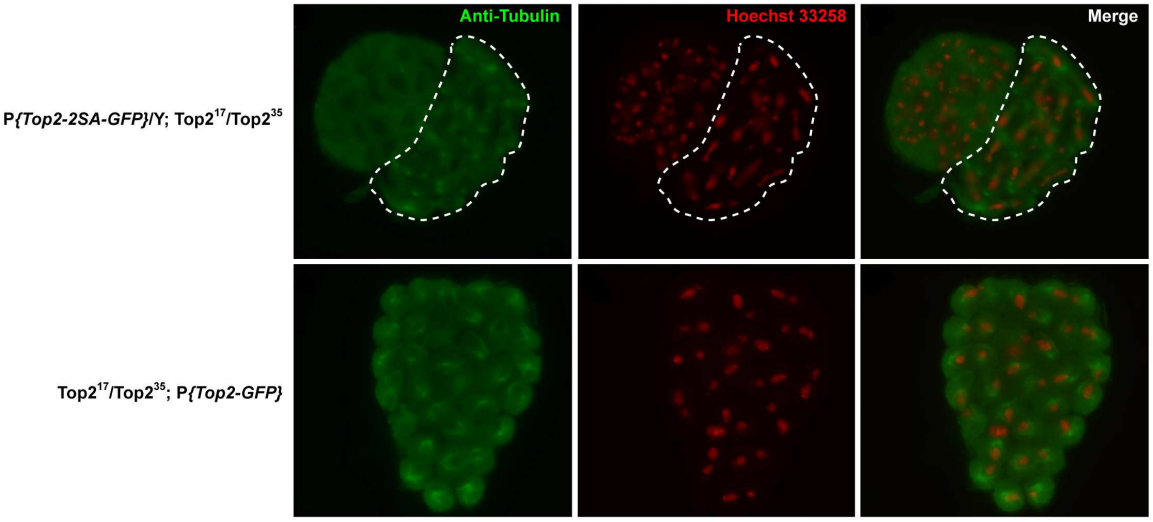

Figure 29: Top2 null flies rescued by Top2-2SA have delayed telophase in meiosis I during spermatogenesis. Cysts of 16 spermacytes in telophase of meiosis I were observed. (Experiment performed by Chia-hsiang Wu).

3.3 Discussion

In this study, we have identified that phosphorylated Ser1428 and Ser1443 of *Drosophila* Top2 are required for interaction with the N-terminus of Mus101. The binding of N-terminal domain of Mus101 to the Top2 CTD was found to inhibit decatenation activity of Top2 *in vitro*. In the cellular assay, Top2-silenced cells rescued by Top2-Δ20 had an increasing population at high DNA content, suggesting that Top2-Mus101 interaction is important for faithful DNA segregation. However, the fly genetic results showed Top2-2SA conferred a male and female sterile phenotype. In an immunofluorescence study on male spermatocytes, we found the fertility defect of Top2-2SA rescued flies was caused by a delay in telophase of meiosis I of

spermatogenesis, which implies that Top2-Mus101 interaction is required during chromosome segregation in meiosis *in vivo*.

3.3.1 Drosophila Top2-Mus101 interaction may function differently from human Top2β-TopBP1 interaction

According to our mapping results from co-IP and pull-down experiments, *Drosophila* Top2 interacts with the N-terminal 350 residues of Mus101 in a doubly phosphorylated manner. This conclusion differs from the yeast two-hybrid screen in the previous study which showed CTD of human Top2β binds the C-terminus of human TopBP1 (Yamane et al., 1997). Based on our results, the function of *Drosophila* Top2-Mus101 interaction was characterized as a part of the DNA segregation process, which is commonly considered to involve Top2α in human but not Top2β (Chen et al., 2013; Nitiss, 2009a). Nevertheless, the binding of two isoforms to TopBP1 in human may not be mutually exclusive. It is possible that human Top2α and Top2β both interact with TopBP1 through separate domains for different cellular functions. To confirm this hypothesis, further investigation is needed for the binding of TopBP1 to human Top2α or Top2β.

3.3.2 Regulation of Top2-Mus101 interaction

BRCT1/2 of Mus101 and its homologs are important for both initiation of replication and DNA damage signaling. On one hand, for assembling the pre-initiation complex during DNA replication, yeast Sld3 and human Treslin, the functional homolog of yeast Sld3, must be doubly phosphorylated by CDK on [S/T-P] motifs for the binding

of BRCT1/2 of yeast Dpb11 and human TopBP1, respectively (Boos et al., 2011; Kumagai et al., 2011; Zegerman and Diffley, 2007). On the other hand, Rad9, a member of the 9-1-1 clamp complex involved in the DNA damage response, interacts with BRCT1/2 of TopBP1 with modification mediated by Casein Kinase 2 on [S/T]-X-X-[D/E] motifs (Takeishi et al., 2010). In this study, we have found that BRCT1/2 of Mus101 are likely involved in a third event, DNA segregation. BRCT1/2 of Mus101 seem to be versatile enough to accommodate the binding of different sequence motifs phosphorylated by kinases from various signaling pathways. According to previous studies, *Drosophila* Top2 has been shown to be phosphorylated by Casein Kinase 2 (Ackerman et al., 1985). After examining the C-terminal sequence of *Drosophila* Top2, Casein Kinase 2 may be responsible for phosphorylating Ser1428 but less likely for Ser1443 which is not in a conserved [S/T]-X-X-[D/E] motif. We suspect that there may be other kinases required for the phosphorylation. Two likely candidate kinases, Aurora B Kinase, and Plk1 (Polo-like kinase 1), were recently discovered to phosphorylate human Top2α and they are both crucial regulators in the mitosis (Li et al., 2008; Losada et al., 2002; Morrison et al., 2002). Given the DNA segregation defect we observed after abolishing Top2-Mus101 interaction, one of these two kinases may modulate the interaction by phosphorylating the C-terminal domain of Top2.

3.3.3 Maintaining DNA segregation fidelity

Previous studies have shown that SUMOylation on the CTD of eukaryotic Top2 is required for its localization at the centromere for DNA segregation (Agostinho et al., 2008; Azuma et al., 2005). Here, we found phosphorylation of *Drosophila* Top2 also has a role in DNA segregation. After chromosomes are condensed by condensin complex and eukaryotic Top2, chromosomes are aligned in the middle of mitotic spindle and pulled by kinetochore-attached microtubules. To prevent aberrant segregation, the spindle assembly checkpoint monitors the proper attachment of microtubules on kinetochores and tension build-up between sister kinetochores. Cohesin also contributes to balance the pulling force by linking sister chromatids with its dimerized ring (Bloom, 2014). For a smooth segregation without physical obstructions in anaphase, Plk1 and Aurora B kinase facilitate the release of cohesion, and upon activation of anaphase-promoting complex, separase/separin removes the remaining cohesin allowing the completion of chromosome segregation (Losada et al., 2002; Onn et al., 2008). As mentioned above, eukaryotic Top2 could be phosphorylated by Plk1 or Aurora B kinase and interact with Mus101 (**Figure 30**). The inhibition of phosphorylated Top2 by the binding of Mus101 would be consistent with inhibition by SUMOylation at Lys660 to prevent recatenation of segregated chromosomes (Ryu et al., 2010). Through the phosphorylation by Plk1 or Aurora B kinase, the level of DNA-DNA catenation and cohesin-DNA interaction can be simultaneously adjusted which helps the proper chromosome segregation in anaphase.

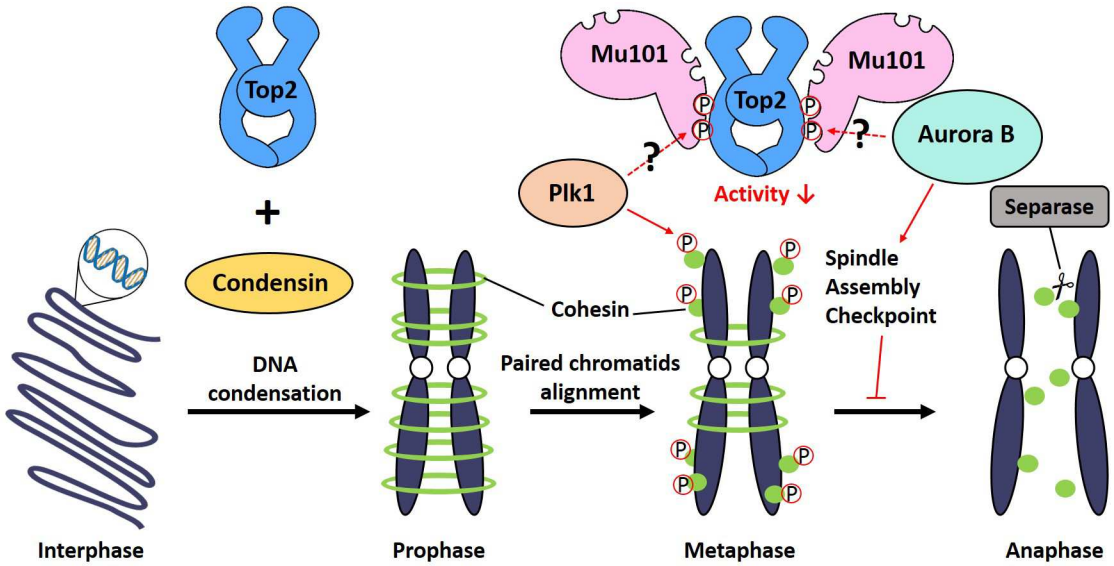

Figure 30: Model for the role of Top2-Mus101 interaction in mitosis. During prophase, Top2 and Condensin help chromatin condense into chromosomes, and paired replicated sister chromosomes are linked by dimerized cohesin. Upon phosphorylation by Plk1, most of the cohesin dimers are released from chromosomes. The remaining cohesin linkage at centromere and Aurora B kinase-mediated activation of spindle assembly checkpoint ensure the establishment of chromosome biorientation and balance the pulling force between bi-oriented sister kinetochores. Top2 might be phosphorylated by Plk1 or Aurora B kinase, and the subsquent Mus101 binding to phosphorylated Top2 inhibits its decatenation activity, which may contribute to balance tension between sister kinetochores by adjusting the level of DNA catenation.

3.4 Experimental procedures

3.4.1 Cloning and DNA Constructs

3.4.1.1 Constructs for co-immunoprecipitation assays

Full-length *Drosophila* Mus101 was cloned into a modified pMT/V5-His vector (Invitrogen), which contained a Flag tag as an N-terminal fusion peptide and the hygromycin resistance gene. Each fragment of Mus101, aa 1-350, aa 351-800, aa 801-1150, or aa 1151-1425, was cloned into another modified pMT/V5-His vector, which contained a nuclear localization signal, aa 582-607 from *Drosophila* RecQ4, as an N-terminal fusion peptide, a Flag tag as a C-terminal fusion peptide, and the hygromycin resistance gene.

Full-length *Drosophila* Top2 was cloned into a pMT-puro vector (Addgene from Sabatini lab) with an N-terminal HA tag. Three truncated Top2 constructs, headless (aa 397-1447), Δ240t (aa 1-1207), or core (397-1207), were individually built in the same way as the full-length Top2 construct, with the addition of a nuclear localization signal, aa 1306-1322 from *Drosophila* Top2, at their C-termini. The CTD was previously determined to be the last 240 amino acids of Top2 (Crenshaw and Hsieh, 1993).

3.4.1.2 C-terminal truncated and mutant forms of Top2 constructs for pull-down assays

All truncated and mutant Top2 constructs, Top2Δ125t (aa 1-1322), Top2Δ59t (aa 1-1388), Top2Δ20t (aa 1-1427), Top2Δ5t (aa 1-1442), Top2(S1392A, S1396A, S1409A, S1410A, S1428A, S1443A), Top2(S1392A, S1396A, S1409A, S1410A), Top2(S1428A,

S1443A), Top2(S1428A), Top2(S1443A), were cloned into pMT-puro vectors with N-terminal HA tags.

3.4.1.3 Mus101 constructs for pull-down assays

Full-length *Drosophila* Mus101 was cloned into a modified pET41a vector (Novagen), to which a linker containing PreScission protease cleavage site was added between an N-terminal Glutathione S-Transferase (GST) fusion tag and Mus101. In addition, the C-terminus of Mus101 was fused with a hexahistidine (6×His) tag.

Mus101[1-350], N-terminus of Mus101 containing aa 1-350, was made by replacing the full-length Mus101 with Mus101 residues 1-350, preserving the N-terminal GST fusion tag plus the PreScission protease cleavage site and the C-terminal 6×His tag.

3.4.1.4 Inducible plasmid-based shRNA system for cellular assays

Our inducible plasmid-based shRNA system was adapted from an intron-mediated shmiR expression system by Haley *et al*. with the following modifications (Haley et al., 2010). In order to make it compatible for easily switching between the shRNA sequences predicted from DSIR algorithm (Vert et al., 2006), 1) HindIII and BamH1 restriction enzyme sites flanking the shRNA sequence were substituted with AvrII and SacI sites, respectively; 2) EcoRI, XbaI, and BglII sites were replaced by BamHI site for connecting ftz intron donor sequence and 5′ miR-1 stem base; 3) SpeI site was changed to BglII site for connecting 3′miR-1 stem base and *ftz* intron accepter sequence. The 3′ of *ftz* intron accepter sequence was ligated with a reporter gene, eGFP or tagBFP

by NheI site. The complete cassette, including *ftz* intron, miR-1 stem base, shRNA sequence, and the reporter gene, was inserted between SpeI and MluI sites of either a pMT-puro vector (Addgene from Sabatini lab) or a modified pMT/V5-His vector (Invitrogen). To simultaneously express Top2 gene (wild-type or mutants), the reporter gene, eGFP or tagBFP, was replaced by sequence of Top2 (wild-type), Top2(S1428A,S1443A), or Top2Δ20 with a GFP as a C-terminal fusion protein.

3.4.1.5 Construction of transgenes P*{Top2-GFP}*, P*{Top2-2SA-GFP}*, and P*{Top2-Δ20-GFP}*

Transgene P*{Top2-GFP}* was constructed in the following two steps: 1) Genomic fragment of Top2 gene including 3′ untranslated region was inserted into pCaSpeR2 vector DNA (Thummel et al., 1988); 2) GFP gene was then inserted at the end of the Top2 gene, right before the termination codon. P*{Top2-2SA-GFP}, and* P*{Top2-Δ20-GFP}* were modified from P*{Top2-GFP}*by using overlap extension PCR to accomplish site-direct mutagenesis or internal deletion of 20 amino acids in the C-terminus (Ho et al., 1989). The sequences of the constructs were confirmed before injecting into *Drosophila* embryos following previously published procedure (Rubin and Spradling, 1982).

3.4.2 Transfection of *Drosophila* S2 cells

16-24 hr before transfection, *Drosophila* S2 cells were seeded at 1×10^6 /mL in 3 mL of Schneider's *Drosophila* medium (Life technologies) containing 10% heat-inactivated fetal bovine serum (FBS, HyClone) and 50 μg/mL of gentamicin (Gibco) using 6-well plates at 27°C. Transfections of plasmids were performed using *Trans*IT-

2020 transfection reagent (Mirus). 2.5 μg of recombinant plasmid DNA and 7.5 μL of *Trans*IT-2020 transfection reagent were added into 250 μL of serum free medium. After mixing the components, the DNA complexes were formed with room temperature incubation for 30 min. The serum free medium containing the complexes was then added drop-wise into cells. 16-24 hr after transfection, the cells were washed and replaced with fresh medium containing 10% FBS. 48 hr later, antibiotics, Hygromycin B 300 μg/mL (HyClone) or puromycin 6 μg/mL (Life technologies), were used for stable transfection.

3.4.3 Immunoprecipitation assay with nuclear extract of *Drosophila* S2 cells

Transfected and stably selected S2 cells were seeded at 2×10^6/ mL in 40 mL of Schneider's *Drosophila* medium containing 10% heat-inactivated FBS and 50 μg/mL of gentamicin (Gibco) using T-150 flask at 27°C. After culturing for 4 days, cells were induced from the metallothionein promoter (pMT/V5-His and pMT-puro vectors) with $CuSO_4$ at the final concentration of 500μM for 16 hr. The cells overexpressing proteins of interest were then harvested by centrifuging at 2000 × g for 3 min and resuspended by phosphate buffered saline, PBS. All solutions were supplemented with homemade protease inhibitor cocktail which contains 1mM PMSF (Sigma), 5 μg/mL E-64 (Peptide international), 5 μg/mL Leupeptin (Peptide international), 2 μg/mL Pepstatin (Peptide international), and 2 μg/mL Aprotinin (Peptide international) unless otherwise specified. In order to obtain the nuclear extract for immunoprecipitation, the cells were lysed by a

dounce homogenizer in hypotonic buffer, 2 mM $MgCl_2$ and 5 mM HEPES buffer pH 7.4, and then placed on ice for 10 min. After centrifuging at 16,000 × g for 5 min, the pellet that contains nuclei was washed with hypotonic buffer before another centrifugation at 16,000 × g for 5 min. The pellet was then resuspended with nuclear extraction solution, 20 mM HEPES buffer pH 7.4, 400 mM NaCl, 10% glycerol, 0.2% NP40 Alternative (CALBIOCHEM), and 1 mM EDTA, on ice for 30 min. Nuclear extraction dilution solution, 20 mM HEPES buffer pH 7.4, 10% glycerol, 0.2% NP40 Alternative, and 1 mM EDTA, was added to bring NaCl down to 250mM before adding 40 µL anti-Flag (Sigma, A2220) or anti-HA agarose beads (Sigma, A2095) in the presence of 100µg/mL ethidium bromide. After incubating at 4°C for 1 hr, antibody agarose beads were spun down at 2000 × g for 5 min, washed 3 times with adjusted nuclear extraction solution (250mM NaCl), resupsended with SDS-PAGE sample buffer, and boiled for 5 min before loading onto 8% SDS-PAGE for western blotting. Rabbit anti-Flag antibody (Sigma, F7425) and mouse anti-HA antibody (Sigma, H9658) were used for detection of Flag- or HA- tagged proteins.

3.4.4 Purification of Mus101 and Mus101[1-350] for pull-down assays

N-terminal GST- and C-terminal 6×His- double tagged full-length Mus101 or Mus101[1-350] was overexpressed by *Escherichia coli* expression strain Rosetta2 (DE3) (Novagen) with 0.4mM Isopropyl b-D-1-thiogalactopyranoside (IPTG) at 16°C for 16 hr at 170 rpm. The cells were then harvested by centrifugation at 4500 × g for 10 min and

washed in 100 mL of 20mM HEPES pH 7.4, and 150 mM NaCl. After washing, cell pellet was collected by centrifugation at 4500 × g before storing at -80°C.

Cell pellet from 12 L of culture for full-length Mus101 or 6 L of culture for Mus101[1-350] was resuspended in 100 mL of lysis buffer, 50 mM HEPES pH 7.4, 0.5 M NaCl, 10% glycerol, and 0.02% Triton X-100. All solutions for purification were supplemented with 5 mM 2-mercaptoethanol (Sigma), 1mM EDTA, and homemade protease inhibitor cocktail unless otherwise specified. 100 mL of cell suspension was treated with 1 mg/mL of lysozyme at room temperature for 30 min and lysed by sonication (7 × 7 sec bursts with 7 sec intervals at 45% amplitude on ice). The lysate was then centrifuged at 15,000 × g for 10 min to remove cell debris. After centrifugation, the supernatant was collected to incubate with 2 mL of a slurry of 76% Glutathione Sepharose 4B resin (GE healthcare) at 4°C for 2 hr. The resin was washed 10 times with 10 mL modified lysis buffer, 50mM HEPES pH 7.4, 0.5 M NaCl, 5% glycerol, and 0.02% Triton X-100 without EDTA, E-64 and Aprotinin. After washing, the resin was resuspended in 15 mL modified lysis buffer before adding 80 units of PreScission protease at 4°C for 16 hr.

After incubation, protein solution was collected by flowing through a poly-prep column (*BIO-RAD*) and directly loaded onto 1 mL Ni-NTA agarose resin (Qiagen). The Ni-NTA agarose resin was washed extensively by 100mL of 20 mM imidazole pH 7.0, 1M NaCl, 5% glycerol, and 0.02% Triton X-100, and the protein was eluted by 10mL of

400 mM imidazole pH 7.0, 1M NaCl, 5% glycerol, and 0.02% Triton X-100. The protein solution was stored at -80°C after three times of dialysis against 300 mL of 25 mM HEPES pH 7.4, 0.5 M NaCl, 0.1mM EDTA without E-64 and Aprotinin.

3.4.5 Immobilizing Top2 proteins on anti-HA agarose resin for pull-down assays

S2 cells stably transfected with a plasmid encoding truncated or mutant Top2 proteins were seeded at 2×10^6/ mL in 40 mL of Schneider's *Drosophila* medium containing 10% heat-inactivated FBS and 50 µg/mL of gentamicin (Gibco) using T-150 flask at 27°C. After 3 days of culturing, 500 µM $CuSO_4$ was added to the cells to induce the metallothionein promoter for expressing protein of interest for 16 hr. The cells were then harvested by centrifuging at 2000 × g for 3 min and washed by PBS. All solutions were supplemented with 5mM 2-mercaptoethanol, 5 mM NaF (Sigma), 1 mM Na_3VO_4 (Sigma), and homemade protease inhibitor cocktail unless otherwise specified. The cells were spun down and lysed by 2 mL of lysis buffer, 20 mM HEPES pH7.4, 400 mM NaCl, 10% glycerol, 0.1 µM okadaic acid (Sigma), 5 mM EDTA, and 1% NP40 Alternative on ice for 20 min. After centrifugation at 16,000 × g for 5 min, the pellet was incubated again with 2 mL of lysis buffer for 20 min. After another centrifugation at 16,000 × g for 5 min, 4 mL of supernatant was collected and incubated with 60 µL of a slurry of 50% anti-HA agarose resin (Sigma, A2095) at 4°C for 2 hr in the presence of 100 µg/mL ethidium bromide. The resin was then washed two times with 1 mL of lysis buffer and three times with 1 mL of high salt lysis buffer, 20 mM HEPES pH7.4, 1 M NaCl, 10% glycerol, 0.1

μM okadaic acid, 5 mM EDTA, and 1% NP40 Alternative. Truncated or mutant Top2 proteins anchored on the resin were stored at -20°C after replacing the solution 3 times with 1 mL storage solution, 20 mM HEPES pH7.4, 500 mM NaCl, 50% glycerol, 0.1 μM okadaic acid, 5 mM EDTA, and 1% NP40 Alternative.

3.4.6 Dephosphorylation of immobilized Top2 by λ-phosphatase

The resin containing immobilized Top2 proteins was washed 2 times with incubation buffer, 20 mM HEPES pH7.4, 200 mM NaCl, 5% glycerol, 1 mM EDTA, 50 μg/mL bovine serum albumin (BSA, Research Organics), 1 mM PMSF, and 5 μg/mL Leupeptin, to eliminate the interference of phosphatase inhibitors. The dephosphorylation of Top2 was accomplished by adding 3 mM $MnCl_2$ and 20 units λ-phosphatase (NEB) per μL of resin at 30°C for 30 min with two controls, one with 3 mM $MnCl_2$ only and the other with 3 mM $MnCl_2$ and λ-phosphatase in the presence of 5 mM NaF, 1 mM Na_3VO_4, and 0.1 μM okadaic acid. After the treatment, the resin was subjected to pull-down assays or elution of proteins.

3.4.7 Pull-down assays

The resin containing 2 pmole of immobilized Top2 proteins was washed 2 times with 200 μL incubation buffer (same composition as mentioned previously), and resuspended with 200 μL incubation buffer before incubating with 64 pmole of Mus101[1-350]-6×His or 4.5 pmole of full-length Mus101 at 4°C for 1 hr. After washing resin 3 times with 200 μL incubation buffer, the sample was loaded onto 8% SDS-PAGE

after boiling with SDS-PAGE sample buffer for 5 min. Proteins were detected by western blotting with rabbit anti-Mus101 antibody for full-length Mus101, mouse anti-His for Mus101[1-350]-6×His (Roche), and mouse anti-HA antibody for HA-tagged Top2 proteins.

3.4.8 Purification of Top2 from Drosophila S2 cells with or without λ-phosphatase treatment

HA tagged Protein purification kit (MBL) was used for purification of Top2 proteins. HA-tagged Top2 proteins overexpressed from 120 mL culture of *Drosophila* S2 cells were immobilized by 40 μL of resin provided in the kit with the same procedure as aforementioned. Immobilized proteins were then treated with or without λ-phosphatase in the presence of 3 mM $MnCl_2$ at 30°C for 30 min as previously mentioned. The resin was washed two times with 200 μL washing solution (part of purification kit) before elution of proteins. The proteins were eluted with 80 μL of peptide solution, 2 μg/μL HA peptide in PBS, and then stored at -80°C.

3.4.9 Decatenation assays

Purified *Drosophila* Top2 with or without λ-phosphatase treatment was used for decatenation activity. 0.5 ng of Top2 proteins were added to a 20 μL reaction buffer containing 0.1 μg kDNA (Topogen), 20 mM HEPES pH 7.4, 100 mM NaCl, 50 mM KCl, 10 mM $MgCl_2$, 0.1 mM, EDTA, BSA 50 μg/mL, 5 mM 2-mercaptoethanol, and ATP 1 mM, in the presence of 0, 0.625, 1.25, or 2.5 μM of Mus101. The samples were then incubated at 30°C for 15 min. The reactions were quenched by adding 4 μL of 6 × DNA dyes

containing 6% sodium dodecyl sulfate (SDS) and 60 mM EDTA and 2 μL of 10 mg/mL proteinase K at 55°C for 10 min. The samples were analyzed by electrophoresis in 1% agarose gel with ethidium bromide. The levels of catenated substrate kDNA and decatenated product DNA were quantified by ImageJ software. The relative ratio of product DNA was measured by dividing the signals of two decatenated product DNA by the total signals in the lane.

3.4.10 Peptide synthesis

C-terminal biotinylated unphosphorylated and doubly phosphorylated peptides containing the last 25 amino acids of Drosophila Top2 were synthesized by the Peptide Synthesis Core Facility of Institute of Cellular and Organismic Biology, Academia Sinica and purified by HPLC. The final products attained > 95% purity and were confirmed by ESI-MS. Peptide Synthesis Core Facility, ICOB, Academia Sinica. Following are the sequences of the peptides.

RAVIESDDDDIEIDEDDDDSDFNC-Biotin

RAVIE(pS)DDDDIEIDEDDDDD(pS)DFNC-Biotin

3.4.11 Surface Plasmon Resonance experiments

Surface plasmon resonance measurements were performed on a BIAcore 2000 (GE healthcare). A streptavidin sensor chip was derivatized with C-terminal biotinylated unphosphorylated peptide (144 response units) or doubly phosphorylated peptide (145 response units) described above. Due to the instability of Mus101[1-350],

the temperature of the BIAcore machine and samples was maintained at 10°C. Solutions (100 µL) of Mus101[1-350] at indicated concentration in 20 mM HEPES pH 7.4, 250 mM NaCl, 5% glycerol, 1 mM EDTA, and 0.005% surfactant P20 (GE healthcare) were flowed across the chip surface at a rate of 20 µL/min. The chip was regenerated by injecting 60 µL of 0.1% SDS (GE healthcare).

3.4.12 Cell cycle analysis by flow cytometry

S2 cells were transfected with constructs for expressing inducible shRNA and selected as described above. For testing the effect of shRNA and co-expression of Top2 gene, 0 µM, 10 µM or 100 µM of CuSO4 was added to S2 cells seeded at 1×10^6 /mL in 3mL using 6-well plates at 27°C. After 96 hr of culture, 3×10^6 /mL S2 cells were collected. The cells were washed with 1 mL PBS and cross-linked with 1% paraformaldehyde at 4°C for 1 hr. The cross-linked cells were then washed by 3 mL PBS before permeabilized by 1 mL 70% ethanol for at least 2 hr. After the treatment, the cells were stained with 40 µg/mL propidium iodide (Biolegend) with 40 µg/mL RNase (Affymetrix) at 37°C for 30 min. Flow cytometer (BD FACSCanto II) were then used to select cells at proper size and singlet. Based on the reporter genes, the eGFP positive, tagBFP positive, or double positive cells were gated for cell cycle analysis.

3.4.13 Karyotype analysis

To investigate the morphology and integrity of the metaphase chromosomes, *Drosophila* S2 cells seeded at 1×10^6 /mL in 3mL using 6-well plates at 27°C for 1 day as

mentioned previously. Before preparing metaphase chromosome spreads, 2.5 μg/mL of colcemid (Sigma-Aldrich) was added to the cells and the plates were incubated on a shaker at 50 rpm for 3 hr. After harvesting the cells, hypotonic buffer, 0.8% Na Citrate, was added drop-wise to the cells with constantly mixing and the cells were incubated at room temperature for 10 min. The samples were then washed by 5 mL fixative, methanol: glacial acetic acid (3:1), drop-wise with constantly mixing. After repeatedly washed by fixative for at least 4 times, samples were stained with 1 μg/mL DAPI before mounting on alcohol cleaned glass slides for microscopy.

4. Summary and Perspective

4.1 Summary

In the project described in chapter 2, we added a new element into a previously developed method, pulse-alkylation mass spectrometry, to monitor dynamic conformation of high-molecular-weight *hs*Top2α by measuring the thiol reactivities with monobromobimane. Most of the measured reactivities are consistent with the level of solvent accessibility predicted from a homology structural model generated by the crystal structures. Next, we found both AMPPNP and ICRF-193 can trigger N-gate closure as indicated by decreased reactivities of cysteines in both GHKL subdomain (Cys 170 and Cys 216) and upper transducer subdomain (Cys 300 and Cys 392). Besides N-gate closure, AMPPNP can simultaneously enhance accessibility at the DNA-gate as well. In an interesting contrast, ICRF-193 binding only allows the N-gate movement but limits solvent accessibility of DNA-gate in *hs*Top2α. Finally, Cys427 located near DNA gate becomes significantly more reactive to monobromobimane after truncating 310 residues from the C-terminus of full-length *hs*Top2α, implying the C-terminal domain of *hs*Top2α localized beside DNA gate.

In the project described in chapter 3, we switched our focus from protein dynamics to protein regulation via protein-protein interaction. Continuing the uncharacterized human Top2β-TopBP1 interaction, we confirmed *Drosophila* Top2 interacts with Mus101, a *Drosophila* TopBP1 homolog. Furthermore, using co-IP, pull-

down, and surface plasmon resonance experiments, phosphorylations of Ser1428 and Ser1443 were identified to be critical for the binding of N-terminus of Mus101. Binding of Mus101 to Top2 in vitro inhibits Top2 decatenation activity. Demonstrated by cellular assays and fly genetics, Top2-Mus101 interaction participates in the DNA segregation process *in vivo*. We proposed that Top2-Mus101 interaction may coordinate with cohesin to modulate the level of catenation and equalize the force pulling from the kinetochore-attached microtubules for maintaining the fidelity of DNA segregation.

4.2 Future directions

4.2.1 Broadening the application of pulse-alkylation mass spectrometry by using arginine specific labeling reagent

Our new probing method detects conformational changes of *hs*Top2α through alkylating cysteines with monobromobimane. However, not all proteins of interest have cysteines evenly distributed for analysis. Therefore, other reagents that selectively label different side chains may be useful for broadening the application of pulse-alkylation mass spectrometry to detect protein dynamics.

Phenylglyoxal was previously reported to selectively react with the guanido group of arginine under ambient conditions (Carven and Stern, 2005; Takahashi, 1968; Wood et al., 1998). Phenylglyoxal has been used to label rabbit muscle creatine kinase followed by a high-resolution tandem mass spectrometry analysis (Wood et al., 1998). The purpose of arginine labeling was to search for the active arginines that are required

for enzyme activity, so the phenylglyoxal labeling was quenched as the enzyme became mostly inactive (below 15% of the original activity). Three arginines in the ATPase motif, Arg 291, Arg 129, and Arg 131, have been found to be modified by phenylglyoxal which suggests these arginines are critical for enzyme function and likely to be important for ATP binding. These arginines indeed locate at the site of the ATP binding pocket according to the crystal structure, which supports the chemical modification approach (Wood et al., 1998).

In another study, a derivative of phenylglyoxal, *p*-hydroxyphenylglyoxal, was used in a combination with other chemical modifiers to study conformational change of HLA-DR1, a class II MHC variant, in the presence or absence of a binding peptide. A cluster of arginines, Arg50α, Arg123α, and Arg189β, are modified only under the condition without the peptide, which helps to identify a region involved in conformational changes upon the binding of the peptide. Thus, phenylglyoxal has been proven to be a useful for probing conformational changes by labeling arginines (Carven and Stern, 2005).

There are 5 non-exchangeable hydrogens on the phenyl ring of phenylglyoxal that can be substituted with deuterium. Using deuterated and normal phenylglyoxal, protein can be labeled differentially under different conditions. 5-Da difference between deuterated and normal phenylglyoxal also allows sufficient separation on the mass spectrometry analysis. Similar to monobromobimane, quantitative analysis on protein

conformational changes can likely be conducted by pulse-alkylation mass spectrometry using phenylglyoxal.

4.2.2 Structural perspective of Top2-Mus101 interaction

As the increasing number of BRCT domains from various proteins are being discovered, there have been differences revealing between BRCT domains, i.e. single BRCT domain or paired BRCT domains; phosphorylation-dependent or phosphorylation-independent (Leung and Glover, 2011). Many paired BRCT domains shown in the crystal structures hold one lysine-containing phosphate binding pocket and interact with singly phosphorylated targets, for example, phosphorylated BACH1 binding to BRCT domains of BRCA1 and BRCT7/8 of TopBP1, and phosphorylated C-terminal tail of γH2Ax binding to BRCT domains of MDC1 (Botuyan et al., 2004; Campbell et al., 2010; Leung et al., 2011). Different from the BRCT pairs described above, the binding of N-terminus of Mus101 to C-terminus of Top2 requires phosphorylation on both Ser1428 and Ser1443. It is highly possible that the paired BRCT1 and BRCT2 of Mus101 are involved in the interaction. Both BRCT1 and BRCT2 harbor lysine-containing phosphate binding pockets for stabilizing phosphorylated sequences. Although Rad9, Sld3, and Treslin were previously found to be doubly phosphorylated for the binding of BRCT1/2, there has not been any structure showing how BRCT1/2 interact with doubly phosphorylated substrates (Boos et al., 2011; Takeishi et al., 2010; Zegerman and Diffley, 2007). Compared with all other doubly phosphorylated

substrates for BRCT1/2, Ser1428 and Ser1443 of *Drosophila* Top2 are only 15 amino acids apart, which is the shortest among all BRCT1/2 binding targets. The doubly phosphorylated peptide we used in our surface plasmon resonance experiment could be useful for a potential co-crystallography or NMR study with BRCT1/2 of Mus101. The crystal structure of Apo-BRCT1/2 has been previously solved using the N-terminus of human TopBP1 (Rappas et al., 2011). In the Apo-BRCT1/2 structure, the relative orientation between BRCT1 and BRCT2 is different from the orientation between canonical paired BRCT domains, which may be clues for how BRCT1/2 accommodate doubly phosphorylated substrates (Kilkenny et al., 2008; Leung et al., 2011; Rappas et al., 2011). However, BRCT1/2 of TopBP1 is missing a direct structural evidence as clear as canonical BRCT domains. In a co-crystal structure of BACH1 peptide and C-terminal domain of BRCA1, the arrangement of the canonical paired BRCT domains allows the phosphate of BACH1 peptide fitting into the lysine-containing pocket of one BRCT domain with the linker region between two BRCT domains stabilizing the +3 phenylalanine (Botuyan et al., 2004). Since there has not been a co-crystal structure of BRCT1/2 domains with doubly phosphorylated substrate, it may provide insight for understanding how BRCT1 and BRCT2 domains coordinate with each other upon the binding of doubly phosphorylated substrate by comparing apo-BRCT1/2 and substrate-bound BRCT1/2.

4.2.3 Other undissected Top2 functions

Disrupting the interaction between Top2 and Mus101 in *Drosophila* helps to clarify one of the Top2 functions in DNA segregation. Other than DNA segregation, Top2 also participates in DNA replication (Chen et al., 2013; Nitiss, 2009a). However, it remains unclear how Top2 is recruited to the sites of topological problems during DNA replication. Despite the discovery of many Top2 binding partners, not many of the interactions have been directly linked to their biological functions. It is likely that the recruitment of Top2 to its targets during DNA replication is mediated through protein-protein interaction.

There has been plenty of evidence showing Top2 is near the replication origin and migrates along with the replicative machinery. In a previous study, human Top2α was examined in a co-immunoprecipitation assay and it did not directly associate with components of ORC complex. However, after centrifuging nuclease treated nuclei, human Top2α was found to co-sediment with ORC complex among the tri-nucleosome fractions, indicating human Top2α is in the vicinity of origin (Hu et al., 2009). By examining proteins from S phase chromatin in *Xenopus* system, Top2 co-migrates with Mcm2-7, a replicative helicase, in a gel filtration analysis (Gambus et al., 2011). Although it is still unclear how Top2 moves along with MCM complex, Top2 does appear to be associated with process of origin firing and replication, which is in accordance with the

notion that Top2 removes the DNA supercoiling and precatenanes generated during DNA replication.

PCNA is a Top2 binding partner in chicken, which could be the missing link that connects Top2 with DNA replication. The interaction was shown in an *in vitro* pull-down experiment using purified C-terminal domain of Top2α and PCNA. The PCNA binding interface of Top2 was further narrowed down to a QTxhxF motif at the C-terminus (Niimi et al., 2001). The interaction can likely be abolished by generating Top2 mutant with alanine substitutions at QTxhxF motif. Similar to our strategy for Top2-Mus101 interaction, the Top2 mutant that abolishes PCNA binding could be used to study Top2-PCNA interaction under the Top2-silenced background in S2 cell line or Top2 null background in fly genetics. By examining the phenotypes of the S2 cells or flies harboring only Top2 mutant, we are able to learn if the biological function of Top2-PCNA interaction is related to DNA replication.

References

Ackerman, P., C.V. Glover, and N. Osheroff. 1985. Phosphorylation of DNA topoisomerase II by casein kinase II: modulation of eukaryotic topoisomerase II activity in vitro. *Proc Natl Acad Sci U S A*. 82:3164-3168.

Agostinho, M., V. Santos, F. Ferreira, R. Costa, J. Cardoso, I. Pinheiro, J. Rino, E. Jaffray, R.T. Hay, and J. Ferreira. 2008. Conjugation of human topoisomerase 2 alpha with small ubiquitin-like modifiers 2/3 in response to topoisomerase inhibitors: cell cycle stage and chromosome domain specificity. *Cancer Res*. 68:2409-2418.

Apuy, J.L., Z.Y. Park, P.D. Swartz, L.J. Dangott, D.H. Russell, and T.O. Baldwin. 2001. Pulsed-alkylation mass spectrometry for the study of protein folding and dynamics: development and application to the study of a folding/unfolding intermediate of bacterial luciferase. *Biochemistry*. 40:15153-15163.

Araki, H. 2011. Initiation of chromosomal DNA replication in eukaryotic cells; contribution of yeast genetics to the elucidation. *Genes & genetic systems*. 86:141-149.

Araki, H., S.H. Leem, A. Phongdara, and A. Sugino. 1995. Dpb11, which interacts with DNA polymerase II(epsilon) in Saccharomyces cerevisiae, has a dual role in S-phase progression and at a cell cycle checkpoint. *Proc Natl Acad Sci U S A*. 92:11791-11795.

Atassi, M.Z., A.M. Suliman, and A.F. Habeeb. 1972. Enzymic and immunochemical properties of lysozyme. VI. Conformation, enzymic activity and immunochemistry of derivatives modified at arginine residues. *Immunochemistry*. 9:907-920.

Azuma, Y., A. Arnaoutov, T. Anan, and M. Dasso. 2005. PIASy mediates SUMO-2 conjugation of Topoisomerase-II on mitotic chromosomes. *EMBO J*. 24:2172-2182.

Bachant, J., A. Alcasabas, Y. Blat, N. Kleckner, and S.J. Elledge. 2002. The SUMO-1 isopeptidase Smt4 is linked to centromeric cohesion through SUMO-1 modification of DNA topoisomerase II. *Mol Cell*. 9:1169-1182.

Baird, C.L., T.T. Harkins, S.K. Morris, and J.E. Lindsley. 1999. Topoisomerase II drives DNA transport by hydrolyzing one ATP. *Proc Natl Acad Sci U S A*. 96:13685-13690.

Bellon, S., J.D. Parsons, Y. Wei, K. Hayakawa, L.L. Swenson, P.S. Charifson, J.A. Lippke, R. Aldape, and C.H. Gross. 2004. Crystal structures of Escherichia coli topoisomerase IV ParE subunit (24 and 43 kilodaltons): a single residue dictates differences in novobiocin potency against topoisomerase IV and DNA gyrase. *Antimicrob Agents Chemother*. 48:1856-1864.

Bender, R.P., A.J. Ham, and N. Osheroff. 2007. Quinone-induced enhancement of DNA cleavage by human topoisomerase IIalpha: adduction of cysteine residues 392 and 405. *Biochemistry*. 46:2856-2864.

Bender, R.P., H.J. Lehmler, L.W. Robertson, G. Ludewig, and N. Osheroff. 2006. Polychlorinated biphenyl quinone metabolites poison human topoisomerase IIalpha: altering enzyme function by blocking the N-terminal protein gate. *Biochemistry*. 45:10140-10152.

Bergerat, A., B. de Massy, D. Gadelle, P.C. Varoutas, A. Nicolas, and P. Forterre. 1997. An atypical topoisomerase II from Archaea with implications for meiotic recombination. *Nature*. 386:414-417.

Bloom, K.S. 2014. Centromeric heterochromatin: the primordial segregation machine. *Annual review of genetics*. 48:457-484.

Boos, D., L. Sanchez-Pulido, M. Rappas, L.H. Pearl, A.W. Oliver, C.P. Ponting, and J.F. Diffley. 2011. Regulation of DNA replication through Sld3-Dpb11 interaction is conserved from yeast to humans. *Curr Biol*. 21:1152-1157.

Botuyan, M.V., Y. Nomine, X. Yu, N. Juranic, S. Macura, J. Chen, and G. Mer. 2004. Structural basis of BACH1 phosphopeptide recognition by BRCA1 tandem BRCT domains. *Structure*. 12:1137-1146.

Boyd, J.B., M.D. Golino, T.D. Nguyen, and M.M. Green. 1976. Isolation and characterization of X-linked mutants of Drosophila melanogaster which are sensitive to mutagens. *Genetics*. 84:485-506.

Bruck, I., and D.L. Kaplan. 2011. Origin single-stranded DNA releases Sld3 protein from the Mcm2-7 complex, allowing the GINS tetramer to bind the Mcm2-7 complex. *J Biol Chem*. 286:18602-18613.

Campbell, S.J., R.A. Edwards, and J.N. Glover. 2010. Comparison of the structures and peptide binding specificities of the BRCT domains of MDC1 and BRCA1. *Structure*. 18:167-176.

Cardenas, M.E., R. Walter, D. Hanna, and S.M. Gasser. 1993. Casein kinase II copurifies with yeast DNA topoisomerase II and re-activates the dephosphorylated enzyme. *J Cell Sci*. 104 (Pt 2):533-543.

Caron, P.R., P. Watt, and J.C. Wang. 1994. The C-terminal domain of Saccharomyces cerevisiae DNA topoisomerase II. *Mol Cell Biol*. 14:3197-3207.

Carven, G.J., and L.J. Stern. 2005. Probing the ligand-induced conformational change in HLA-DR1 by selective chemical modification and mass spectrometric mapping. *Biochemistry*. 44:13625-13637.

Chen, S.H., N.L. Chan, and T.S. Hsieh. 2013. New mechanistic and functional insights into DNA topoisomerases. *Annu Rev Biochem*. 82:139-170.

Chen, V.B., I.W. Davis, and D.C. Richardson. 2009. KING (Kinemage, Next Generation): a versatile interactive molecular and scientific visualization program. *Protein Sci*. 18:2403-2409.

Chikamori, K., D.R. Grabowski, M. Kinter, B.B. Willard, S. Yadav, R.H. Aebersold, R.M. Bukowski, I.D. Hickson, A.H. Andersen, R. Ganapathi, and M.K. Ganapathi. 2003. Phosphorylation of serine 1106 in the catalytic domain of topoisomerase II alpha regulates enzymatic activity and drug sensitivity. *J Biol Chem*. 278:12696-12702.

Choi, J.H., L.A. Lindsey-Boltz, and A. Sancar. 2007. Reconstitution of a human ATR-mediated checkpoint response to damaged DNA. *Proc Natl Acad Sci U S A*. 104:13301-13306.

Choi, J.H., L.A. Lindsey-Boltz, and A. Sancar. 2009. Cooperative activation of the ATR checkpoint kinase by TopBP1 and damaged DNA. *Nucleic Acids Res*. 37:1501-1509.

Classen, S., S. Olland, and J.M. Berger. 2003. Structure of the topoisomerase II ATPase region and its mechanism of inhibition by the chemotherapeutic agent ICRF-187. *Proc Natl Acad Sci U S A*. 100:10629-10634.

Corbett, K.D., A.J. Schoeffler, N.D. Thomsen, and J.M. Berger. 2005. The structural basis for substrate specificity in DNA topoisomerase IV. *J Mol Biol*. 351:545-561.

Costenaro, L., J.G. Grossmann, C. Ebel, and A. Maxwell. 2005. Small-angle X-ray scattering reveals the solution structure of the full-length DNA gyrase a subunit. *Structure*. 13:287-296.

Crenshaw, D.G., and T. Hsieh. 1993. Function of the hydrophilic carboxyl terminus of type II DNA topoisomerase from Drosophila melanogaster. I. In vitro studies. *J Biol Chem*. 268:21328-21334.

Delacroix, S., J.M. Wagner, M. Kobayashi, K. Yamamoto, and L.M. Karnitz. 2007. The Rad9-Hus1-Rad1 (9-1-1) clamp activates checkpoint signaling via TopBP1. *Genes Dev*. 21:1472-1477.

Depew, R.E., L.F. Liu, and J.C. Wang. 1978. Interaction between DNA and Escherichia coli protein omega. Formation of a complex between single-stranded DNA and omega protein. *J Biol Chem*. 253:511-518.

DeVore, R.F., A.H. Corbett, and N. Osheroff. 1992. Phosphorylation of topoisomerase II by casein kinase II and protein kinase C: effects on enzyme-mediated DNA cleavage/religation and sensitivity to the antineoplastic drugs etoposide and 4'-(9-acridinylamino)methane-sulfon-m-anisidide. *Cancer Res*. 52:2156-2161.

Duursma, A.M., R. Driscoll, J.E. Elias, and K.A. Cimprich. 2013. A role for the MRN complex in ATR activation via TOPBP1 recruitment. *Mol Cell*. 50:116-122.

Dykhuizen, E.C., D.C. Hargreaves, E.L. Miller, K. Cui, A. Korshunov, M. Kool, S. Pfister, Y.J. Cho, K. Zhao, and G.R. Crabtree. 2013. BAF complexes facilitate decatenation of DNA by topoisomerase IIalpha. *Nature*. 497:624-627.

Fass, D., C.E. Bogden, and J.M. Berger. 1999. Quaternary changes in topoisomerase II may direct orthogonal movement of two DNA strands. *Nat Struct Biol*. 6:322-326.

Gadelle, D., J. Filee, C. Buhler, and P. Forterre. 2003. Phylogenomics of type II DNA topoisomerases. *Bioessays*. 25:232-242.

Gambus, A., G.A. Khoudoli, R.C. Jones, and J.J. Blow. 2011. MCM2-7 form double hexamers at licensed origins in xenopus egg extract. *J Biol Chem*.

Garcia, V., K. Furuya, and A.M. Carr. 2005. Identification and functional analysis of TopBP1 and its homologs. *DNA Repair (Amst)*. 4:1227-1239.

Germann, S.M., V. Schramke, R.T. Pedersen, I. Gallina, N. Eckert-Boulet, V.H. Oestergaard, and M. Lisby. 2014. TopBP1/Dpb11 binds DNA anaphase bridges to prevent genome instability. *J Cell Biol*. 204:45-59.

Habeeb, A.F., R.E. Schrohenloher, and J.C. Bennett. 1972. Studies of the component chains of human IgM by citraconylation. *Biochim Biophys Acta*. 263:339-350.

Haley, B., B. Foys, and M. Levine. 2010. Vectors and parameters that enhance the efficacy of RNAi-mediated gene disruption in transgenic Drosophila. *Proc Natl Acad Sci U S A*. 107:11435-11440.

Hanai, R., and J.C. Wang. 1994. Protein footprinting by the combined use of reversible and irreversible lysine modifications. *Proc Natl Acad Sci U S A*. 91:11904-11908.

Harkins, T.T., T.J. Lewis, and J.E. Lindsley. 1998. Pre-steady-state analysis of ATP hydrolysis by Saccharomyces cerevisiae DNA topoisomerase II. 2. Kinetic mechanism for the sequential hydrolysis of two ATP. *Biochemistry*. 37:7299-7312.

Hartman, P.S., and R.K. Herman. 1982. Radiation-sensitive mutants of Caenorhabditis elegans. *Genetics*. 102:159-178.

Hashimoto, Y., and H. Takisawa. 2003. Xenopus Cut5 is essential for a CDK-dependent process in the initiation of DNA replication. *EMBO J*. 22:2526-2535.

Herold, S., A. Hock, B. Herkert, K. Berns, J. Mullenders, R. Beijersbergen, R. Bernards, and M. Eilers. 2008. Miz1 and HectH9 regulate the stability of the checkpoint protein, TopBP1. *EMBO J*. 27:2851-2861.

Hirano, T., S. Funahashi, T. Uemura, and M. Yanagida. 1986. Isolation and characterization of Schizosaccharomyces pombe cutmutants that block nuclear division but not cytokinesis. *EMBO J*. 5:2973-2979.

Ho, S.N., H.D. Hunt, R.M. Horton, J.K. Pullen, and L.R. Pease. 1989. Site-directed mutagenesis by overlap extension using the polymerase chain reaction. *Gene*. 77:51-59.

Hu, H.G., M. Baack, and R. Knippers. 2009. Proteins of the origin recognition complex (ORC) and DNA topoisomerases on mammalian chromatin. *BMC Mol Biol*. 10:36.

Hu, T., H. Sage, and T.S. Hsieh. 2002. ATPase domain of eukaryotic DNA topoisomerase II. Inhibition of ATPase activity by the anti-cancer drug bisdioxopiperazine and ATP/ADP-induced dimerization. *J Biol Chem*. 277:5944-5951.

Iida, M., M. Matsuda, and H. Komatani. 2008. Plk3 phosphorylates topoisomerase IIalpha at Thr(1342), a site that is not recognized by Plk1. *Biochem J*. 411:27-32.

Imbalzano, A.N., H. Kwon, M.R. Green, and R.E. Kingston. 1994. Facilitated binding of TATA-binding protein to nucleosomal DNA. *Nature*. 370:481-485.

Jensen, L.H., A.V. Thougaard, M. Grauslund, B. Sokilde, E.V. Carstensen, H.K. Dvinge, D.A. Scudiero, P.B. Jensen, R.H. Shoemaker, and M. Sehested. 2005. Substituted purine analogues define a novel structural class of catalytic topoisomerase II inhibitors. *Cancer Res*. 65:7470-7477.

Jeon, Y., K.Y. Lee, M.J. Ko, Y.S. Lee, S. Kang, and D.S. Hwang. 2007. Human TopBP1 participates in cyclin E/CDK2 activation and preinitiation complex assembly during G1/S transition. *J Biol Chem*. 282:14882-14890.

Johnson, E.S., and G. Blobel. 1999. Cell cycle-regulated attachment of the ubiquitin-related protein SUMO to the yeast septins. *J Cell Biol*. 147:981-994.

Jones, D.T., N. Jager, M. Kool, T. Zichner, B. Hutter, M. Sultan, Y.J. Cho, T.J. Pugh, V. Hovestadt, A.M. Stutz, T. Rausch, H.J. Warnatz, M. Ryzhova, S. Bender, D. Sturm, S. Pleier, H. Cin, E. Pfaff, L. Sieber, A. Wittmann, M. Remke, H. Witt, S. Hutter, T. Tzaridis, J. Weischenfeldt, B. Raeder, M. Avci, V. Amstislavskiy, M. Zapatka, U.D. Weber, Q. Wang, B. Lasitschka, C.C. Bartholomae, M. Schmidt, C. von Kalle, V. Ast, C. Lawerenz, J. Eils, R. Kabbe, V. Benes, P. van Sluis, J. Koster, R. Volckmann, D. Shih, M.J. Betts, R.B. Russell, S. Coco, G.P. Tonini, U. Schuller, V. Hans, N. Graf, Y.J. Kim, C. Monoranu, W. Roggendorf, A. Unterberg, C. Herold-Mende, T. Milde, A.E. Kulozik, A. von Deimling, O. Witt, E. Maass, J. Rossler, M. Ebinger, M.U. Schuhmann, M.C. Fruhwald, M. Hasselblatt, N. Jabado, S. Rutkowski, A.O. von Bueren, D. Williamson, S.C. Clifford, M.G. McCabe, V.P. Collins, S. Wolf, S. Wiemann, H. Lehrach, B. Brors, W. Scheurlen, J. Felsberg, G. Reifenberger, P.A. Northcott, M.D. Taylor, M. Meyerson, S.L. Pomeroy, M.L. Yaspo, J.O. Korbel, A. Korshunov, R. Eils, S.M. Pfister, and P. Lichter. 2012. Dissecting the genomic complexity underlying medulloblastoma. *Nature*. 488:100-105.

Kennelly, P.J., and E.G. Krebs. 1991. Consensus sequences as substrate specificity determinants for protein kinases and protein phosphatases. *J Biol Chem*. 266:15555-15558.

Kilkenny, M.L., A.S. Dore, S.M. Roe, K. Nestoras, J.C. Ho, F.Z. Watts, and L.H. Pearl. 2008. Structural and functional analysis of the Crb2-BRCT2 domain reveals distinct roles in checkpoint signaling and DNA damage repair. *Genes Dev*. 22:2034-2047.

Kim, Y.J., L.K. Pannell, and D.L. Sackett. 2004. Mass spectrometric measurement of differential reactivity of cysteine to localize protein-ligand binding sites. Application to tubulin-binding drugs. *Anal Biochem*. 332:376-383.

Kondo, S., and N. Perrimon. 2011. A genome-wide RNAi screen identifies core components of the G(2)-M DNA damage checkpoint. *Sci Signal*. 4:rs1.

Kumagai, A., J. Lee, H.Y. Yoo, and W.G. Dunphy. 2006. TopBP1 activates the ATR-ATRIP complex. *Cell*. 124:943-955.

Kumagai, A., A. Shevchenko, and W.G. Dunphy. 2010. Treslin collaborates with TopBP1 in triggering the initiation of DNA replication. *Cell*. 140:349-359.

Kumagai, A., A. Shevchenko, A. Shevchenko, and W.G. Dunphy. 2011. Direct regulation of Treslin by cyclin-dependent kinase is essential for the onset of DNA replication. *J Cell Biol*. 193:995-1007.

Kurz, E.U., K.B. Leader, D.J. Kroll, M. Clark, and F. Gieseler. 2000. Modulation of human DNA topoisomerase IIalpha function by interaction with 14-3-3epsilon. *J Biol Chem*. 275:13948-13954.

Labib, K. 2010. How do Cdc7 and cyclin-dependent kinases trigger the initiation of chromosome replication in eukaryotic cells? *Genes Dev*. 24:1208-1219.

Lane, A.B., J.F. Gimenez-Abian, and D.J. Clarke. 2013. A novel chromatin tether domain controls topoisomerase IIalpha dynamics and mitotic chromosome formation. *J Cell Biol*. 203:471-486.

Lee, M.P., and T.S. Hsieh. 1994. Linker insertion mutagenesis of Drosophila topoisomerase II. Probing the structure of eukaryotic topoisomerase II. *J Mol Biol*. 235:436-447.

Leung, C.C., and J.N. Glover. 2011. BRCT domains: easy as one, two, three. *Cell Cycle*. 10:2461-2470.

Leung, C.C., Z. Gong, J. Chen, and J.N. Glover. 2011. Molecular basis of BACH1/FANCJ recognition by TopBP1 in DNA replication checkpoint control. *J Biol Chem*. 286:4292-4301.

Leung, C.C., L. Sun, Z. Gong, M. Burkat, R. Edwards, M. Assmus, J. Chen, and J.N. Glover. 2013. Structural insights into recognition of MDC1 by TopBP1 in DNA replication checkpoint control. *Structure*. 21:1450-1459.

Li, H., Y. Wang, and X. Liu. 2008. Plk1-dependent phosphorylation regulates functions of DNA topoisomerase IIalpha in cell cycle progression. *J Biol Chem*. 283:6209-6221.

Li, W., and J.C. Wang. 1997. Footprinting of yeast DNA topoisomerase II lysyl side chains involved in substrate binding and interdomainal interactions. *J Biol Chem*. 272:31190-31195.

Lin, R.K., N. Zhou, Y.L. Lyu, Y.C. Tsai, C.H. Lu, J. Kerrigan, Y.T. Chen, Z. Guan, T.S. Hsieh, and L.F. Liu. 2011. Dietary isothiocyanate-induced apoptosis via thiol modification of DNA topoisomerase IIalpha. *J Biol Chem*. 286:33591-33600.

Liu, K., J.D. Graves, J.D. Scott, R. Li, and W.C. Lin. 2013. Akt switches TopBP1 function from checkpoint activation to transcriptional regulation through phosphoserine binding-mediated oligomerization. *Mol Cell Biol*. 33:4685-4700.

Liu, K., J.C. Paik, B. Wang, F.T. Lin, and W.C. Lin. 2006. Regulation of TopBP1 oligomerization by Akt/PKB for cell survival. *EMBO J*. 25:4795-4807.

Liu, L.F., T.C. Rowe, L. Yang, K.M. Tewey, and G.L. Chen. 1983. Cleavage of DNA by mammalian DNA topoisomerase II. *J Biol Chem*. 258:15365-15370.

Liu, L.F., and J.C. Wang. 1979. Interaction between DNA and Escherichia coli DNA topoisomerase I. Formation of complexes between the protein and superhelical and nonsuperhelical duplex DNAs. *J Biol Chem*. 254:11082-11088.

Liu, S., B. Shiotani, M. Lahiri, A. Marechal, A. Tse, C.C. Leung, J.N. Glover, X.H. Yang, and L. Zou. 2011. ATR autophosphorylation as a molecular switch for checkpoint activation. *Mol Cell*. 43:192-202.

Losada, A., M. Hirano, and T. Hirano. 2002. Cohesin release is required for sister chromatid resolution, but not for condensin-mediated compaction, at the onset of mitosis. *Genes Dev*. 16:3004-3016.

Love, C., Z. Sun, D. Jima, G. Li, J. Zhang, R. Miles, K.L. Richards, C.H. Dunphy, W.W. Choi, G. Srivastava, P.L. Lugar, D.A. Rizzieri, A.S. Lagoo, L. Bernal-Mizrachi, K.P. Mann, C.R. Flowers, K.N. Naresh, A.M. Evens, A. Chadburn, L.I. Gordon, M.B. Czader, J.I. Gill, E.D. Hsi, A. Greenough, A.B. Moffitt, M. McKinney, A. Banerjee, V. Grubor, S. Levy, D.B. Dunson, and S.S. Dave. 2012. The genetic landscape of mutations in Burkitt lymphoma. *Nat Genet*. 44:1321-1325.

Luo, K., J. Yuan, J. Chen, and Z. Lou. 2009. Topoisomerase IIalpha controls the decatenation checkpoint. *Nat Cell Biol*. 11:204-210.

Lyu, Y.L., J.E. Kerrigan, C.P. Lin, A.M. Azarova, Y.C. Tsai, Y. Ban, and L.F. Liu. 2007. Topoisomerase IIbeta mediated DNA double-strand breaks: implications in doxorubicin cardiotoxicity and prevention by dexrazoxane. *Cancer Res*. 67:8839-8846.

Makiniemi, M., T. Hillukkala, J. Tuusa, K. Reini, M. Vaara, D. Huang, H. Pospiech, I. Majuri, T. Westerling, T.P. Makela, and J.E. Syvaoja. 2001. BRCT domain-containing protein TopBP1 functions in DNA replication and damage response. *J Biol Chem*. 276:30399-30406.

Masumoto, H., S. Muramatsu, Y. Kamimura, and H. Araki. 2002. S-Cdk-dependent phosphorylation of Sld2 essential for chromosomal DNA replication in budding yeast. *Nature*. 415:651-655.

McClendon, A.K., A.C. Gentry, J.S. Dickey, M. Brinch, S. Bendsen, A.H. Andersen, and N. Osheroff. 2008. Bimodal recognition of DNA geometry by human topoisomerase II alpha: preferential relaxation of positively supercoiled DNA requires elements in the C-terminal domain. *Biochemistry*. 47:13169-13178.

Meczes, E.L., K.L. Gilroy, K.L. West, and C.A. Austin. 2008. The impact of the human DNA topoisomerase II C-terminal domain on activity. *PLoS One*. 3:e1754.

Mirski, S.E., J.H. Gerlach, H.J. Cummings, R. Zirngibl, P.A. Greer, and S.P. Cole. 1997. Bipartite nuclear localization signals in the C terminus of human topoisomerase II alpha. *Exp Cell Res*. 237:452-455.

Montecucco, A., R. Rossi, D.S. Levin, R. Gary, M.S. Park, T.A. Motycka, G. Ciarrocchi, A. Villa, G. Biamonti, and A.E. Tomkinson. 1998. DNA ligase I is recruited to sites of DNA replication by an interaction with proliferating cell nuclear antigen: identification of a common targeting mechanism for the assembly of replication factories. *EMBO J*. 17:3786-3795.

Morrison, A., and N.R. Cozzarelli. 1979. Site-specific cleavage of DNA by E. coli DNA gyrase. *Cell*. 17:175-184.

Morrison, C., A.J. Henzing, O.N. Jensen, N. Osheroff, H. Dodson, S.E. Kandels-Lewis, R.R. Adams, and W.C. Earnshaw. 2002. Proteomic analysis of human metaphase chromosomes reveals topoisomerase II alpha as an Aurora B substrate. *Nucleic Acids Res*. 30:5318-5327.

Moyer, S.E., P.W. Lewis, and M.R. Botchan. 2006. Isolation of the Cdc45/Mcm2-7/GINS (CMG) complex, a candidate for the eukaryotic DNA replication fork helicase. *Proc Natl Acad Sci U S A*. 103:10236-10241.

Niimi, A., N. Suka, M. Harata, A. Kikuchi, and S. Mizuno. 2001. Co-localization of chicken DNA topoisomerase IIalpha, but not beta, with sites of DNA replication and possible involvement of a C-terminal region of alpha through its binding to PCNA. *Chromosoma*. 110:102-114.

Nitiss, J.L. 2009a. DNA topoisomerase II and its growing repertoire of biological functions. *Nat Rev Cancer*. 9:327-337.

Nitiss, J.L. 2009e. Targeting DNA topoisomerase II in cancer chemotherapy. *Nat Rev Cancer*. 9:338-350.

Onn, I., J.M. Heidinger-Pauli, V. Guacci, E. Unal, and D.E. Koshland. 2008. Sister chromatid cohesion: a simple concept with a complex reality. *Annual review of cell and developmental biology*. 24:105-129.

Parsons, D.W., M. Li, X. Zhang, S. Jones, R.J. Leary, J.C. Lin, S.M. Boca, H. Carter, J. Samayoa, C. Bettegowda, G.L. Gallia, G.I. Jallo, Z.A. Binder, Y. Nikolsky, J. Hartigan, D.R. Smith, D.S. Gerhard, D.W. Fults, S. VandenBerg, M.S. Berger, S.K. Marie, S.M. Shinjo, C. Clara, P.C. Phillips, J.E. Minturn, J.A. Biegel, A.R. Judkins, A.C. Resnick, P.B. Storm, T. Curran, Y. He, B.A. Rasheed, H.S. Friedman, S.T. Keir, R. McLendon, P.A. Northcott, M.D. Taylor, P.C. Burger, G.J. Riggins, R. Karchin, G. Parmigiani, D.D. Bigner, H. Yan, N. Papadopoulos, B. Vogelstein, K.W. Kinzler, and V.E. Velculescu. 2011. The genetic landscape of the childhood cancer medulloblastoma. *Science*. 331:435-439.

Pospiech, H., F. Grosse, and F.M. Pisani. 2010. The initiation step of eukaryotic DNA replication. *Subcell Biochem*. 50:79-104.

Pugh, T.J., S.D. Weeraratne, T.C. Archer, D.A. Pomeranz Krummel, D. Auclair, J. Bochicchio, M.O. Carneiro, S.L. Carter, K. Cibulskis, R.L. Erlich, H. Greulich, M.S. Lawrence, N.J. Lennon, A. McKenna, J. Meldrim, A.H. Ramos, M.G. Ross, C. Russ, E. Shefler, A. Sivachenko, B. Sogoloff, P. Stojanov, P. Tamayo, J.P. Mesirov, V. Amani, N. Teider, S. Sengupta, J.P. Francois, P.A. Northcott, M.D. Taylor, F. Yu, G.R. Crabtree, A.G. Kautzman, S.B. Gabriel, G. Getz, N. Jager, D.T. Jones, P. Lichter, S.M. Pfister, T.M. Roberts, M. Meyerson, S.L. Pomeroy, and Y.J. Cho. 2012. Medulloblastoma exome sequencing uncovers subtype-specific somatic mutations. *Nature*. 488:106-110.

Qi, X., S. Hou, A. Lepp, R. Li, Z. Basir, Z. Lou, and G. Chen. 2011. Phosphorylation and Stabilization of Topoisomerase II{alpha} Protein by p38{gamma} Mitogen-activated Protein Kinase Sensitize Breast Cancer Cells to Its Poisons. *J Biol Chem*. 286:35883-35890.

Rappas, M., A.W. Oliver, and L.H. Pearl. 2011. Structure and function of the Rad9-binding region of the DNA-damage checkpoint adaptor TopBP1. *Nucleic Acids Res*. 39:313-324.

Richter, J., M. Schlesner, S. Hoffmann, M. Kreuz, E. Leich, B. Burkhardt, M. Rosolowski, O. Ammerpohl, R. Wagener, S.H. Bernhart, D. Lenze, M. Szczepanowski, M. Paulsen, S. Lipinski, R.B. Russell, S. Adam-Klages, G. Apic, A. Claviez, D. Hasenclever, V. Hovestadt, N. Hornig, J.O. Korbel, D. Kube, D. Langenberger, C. Lawerenz, J. Lisfeld, K. Meyer, S. Picelli, J. Pischimarov, B. Radlwimmer, T. Rausch, M. Rohde, M. Schilhabel, R. Scholtysik, R. Spang, H. Trautmann, T. Zenz, A. Borkhardt, H.G. Drexler, P. Moller, R.A. MacLeod, C. Pott, S. Schreiber, L. Trumper, M. Loeffler, P.F. Stadler, P. Lichter, R. Eils, R. Kuppers, M. Hummel, W. Klapper, P. Rosenstiel, A. Rosenwald, B. Brors, R. Siebert, and I.M.-S. Project. 2012. Recurrent mutation of the ID3 gene in Burkitt lymphoma identified by integrated genome, exome and transcriptome sequencing. *Nat Genet*. 44:1316-1320.

Robinson, G., M. Parker, T.A. Kranenburg, C. Lu, X. Chen, L. Ding, T.N. Phoenix, E. Hedlund, L. Wei, X. Zhu, N. Chalhoub, S.J. Baker, R. Huether, R. Kriwacki, N. Curley, R. Thiruvenkatam, J. Wang, G. Wu, M. Rusch, X. Hong, J. Becksfort, P. Gupta, J. Ma, J. Easton, B. Vadodaria, A. Onar-Thomas, T. Lin, S. Li, S. Pounds, S. Paugh, D. Zhao, D. Kawauchi, M.F. Roussel, D. Finkelstein, D.W. Ellison, C.C. Lau, E. Bouffet, T. Hassall, S. Gururangan, R. Cohn, R.S. Fulton, L.L. Fulton, D.J. Dooling, K. Ochoa, A. Gajjar, E.R. Mardis, R.K. Wilson, J.R. Downing, J. Zhang, and R.J. Gilbertson. 2012. Novel mutations target distinct subgroups of medulloblastoma. *Nature*. 488:43-48.

Roca, J., R. Ishida, J.M. Berger, T. Andoh, and J.C. Wang. 1994. Antitumor bisdioxopiperazines inhibit yeast DNA topoisomerase II by trapping the enzyme in the form of a closed protein clamp. *Proc Natl Acad Sci U S A*. 91:1781-1785.

Roca, J., and J.C. Wang. 1992. The capture of a DNA double helix by an ATP-dependent protein clamp: a key step in DNA transport by type II DNA topoisomerases. *Cell*. 71:833-840.

Roy, A., A. Kucukural, and Y. Zhang. 2010. I-TASSER: a unified platform for automated protein structure and function prediction. *Nat Protoc*. 5:725-738.

Rubin, G.M., and A.C. Spradling. 1982. Genetic transformation of Drosophila with transposable element vectors. *Science*. 218:348-353.

Ryu, H., M. Furuta, D. Kirkpatrick, S.P. Gygi, and Y. Azuma. 2010. PIASy-dependent SUMOylation regulates DNA topoisomerase IIalpha activity. *J Cell Biol*. 191:783-794.

Sampson, D.A., M. Wang, and M.J. Matunis. 2001. The small ubiquitin-like modifier-1 (SUMO-1) consensus sequence mediates Ubc9 binding and is essential for SUMO-1 modification. *J Biol Chem*. 276:21664-21669.

Sander, M., and T. Hsieh. 1983. Double strand DNA cleavage by type II DNA topoisomerase from Drosophila melanogaster. *J Biol Chem*. 258:8421-8428.

Sander, M., J.M. Nolan, and T. Hsieh. 1984. A protein kinase activity tightly associated with Drosophila type II DNA topoisomerase. *Proc Natl Acad Sci U S A*. 81:6938-6942.

Schmidt, B.H., N. Osheroff, and J.M. Berger. 2012. Structure of a topoisomerase II-DNA-nucleotide complex reveals a new control mechanism for ATPase activity. *Nat Struct Mol Biol*. 19:1147-1154.

Schoeffler, A.J., and J.M. Berger. 2008. DNA topoisomerases: harnessing and constraining energy to govern chromosome topology. *Q Rev Biophys*. 41:41-101.

Sheflin, L.G., and S.W. Spaulding. 1989. High mobility group protein 1 preferentially conserves torsion in negatively supercoiled DNA. *Biochemistry*. 28:5658-5664.

Sjottem, E., C. Rekdal, G. Svineng, S.S. Johnsen, H. Klenow, R.D. Uglehus, and T. Johansen. 2007. The ePHD protein SPBP interacts with TopBP1 and together they co-operate to stimulate Ets1-mediated transcription. *Nucleic Acids Res*. 35:6648-6662.

Sohn, S.Y., and Y. Cho. 2009. Crystal structure of the human rad9-hus1-rad1 clamp. *J Mol Biol*. 390:490-502.

Sokka, M., S. Parkkinen, H. Pospiech, and J.E. Syvaoja. 2010. Function of TopBP1 in genome stability. *Subcell Biochem*. 50:119-141.

Stros, M., A. Bacikova, E. Polanska, J. Stokrova, and F. Strauss. 2007. HMGB1 interacts with human topoisomerase IIalpha and stimulates its catalytic activity. *Nucleic Acids Res*. 35:5001-5013.

Stros, M., D. Cherny, and T.M. Jovin. 2000. HMG1 protein stimulates DNA end joining by promoting association of DNA molecules via their ends. *Eur J Biochem*. 267:4088-4097.

Stros, M., J. Stokrova, and J.O. Thomas. 1994. DNA looping by the HMG-box domains of HMG1 and modulation of DNA binding by the acidic C-terminal domain. *Nucleic Acids Res*. 22:1044-1051.

Tak, Y.S., Y. Tanaka, S. Endo, Y. Kamimura, and H. Araki. 2006. A CDK-catalysed regulatory phosphorylation for formation of the DNA replication complex Sld2-Dpb11. *EMBO J*. 25:1987-1996.

Takahashi, K. 1968. The reaction of phenylglyoxal with arginine residues in proteins. *J Biol Chem*. 243:6171-6179.

Takahashi, Y., V. Yong-Gonzalez, Y. Kikuchi, and A. Strunnikov. 2006. SIZ1/SIZ2 control of chromosome transmission fidelity is mediated by the sumoylation of topoisomerase II. *Genetics*. 172:783-794.

Takeishi, Y., E. Ohashi, K. Ogawa, H. Masai, C. Obuse, and T. Tsurimoto. 2010. Casein kinase 2-dependent phosphorylation of human Rad9 mediates the interaction between human Rad9-Hus1-Rad1 complex and TopBP1. *Genes to cells : devoted to molecular & cellular mechanisms*. 15:761-771.

Tanaka, S., T. Umemori, K. Hirai, S. Muramatsu, Y. Kamimura, and H. Araki. 2007. CDK-dependent phosphorylation of Sld2 and Sld3 initiates DNA replication in budding yeast. *Nature*. 445:328-332.

Thomas, J.O., and A.A. Travers. 2001. HMG1 and 2, and related 'architectural' DNA-binding proteins. *Trends in biochemical sciences*. 26:167-174.

Thummel, C.S., A.M. Boulet, and H.D. Lipshitz. 1988. Vectors for Drosophila P-element-mediated transformation and tissue culture transfection. *Gene*. 74:445-456.

Tu, B.P., and J.C. Wang. 1999. Protein footprinting at cysteines: probing ATP-modulated contacts in cysteine-substitution mutants of yeast DNA topoisomerase II. *Proc Natl Acad Sci U S A*. 96:4862-4867.

Van Hatten, R.A., A.V. Tutter, A.H. Holway, A.M. Khederian, J.C. Walter, and W.M. Michael. 2002. The Xenopus Xmus101 protein is required for the recruitment of Cdc45 to origins of DNA replication. *J Cell Biol*. 159:541-547.

Vert, J.P., N. Foveau, C. Lajaunie, and Y. Vandenbrouck. 2006. An accurate and interpretable model for siRNA efficacy prediction. *BMC bioinformatics*. 7:520.

Vos, S.M., E.M. Tretter, B.H. Schmidt, and J.M. Berger. 2011. All tangled up: how cells direct, manage and exploit topoisomerase function. *Nat Rev Mol Cell Biol*. 12:827-841.

Wang, J., Z. Gong, and J. Chen. 2011. MDC1 collaborates with TopBP1 in DNA replication checkpoint control. *J Cell Biol*. 193:267-273.

Warbrick, E. 1998. PCNA binding through a conserved motif. *Bioessays*. 20:195-199.

Wardlaw, C.P., A.M. Carr, and A.W. Oliver. 2014. TopBP1: A BRCT-scaffold protein functioning in multiple cellular pathways. *DNA Repair (Amst)*. 22:165-174.

Wasserman, R.A., C.A. Austin, L.M. Fisher, and J.C. Wang. 1993. Use of yeast in the study of anticancer drugs targeting DNA topoisomerases: expression of a functional recombinant human DNA topoisomerase II alpha in yeast. *Cancer Res*. 53:3591-3596.

Wei, H., A.J. Ruthenburg, S.K. Bechis, and G.L. Verdine. 2005. Nucleotide-dependent domain movement in the ATPase domain of a human type IIA DNA topoisomerase. *J Biol Chem*. 280:37041-37047.

Wells, N.J., C.M. Addison, A.M. Fry, R. Ganapathi, and I.D. Hickson. 1994. Serine 1524 is a major site of phosphorylation on human topoisomerase II alpha protein in vivo and is a substrate for casein kinase II in vitro. *J Biol Chem*. 269:29746-29751.

Wigley, D.B., G.J. Davies, E.J. Dodson, A. Maxwell, and G. Dodson. 1991. Crystal structure of an N-terminal fragment of the DNA gyrase B protein. *Nature*. 351:624-629.

Wood, T.D., Z. Guan, C.L. Borders, Jr., L.H. Chen, G.L. Kenyon, and F.W. McLafferty. 1998. Creatine kinase: essential arginine residues at the nucleotide binding site identified by chemical modification and high-resolution tandem mass spectrometry. *Proc Natl Acad Sci U S A*. 95:3362-3365.

Word, J.M., S.C. Lovell, T.H. LaBean, H.C. Taylor, M.E. Zalis, B.K. Presley, J.S. Richardson, and D.C. Richardson. 1999. Visualizing and quantifying molecular goodness-of-fit: small-probe contact dots with explicit hydrogen atoms. *J Mol Biol*. 285:1711-1733.

Wu, X., H. Liang, K.A. O'Hara, J.C. Yalowich, and B.B. Hasinoff. 2008. Thiol-modulated mechanisms of the cytotoxicity of thimerosal and inhibition of DNA topoisomerase II alpha. *Chem Res Toxicol*. 21:483-493.

Yamamoto, R.R., J.M. Axton, Y. Yamamoto, R.D. Saunders, D.M. Glover, and D.S. Henderson. 2000. The Drosophila mus101 gene, which links DNA repair, replication and condensation of heterochromatin in mitosis, encodes a protein with seven BRCA1 C-terminus domains. *Genetics*. 156:711-721.

Yamane, K., M. Kawabata, and T. Tsuruo. 1997. A DNA-topoisomerase-II-binding protein with eight repeating regions similar to DNA-repair enzymes and to a cell-cycle regulator. *Eur J Biochem*. 250:794-799.

Zegerman, P., and J.F. Diffley. 2007. Phosphorylation of Sld2 and Sld3 by cyclin-dependent kinases promotes DNA replication in budding yeast. *Nature*. 445:281-285.

Zhang, Y. 2007. Template-based modeling and free modeling by I-TASSER in CASP7. *Proteins*. 69 Suppl 8:108-117.

Biography

Yu-tsung Shane Chen was born in Taipei, Taiwan on May 8th, 1981. He graduated from School of Pharmacy in National Taiwan University with a Bachelor of Science and qualified as a pharmacist in 2003. He then attended the Institute of Biochemistry and Molecular Biology for his master degree to study SARS coronavirus nucleocapsid protein in Dr. Lu-Ping Chow's lab. In 2007 after serving one year military obligation, he joined Dr. Tao-shih Hsieh's lab at Duke University as a research assistant, where he studied enzyme kinetics of *Drosophila* Topoisomerase 2. Mentored by both Dr. Tao-shih Hsieh and Dr. Paul Modrich, he started his Ph.D. training in Department of Biochemistry at Duke University in 2009, and published two peer-reviewed articles, "Dietary isothiocyanate-induced apoptosis via thiol modification of DNA topoisomerase IIα" and "Probing conformational changes in human DNA topoisomerase IIα by pulsed alkylation mass spectrometry" in Journal of Biological Chemistry in 2011 and 2012, respectively.